UNIVERSITY OF CALIFORNIA, SAN DIEGO
SAN DIEGO STATE UNIVERSITY

Identification and Modification of Fatty Acid Modifying Enzyme From *Staphylococcus aureus*

A dissertation submitted in partial satisfaction of the
requirements for the degree Doctor of Philosophy

in

Chemistry

by

Benjamin David Saylor

Committee in charge:

University of California, San Diego

Professor Michael Burkart
Professor Navtej Toor

San Diego State University

Professor John J. Love, Chair
Professor Richard Bizzoco
Professor William Stumph

2016

The dissertation of Benjamin David Saylor is approved, and it is acceptable in quality and form for publication on microfilm and electronically:

_____

_____

_____

_____

_____

Chair

University of California, San Diego

San Diego State University

2016

TABLE OF CONTENTS

Signature Page.....iii

Table of Contents.....iv

List of Abbreviations.....viii

List of Figures.....x

List of Tables.....xiii

Acknowledgments.....xiv

Vita and Publications.....xv

Abstract of the Dissertation.....xvi

Chapter I: Introduction

1.1 Practical Considerations in Alternative Fuel Development.....1

1.2 Biodiesel: Benefits and Challenges.....2

1.3 An Introduction to Lipases.....4

1.4 Real and Potential Applications of Lipases.....8

1.5 *Staphylococcus aureus* and Lipase Activity.....9

1.6 FAME Limitations and Substrate Localization.....14

1.7 Rebinding.....17

1.8 LUSH.....20

1.9 References.....23

Chapter II: Materials and Methods

2.1 Introduction.....29

2.2 Reagents.....30

2.3 Instrumentation.....30

2.4 *Staphylococcus aureus* Cultures.....31

2.5 GC-MS Method of FAME Activity Assessment.....32

2.6 *S. aureus* Culture Fractionation and LC-MS Sequencing.....33

2.7 Cloning of NWMN_0624, NWMN_2434, SAUSA300_2518, SAUSA300_0320, and SAUSA300_2603.....34

2.8 Recombinant Expression of FAME Proteins.....41

2.9 Assaying of the “Selected” Proteins.....44

2.10 NPA Assaying of Recombinant Isolated Proteins.....44

2.11 Turbidity of Oleic Acid Suspensions.....46

2.12 Design and Cloning of FAME-LUSH Fusion.....49

2.13 Design and Cloning of FAME-LUSH Fusion T57A mutant.....52

2.14 Purification of Recombinant FAME Constructs.....54

2.15 ANS Fluorescence Titration of FAME and FAME-LUSH fusion.....57

2.16 GC-MS Assessment of FAME-LUSH Fusion.....59

2.17 References.....61

Chapter III: Identification of Staphylococcal FAME

3.1 Introduction.....63

3.2 NWMN_0624 and NWMN_2434 are Non-FAME Proteins.....64

3.3 Square One: *Staphylococcus aureus* Culture Fractionation.....65

3.4 Para-Nitrophenyl Acetate Hydrolysis Results.....71

3.5 SAUSA300_0320, SAUSA300_2603 and *in vitro* FAME Activity.....74

3.6 Features of SAUSA300_0320 and SAUSA300_2603.....77

3.7 Conclusion.....84

3.8 References.....87

Chapter IV: Design and Analysis of Staphylococcal FAME-LUSH fusions

4.1 Introduction.....92

4.2 Alcohol Binding Proteins.....99

4.3 FAME-LUSH Design.....102

4.4 FAME-LUSH-T57A.....103

4.5 FAME-LUSH Fusion Purification.....104

4.6 FAME-LUSH Ethanol Binding and Fluorescence Spectroscopy.....105

4.7 FAME Activity of FAME-LUSH Fusions.....107

4.8 Kinetic Data Interpretation.....111

4.9 Conclusion.....114

4.10 References.....118

Chapter V: Outer Membrane Phospholipase A

5.1 OMPLA.....122

5.2 Mutating OMPLA.....125

5.3 Assessing OMPLA.....125

5.4 Reagents.....128

5.5 Instrumentation.....128

5.6 Cloning of OMPLA for Recombinant Expression.....128

5.7 Recombinant OMPLA Denaturation and Refolding.....132

5.8 bis-BODIPY Fluorescence Assay for Phospholipase Activity.....133

5.9 Results: OMPLA Expression in *E. coli*.....134

5.10 Fluorescence Assay Complications.....134

5.11 Termination of the OMPLA Project.....138

5.12 References.....141

Appendix I: Manuscript in Review

Abstract.....144

A.1 Introduction.....145

A.2 Experimental.....150

A.3 Results and Discussion.....155

A.4 Conclusion.....167

A.5 References.....169

LIST OF ABBREVIATIONS

°C	degrees Celsius
cDNA	complementary DNA
FAME	Fatty Acid Modifying Enzyme
FPLC	Fast Protein Liquid Chromatography
kD	kilo-Dalton
LB	Luria-Bertani media
MRSA	Methicillin Resistant *Staphylococcus aureus*
PCR	Polymerase Chain Reaction
GC-FID	Gas Chromatography-Flame Ionization Detector
GC-MS	Gas Chromatography-Mass Spectrometry
LC-MS	Liquid Chromatography-Mass Spectrometry
SDS-PAGE	Sodium Dodecyl Sulfate Polyacrylamide Gel Electrophoresis
SEC	Size Exclusion Chromatography
TSB	Tryptic Soy Broth

Small molecules:

ANS	8-Anilino-1-Naphthalene-Sulfonic acid
bis-Tris	bis tris hydroxymethyl aminomethane
EtOH	Ethanol
IPTG	Isopropyl β-D-1-thiogalactopyranoside

mβCD	Methyl-Beta-Cyclodextrin
NPA	para-Nitrophenol Acetate
POPC	Phosphatidylcholine

Proteins:

FGF-2	Fibroblast Growth Factor 2
HSPG	Heparan Sulfate Proteoglycan
LUSH	a *Drosophila melanogaster* ethanol binding protein
OMPLA	*Escherichia coli* Outer Membrane Phospholipase A
SAUSA300_0320	aka SAL-2, a *Staphylococcus aureus* lipase and FAME
SAUSA300_0641	aka NWMN_0624, a *S. aureus* cytoplasmic lipase
SAUSA300_2473	aka NWMN_2434, a *Staphylococcus aureus* protein
SAUSA300_2518	a *Staphylococcus aureus* cytoplasmic lipase
SAUSA300_2603	aka SAL-1, a *Staphylococcus aureus* lipase and FAME
SAL-3	a *Staphylococcus aureus* lipase, homologue of SAL-1
SEL-1	a *Staphylococcus epidermidis* lipase, homologue of SAL-1
SEL-2	a *Staphylococcus epidermidis* lipase, homologue of SAL-2
SHyL	*Staphylococcus hyicus* phospholipase

LIST OF FIGURES

Figure 1-1. Aquaculture Systems for the Production of Algae.....3

Figure 1-2. Lipase-Catalyzed Reactions.....6

Figure 1-3. The Basic Architecture of the α/β Hydrolase Fold.....7

Figure 1-4. Bacterial Resistance to Environmental Free Fatty Acids.....11

Figure 1-5. Schematic of Six Secreted Staphylococcal Lipases.....13

Figure 1-6. Graphical Representation of Rebinding.....18

Figure 1-7. LUSH Visualized *in vivo* via Immunofluorescence.....21

Figure 2-1. Expression Region of the pET22b(+) Plasmid.....38

Figure 2-2. SDS-PAGE Evaluation of Recombinant Protein Expression.....43

Figure 2.3. Nitrophenyl Acetate Assay for Lipase Activity.....45

Figure 2-4. FAME Activity Reduces Oleic Acid Droplet Turbidity.....48

Figure 2-5. PCR Scheme for Construction of the LUSH Gene.....50

Figure 2-6. SDS-PAGE Showing Purified FAME Constructs.....57

Figure 2-7. ANS Fluorescence Titration.....58

Figure 2-8. Mass Spectra of Butyl Oleate and Ethyl Oleate.....60

Figure 3-1. FAME Activity in Staphylococcal Culture Supernatants.....66

Figure 3-2. FAME Activity in Size Exclusion Eluent Fractions.....68

Figure 3-3. NPA Hydrolysis by Recombinant Staphylococcal Lipases.....72

Figure 3-4. Sequence Alignment of FAMEs and *S. hyicus* phospholipase.....79

Figure 3-5. Structure Comparison of FAMEs to *S. hyicus* phospholipase.....80

Figure 3-6. Members of the Secreted Staphylococcal Lipase Family.....85
Figure 4-1. Hypothetical Screening of a Mutagenized FAME Library.....94
Figure 4-2. Interfacial Activation.....97
Figure 4-3. Crystal Models of Alcohol-Binding Proteins.....101
Figure 4-4. The Gene for the FAME-LUSH Fusion Variant.....103
Figure 4-5. Loss of ANS Fluorescence due to Ethanol Binding.....107
Figure 4-6. Ethyl Oleate Synthesis by Recombinant FAME.....109
Figure 5-1. The Crystal Model of OMPLA.....122
Figure 5-2. Phospholipase A1/A2/B Catalyzed Reactions.....124
Figure 5-3. Example of Thin Layer Chromatography.....126
Figure 5-4. bis-BODIPY Phosphatidylcholine.....127
Figure 5-5. Expression Region of the pET21a(+) Plasmid.....129
Figure 5-6. SDS-PAGE Evaluation of Recombinant OMPLA Expression.....131
Figure 5-7. Baseline bis-BODIPY Phosphatidylcholine Fluorescence.....135
Figure 5-8. Gain in bis-BODIPY Phosphatidylcholine Fluorescence.....136
Figure A-1. FAME Activity of Different Staphylococcal Strains.....175
Figure A-2. Nitrophenyl acetate hydrolysis by recombinant Staphylococcal lipases.....176
Figure A-3. Ester synthesis by staphylococcal lipases.....177
Figure A-4. ANS Fluorescence Loss due to Ethanol Binding.....178
Figure A-5. Ethyl Oleate Synthesis by recombinant FAME.....179

Supplementary figure A-1. FAME activity of SEC fractions.....182

Supplementary figure A-2. SDS-PAGE showing 2603 FAME.....183

Supplementary figure A-3. Kalign CLUSTAL protein sequence alignment of USA300 strain *Staphylococcus aureus* lipases.....184

LIST OF TABLES

Table 3-1. Protein Contents of FAME-Active Supernatant Fraction.....69

Table 3-2. Recombinant Staphylococcal Protein Enzymatic Activities.....75

Table 4-1. Effective K_Ms of FAME Constructs With Respect to Ethanol.....111

Table A-1. Analysis of the data using GraphPad Prism.....181

ACKNOWLEDGMENTS

I would like to thank everyone in the Love lab for their help and advice over the years, in particular Lisa, Youly, Markus, Mario, Melissa, Brian, Peter, Ariana, and Myung. I'd also like to thank members of the other labs at SDSU, in particular Drs. Tom Huxford, William Stumph, and Aileen Knowles for their help both with my project and in their capacities as seminar leaders.

Much of the equipment used for this project was generously made available by other laboratories. I want to specifically thank Drs. Eunha Hoh, Kelly Doran, Sam Somanathan, Dale Chatfield, and Robert Pomeroy for granting access and training with important instruments.

Finally, I would like to thank my family and friends, who mean more to me than I could possibly convey here.

Appendix I, in part is currently submitted for publication of the material. Saylor, Benjamin D.; Love, John J. The dissertation author was the primary investigator and author of this material.

VITA

Education

2006 B.S. Biology
University of California, Riverside, Riverside, California

2015 M.A. Chemistry and Biochemistry
San Diego State University, San Diego, California

2016 Ph.D. Chemistry
San Diego State University, University of California, San Diego

Publications

Saylor B.D., Love J.J. “A Secreted *Staphylococcus aureus* Lipase Engineered for Enhanced Alcohol Affinity for Fatty Acid Esterification” manuscript in review.

Awards

Recipient of the 2013-2014 Arne N. Wick Predoctoral Research Fellowship from the California Metabolic Research Foundation.

ABSTRACT OF THE DISSERTATION

Identification and Modification of Fatty Acid Modifying Enzyme From *Staphylococcus aureus*

by

Benjamin David Saylor

Doctor of Philosophy in Chemistry

University of Califoria, San Diego 2016
San Diego State University 2016

Professor John J. Love, Chair

Biodiesel, as well as other commercially and industrially useful lipids, can be synthesized enzymatically in lieu of other methods. Enzymatic synthesis offers improved specificity and potentially lower manufacturing costs, as non-enzymatic synthesis requires the addition of heat and expensive or dangerous reagents. Numerous microbial enzymes in the lipase family have already been shown to catalyze the synthesis of esters, including biodiesel, under hydrophobic conditions. Enzymatic synthesis of biodiesel by naturally occurring lipases is often hampered by dependence on long-chain alcohol substrates. Enzymes that can employ small alcohols (methanol or ethanol) as substrates are at an advantage because said alcohols are generally much cheaper and less toxic.

We have isolated two enzymes from methicillin resistant *Staphylococcus aureus* that can catalyze the esterification of fatty acid to ethanol to form fatty acid ethyl esters, as they appear to do *in vivo*.

Lipase activity, as well as other lipase-catalyzed reactions such as the synthesis of fatty acid alkyl esters, is often dependent on localization of enzyme and substrate due to the propensity of the substrates to partition in aqueous environments. Lipases have been shown to exhibit unique conformational changes when associating with lipid substrate. These changes thermodynamically enhance enzyme-lipid association, and we have sought to exploit this co-localization by mutating a lipase to recruit additional alcohol to the microenvironment of the lipid substrate. The “rebinding” effect, which has been shown to occur when multiple receptors are closely grouped, reduces diffusion of ligand (or substrate) away from the receptor cluster, increasing the equilibrium ligand concentration local to the cluster. The addition of an alcohol-binding domain derived from the *Drosophila melanogaster* protein LUSH to the staphylococcal lipase creates a fusion protein with superior substrate co-localization ability. As a result, the rate of fatty acid ethyl ester synthesis is enhanced, in comparison to the wild type lipase, at low ethanol concentrations.

Chapter I: Introduction

1.1 Practical Considerations in Alternative Fuel Development

For much of the past decade, there has been increased interest in the development of fuels that constitute a viable alternative to petroleum-based liquid fuels (gasoline). This has been driven at various points by concerns about the environmental impact of carbon dioxide emissions resulting from the use of fossil fuels for transportation and electricity, and concerns about the future availability of petroleum and fossil fuels in general. Although the latter consideration has recently waned in importance due to recent circumstances such as the development of hydraulic fracturing and changes in the policies of some petroleum exporting nations, the nonrenewable nature of fossil fuels makes the eventual decline of global petroleum production an inevitability [12].

Nevertheless, petroleum fuels remain entrenched as the fuel of choice for most transportation needs worldwide, primarily for two reasons. The first is that the existing vehicle population, including automotives, ships, and aircraft, is overwhelmingly petroleum-fueled. While other engine types, such as electric motors, are commercially available, the infrastructure required to supply them with new energy is not as pervasive or well-developed as that of gasoline-driven vehicles. As a result, alternative engine types may seem less appealing to individual consumers and institutions, slowing the pace at which those types are

adopted. The slow adoption of new fuel sources in turn slows the development of the infrastructure required to resupply them, creating a negative feedback loop of industrial inertia.

The second reason for the persistence of fossil fuels as the power source of choice for most of the world is chemical rather than commercial. Gasoline, kerosene, and petrodiesel, which are heterogeneous mixtures of reduced hydrocarbons, have tremendously high energy densities as combustible fuels, [54]. Alcohol fuels such as ethanol are already partially oxidized, and therefore release less heat energy (both by weight and by volume) upon combustion with oxygen. Hydrogen is similarly less energy-dense by volume, even when compressed into a liquid state. Any fuel that is low in energy density necessitates a more cumbersome fuel reservoir. Therefore, any viable alternative fuel must approach the energy density of petroleum fuels in order to be widely adopted. Biodiesel, including algae-sourced biodiesel, is one such fuel (Figure 1-1) [12].

1.2 Biodiesel: Benefits and Challenges

Biodiesel, a colloquial term for homogeneous or heterogeneous fatty acid alkyl esters, is appealing as an alternative fuel because it is compatible with a great deal of the existing energy infrastructure. It is compatible with diesel engines whereas ethanol and ethanolic fuels typically require specialized internal combustion engines.

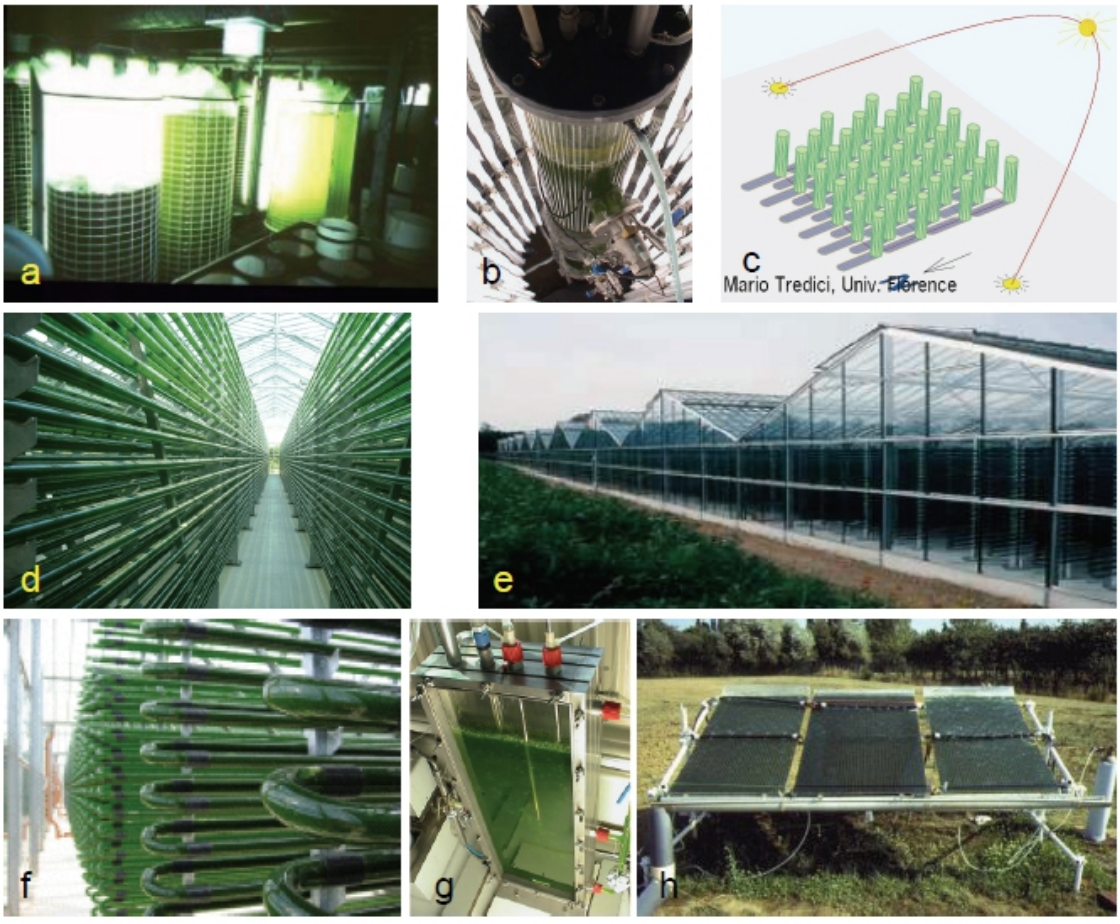

Figure 1-1. Several aquaculture systems for industrial production of algae [12].

Other energy sources, such as gas-electric engines and fully electric engines, are on the rise in the field of consumer vehicles, but it is not likely that they will be widespread in industrial or military sectors for many years. Therefore the refinement of biodiesel production merits investigation. Biodiesel is typically synthesized by heating a mixture of triglycerides or fatty acids and alcohols at

high pH. The costs associated with supplying heat and alkaline catalysts are ultimately passed on to consumers by inflating the cost of the resulting biodiesel, thereby reducing its appeal as a fuel source. Additionally, unwanted side products are produced in the presence of water, but many potential sources of feedstock oil, such as plant oils and algal oil, are difficult to fully dry without the investment of significant amounts of additional energy. Therefore, enzymes in the lipase/esterase family offer a potentially appealing alternative, as they are adapted to potentially catalyze the synthesis of fatty acid acyl esters at lower temperatures and pH values and in aqueous environments. Although the enzyme-catalyzed synthesis of alternative fuels poses its own set of technical challenges, it circumvents many of the challenges currently confronting the field [4,12,13,20,31,48].

1.3 An Introduction to Lipases

Esterases, as their name implies, are the family of hydrolases that catalyze the hydrolysis of ester bonds within substrates. Esterases generally feature a “catalytic triad” composed of a basic amino acid side chain (usually histidine), an acidic side chain, and a potential nucleophile (usually serine or cysteine) [9,27,30,32,36,40,42]. The acid and base groups activate the third side chain by deprotonating it, creating a nucleophile that can attack the carbonyl carbon of a nearby ester substrate molecule, creating a tetrahedral intermediate.

The tetrahedral intermediate then decomposes, releasing an alcohol product. A water molecule can then make a nucleophilic attack on the remaining enzyme-substrate complex, forming another tetrahedral intermediate that can then decompose into a carboxylic acid and free enzyme. Lipases are the subcategory of esterases that hydrolyze the ester bonds found in lipids, such as those linking the fatty acid moieties of a triacylglycerol or phospholipid to the glycerol backbone. The release of fatty acids from these molecules plays a significant role in both metabolism and intracellular signaling [32]. However, the versatility of the catalytic mechanism gives lipases the ability to catalyze other reactions (Figure 1-2).

Many hydrolases that fall within the esterase functional category also fall into the α/β hydrolase structural category [32,40]. α/β hydrolases are found in every kingdom of life, their similarities potentially arising from common ancestry (homology) although they have no universally recognizable sequence similarity and catalyze many different hydrolysis reactions. The characteristic fold of α/β hydrolases is a single globular domain consisting of a central beta sheet surrounded on both sides by alpha helices (Figure 1-3). The positions of the catalytic triad and oxyanion hole are well conserved, but the α/β hydrolase family contains proteases, epoxide hydrolases, transferases, and various esterases including lipases.

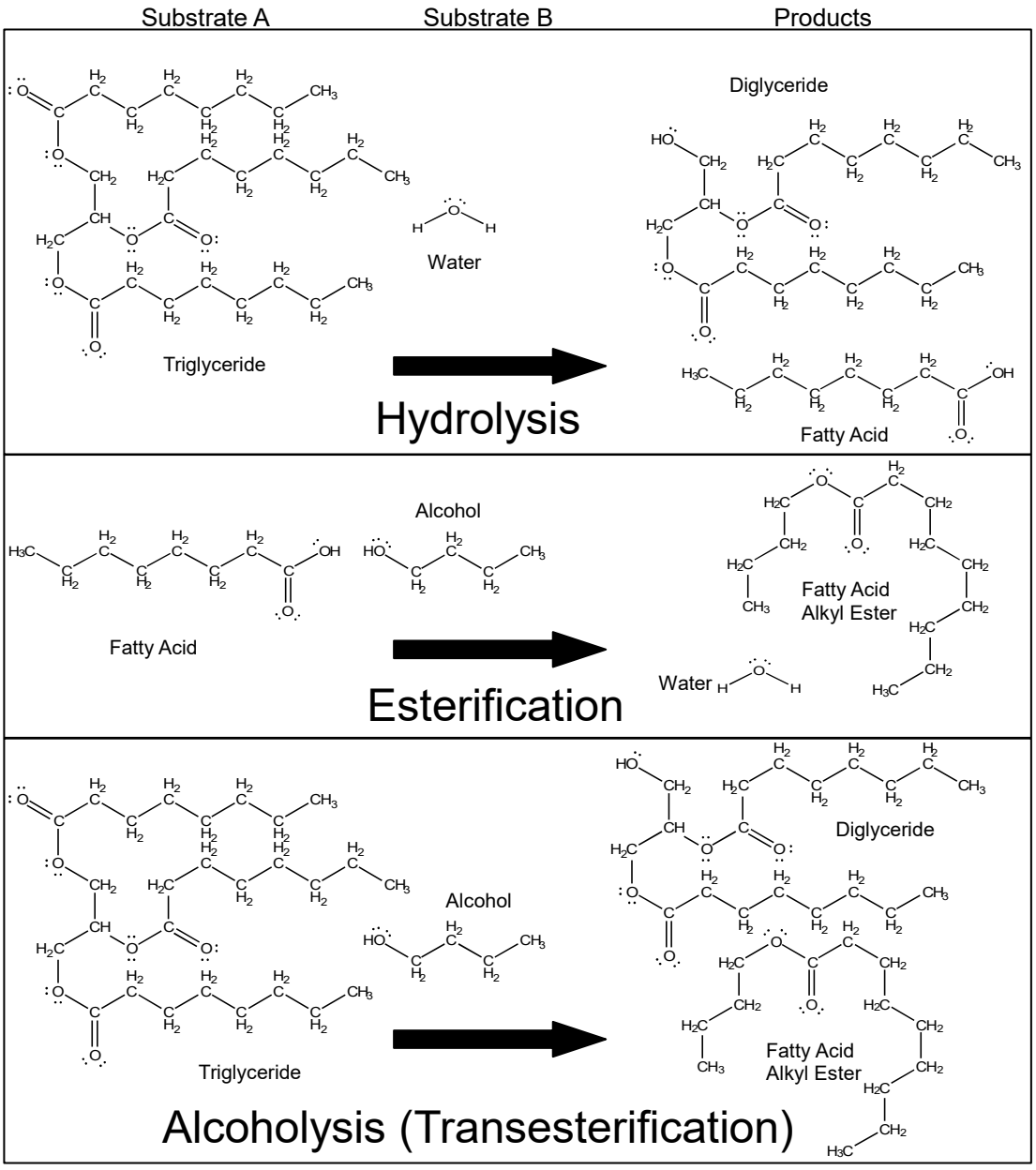

Figure 1-2. Lipase-catalyzed reactions that can lead to biodiesel (fatty acid alkyl ester) synthesis.

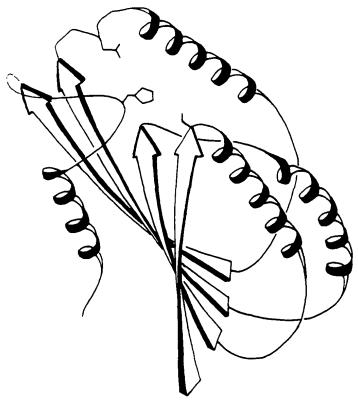

Figure 1-3. The basic architecture of the α/β hydrolase fold, as described by Ollis et. al. in 1992 [40]; members of the superfamily vary with respect to the numbers of surface helices and core strands.

Because the reactions catalyzed by α/β hydrolase lipases using the mechanism previously described occur independently of cofactors such as ATP or NADH they are, in principle, readily reversible [31,52]. An enzyme is traditionally described as catalyzing a single reaction, with the understanding that it may simply be stabilizing the high-energy intermediate between substrate and product, thereby driving a reversible reaction toward equilibrium. Because the chemical components in living systems do not exist at equilibrium, an enzyme often serves to drive a reaction almost solely in one direction *in vivo*, but can drive the reverse reaction *in vitro*. When an α/β esterase that catalyzes a reversible reaction is incubated with an excess of “product” and little “substrate” (that is to say, ester), its activity becomes that of an ester synthase rather than

an esterase. This feature of esterases may be exploited as a potential avenue for the production of alternative fuels.

1.4 Real and Potential Applications of Lipases

Enzymes in the lipase/esterase family are already in use in manufacturing, as they can synthesize organic molecules with high specificity, eliminating the costs associated with separating a desired product from side products that would be produced during synthesis of the desired product by more traditional means [2,52]. Esterases can, under the proper conditions, catalyze the formation of esters. This is presumably due to the fact that they stabilize the transition state between the esterified and hydrolyzed states of the substrate molecules. This catalysis has been observed to occur in fungal and bacterial populations [2,8,14,23,25,33,35,37]. Provided with an overabundance of lipid hydrolysis products, many lipases have been shown to synthesize lipids, often under low-dielectric and aliphatic solvent conditions that are hostile to most non-lipase wild type proteins [4,5,7,16,17,18,20,22,31,43,52]. Optimization of these processes may involve mutation of the wild-type lipase for higher substrate affinity [10], stabilization of the active conformation as with the engineering of the *Thermomyces lanuginosus* lipase to lock the activation “lid” into an open state [48,51], or localization of enzyme and substrate such as the crosslinking of *Staphylococcus haemolyticus* lipase onto magnetic beads [31].

Synthesizing compounds with ester groups under highly non-natural conditions typically involves using organic solvents such as hexane in lieu of water. This drives the hydrolysis/synthesis equilibrium toward the ester form since water molecules are required as hydrolysis substrates. However, catalysis under these conditions fails to obviate the need for organic solvents. Aqueous catalysis of ester synthesis would make the reaction more compatible with earlier steps in biodiesel production. This possibility has been explored and met with some success, but only using large hydrophobic alcohols [9] instead of the more available ethanol. The advantage of this approach is that algal fatty acids and triglycerides are costly to separate from the water in which algae grows; aqueous synthesis of biodiesel molecules may allow for in-culture production rather than post-culture production.

1.5 *Staphylococcus aureus* and Lipase Activity

One instance of lipase/esterase-catalyzed fatty alkyl ester synthesis has been observed in the presence of some (but not all) strains of *Staphylococcus*, in both host abscesses and liquid culture [8,14,23,25,26,33]. Previous research has demonstrated that staphylococcal populations are adversely affected by the presence of free fatty acids in their environment. Although it has previously been hypothesized that the accumulation of the fatty acids was a side effect of bacterial metabolism, more recent work suggests that bactericidal fatty acids are

released by host organisms as a measure of defense against bacterial infection (Figure 1-4). In light of this, it is reasonable to hypothesize that the synthesis of fatty alkyl esters, which do not share free fatty acids' bactericidal properties, may be more than a mere coincidence. Just as the secretion of fatty acids by host species provides a selective advantage by increasing the likelihood of such a host surviving a bacterial infection, the production of enzymes that can reduce the concentration of free fatty acids in a bacterial abscess creates more favorable conditions for the bacterial population, thereby affording a selective advantage to the bacteria. The hypothetical protein responsible for this esterification was dubbed Fatty Acid Modifying Enzyme (FAME, not to be confused with “fatty acid methyl ester,” a form of biodiesel but a subset of the fatty acid alkyl esters; it will not be discussed further herein).

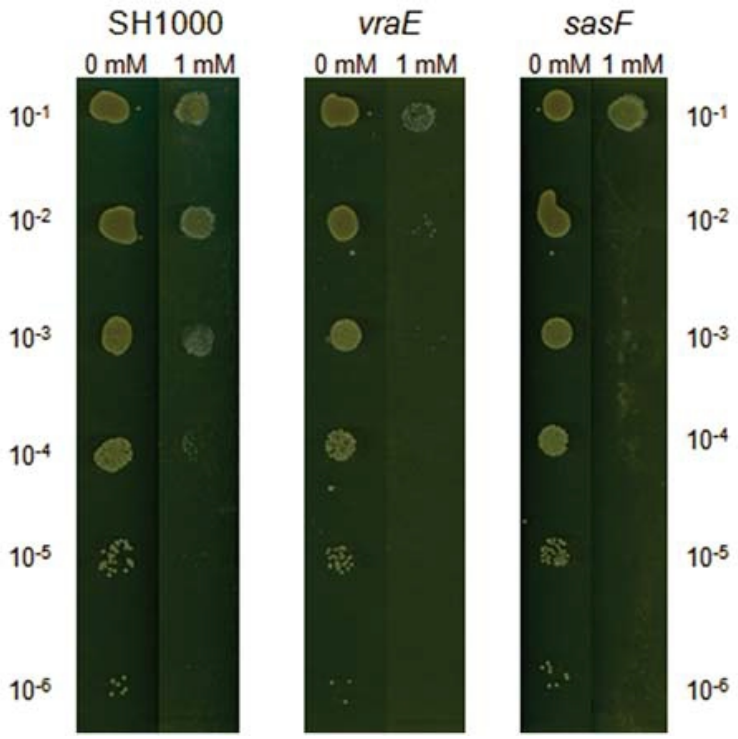

Figure 1-4. Bacterial resistance to environmental free fatty acids, shown by Kenny et. al. with serial dilutions (y-axis) of *Staphylococcus aureus* cultures. Two single-gene mutations in wild type (far left) SH1000 strain *S. aureus* diminish their resistance to 1 mM linoleic acid [26].

With this FAME activity in mind, investigators have determined many of the features of the esterification activity *in vitro*, such as the pH optima of the catalysis as well as the optimal temperature [21]. Previous studies have also shown that the enzyme catalyzes the esterification of free fatty acids to bulky alcohols such as cholesterol better than it catalyzes the esterification of free fatty

acids to small alcohols such as methanol [8]. This is consistent with the hypothesis that the FAME would be adapted to act on the substrate alcohols most commonly available in the environment of a host abscess, where small alcohols are scarce but sterols are available. However, the actual protein responsible for the observed *in vivo* esterification of small alcohols by *Staphylococcus aureus* has not been previously determined.

Staphylococcal genomes encode a number of lipases, but few are secreted lipases. Based on sequence homology and functional similarities, one subset of staphylococcal lipases has come to be grouped into a secreted staphylococcal lipase family [5,15,20,24,34,42,46]. This family is studied for its potential as a source of ester-synthesizing enzymes, and in the process of investigating staphylococcal pathogenesis [45]. As mentioned above, multiple *Staphylococcus aureus* lipases have been shown to catalyze the synthesis of alkyl oleates in hexane. In addition, a *Staphylococcus epidermidis* lipase has been shown to catalyze the synthesis of alkyl oleates in aqueous conditions, but was not shown to act on alcohol substrates smaller than butanol [8]. There appear to be many highly similar enzymes within the secreted staphylococcal lipase family, which differ only slightly from strain to strain and species to species (Figure 1-5). However, they appear to have at least some crucial differences in function.

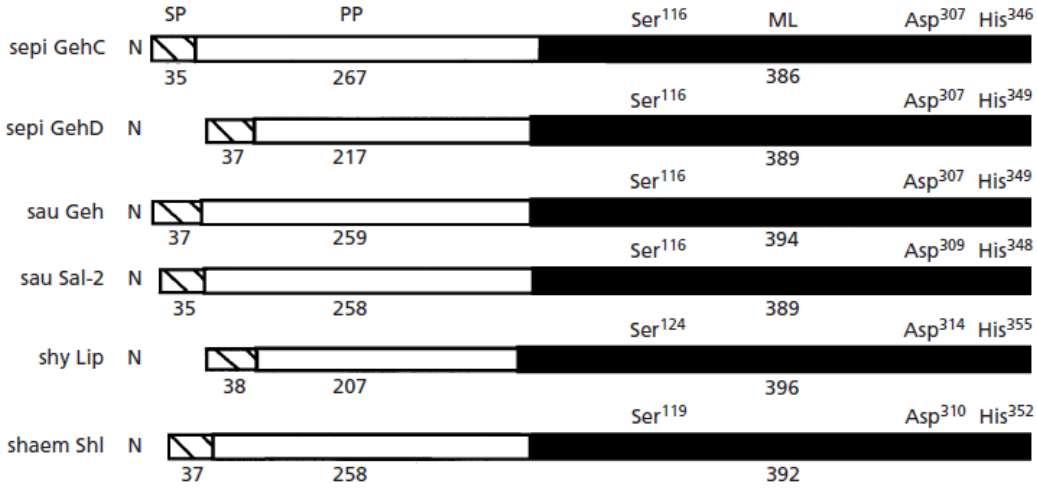

Figure 1-5. Schematic of six secreted staphylococcal lipases. The positions of the catalytic Ser-Asp-His triad are indicated. Dashed lines show the N-terminal secretion signal sequence, the unlined area is the inhibitory pre-protein domain, and the solid black bar is the mature lipase domain with an α/β hydrolase fold in solution [34].

Secreted staphylococcal lipases have not universally been shown to be capable of catalyzing esterification in aqueous media (where substrate availability is kinetically constraining)[35]. Similarly, at least some secreted staphylococcal lipases cannot effectively use small alcohols (methanol and ethanol) as substrates. Members of the family also vary with respect to thermal stability and calcium dependence [21,38,39,42,47]. This variation is significant as literature indicates that not all staphylococcal strains show FAME activity *in vivo*

despite the prevalence of staphylococcal lipases; only some staphylococcal lipases are FAMEs, and the others are not [8,33]. We report, based on mass spectrometric analysis of staphylococcal culture supernatant followed by recombinant expression, that two enzymes secreted by MRSA strains of *Staphylococcus aureus* are capable of fatty acid alkyl ester synthesis, including ethyl ester synthesis in aqueous solutions. These two enzymes are previously partially characterized in their capacity as lipases [5,42]. Although one of them has been used to synthesize esters in an organic solution, it has not previously been shown that both are in fact capable of FAME activity in aqueous solutions. In addition, we have shown that aqueous FAME activity is not a general feature of *S. aureus* lipases, based on GC-MS analysis of another recombinant lipase from *S. aureus*.

1.6 FAME Limitations and Substrate Localization

There are numerous potential approaches that might conceivably be taken to redesign and improve upon a naturally occurring enzyme in an effort to optimize it for biofuel production. One might conceivably, through rational design or the creation of a mutagenized enzyme library, attempt to increase the longevity of the proteins by increasing their thermal stability [9,20,48]. This approach, as well as pH optimization and detergent resistance [21], has been a consideration in previous work with microbial lipases and their applications in

industry. Alternatively, one could use rational design or mutagenesis to attempt to better fit the enzyme's binding site to the specific substrates (or products) intended for use [9,10]. However, there is another consideration for optimization of aqueous reaction conditions. In organic conditions, the rate of ester synthesis can be accelerated to near V_{max} by using very high substrate (fatty acid and alcohol) concentrations. In aqueous conditions, unlike those using hexane or other organic solvents, substrate concentrations have lower concentration maxima. The reasons for this are twofold: the substrates generally have lower solubilities in water than in organic solvents, and the substrates themselves may be less compatible with other components of the system (live algae, for example). One challenge, then, to optimizing FAME activity in aqueous media is to improve substrate binding by the enzyme without recourse to high substrate concentrations. In this case, that would mean attempting to identify the alcohol substrate binding site in the FAME and engineering it in such a way as to better bind smaller molecules.

We originally intended to attempt this latter approach. However, sequence alignment of the FAME enzymes with proteins with structures already modeled on the protein data bank [44] showed that FAME's likely substrate binding sites are deeply recessed within one face of the protein. This fact potentially confounds any attempts to rationally design stable variants with binding pockets with higher affinity for small alcohols, as it would entail the introduction,

modification, or elimination of hydrophobic side chains close to the protein's core.

However, there is an additional consideration in the analysis and alteration of esterase/lipase kinetics. At this point it is worthwhile to consider the effect of co-localization of the critical components of a reaction (substrates and catalyst) within a greater system. Because the various products and substrates of the esterase are hydrophobic to different degrees, they cannot readily remain homogeneously distributed through an aqueous solution. The hydrophobic esters, fatty acids, or bulky alcohols are thermodynamically predisposed to effectively leave the aqueous phase of a system, either by associating with each other or partitioning into an available lipid solvent. *In vivo*, this solvent typically takes the form of a plasma membrane or lipid droplet. The cumulative effect of substrate partitioning and enzyme localization is that the effective concentration of the components of the system at the site of the reaction is greater than the components' concentration in the system as a whole. There is some indication that this phenomenon appears even in the case of highly organic lipase-driven catalysis [18]. Even for moderately soluble alcohols such as butanol, preferential partitioning into a hydrophobic phase will create a greater butanol concentration in the regions of the aqueous phase closest to the hydrophobic phase. In lieu of other protein engineering approaches, it may be possible to enhance overall catalytic activity of FAME by enhancing this localization, effectively increasing the

substrate concentration in the immediate region of the enzyme. We have developed a construct that employs an additional alcohol-binding domain to gain greater effective affinity for small alcohol substrates.

1.7 Rebinding

It has been known for some time that cells modulate certain ligand-receptor signal transduction events by clustering multiple copies of receptor proteins together on cell surfaces [6]. Simple, canonical mathematical models can readily describe the sensitivity of protein-ligand interactions in solution, or when receptor proteins are uniformly distributed around a cell surface. However, for any given receptor protein copy number, there is a meaningful difference in ligand signal response between two states: one in which receptors are uniformly distributed across the surface of the cell, and another in which the receptors are clustered into groups [19]. The cell's sensitivity to molecular signals is sometimes enhanced in the latter case, due to the effect of “rebinding” (Figure 1-6).

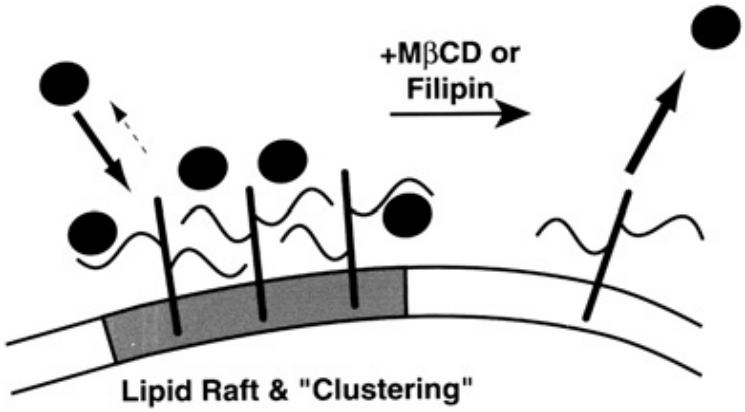

Figure 1-6. Graphical representation of rebinding. When receptors are clustered together (shown on the left), dissociated ligand (black circles) is more likely to rebind before diffusing away, resulting in an equilibrium (the arrows on the left) that favors high ligand concentration near the cluster. MβCD or Filipin disrupts the lipid raft that keeps the receptors clustered together, eliminating the rebinding effect and allowing more ligand to diffuse away (shown on the right) [11].

To explain this, consider a model in which we compare the ligand population in the immediate microenvironment around a cell with the ligand population in the more distant surroundings. A ligand molecule in the microenvironment near its receptor protein cognate can ultimately either bind to the receptor or diffuse away from the microenvironment (in the case of the aforementioned model, this would be away from the cell into the surroundings). However, each additional receptor in the vicinity of the ligand affords an

additional opportunity to bind rather than diffuse away. As a consequence of this, as the number of receptors in the microenvironment increases, the probability that the ligand will remain in the environment rather than enter the surroundings increases. Since the rate at which ligands are entering the microenvironment is proportional to the ligand concentration in the surroundings, and independent of ligand concentration in the immediate microenvironment, the addition of more receptors increases the equilibrium concentration in the microenvironment. In other words, if the rate constant for ligand exiting the microenvironment is reduced but the rate constant for ligand entering the microenvironment remains the same, the equilibrium constant for the two ligand populations is shifted toward a higher proportion of total ligand in the microenvironment. Following observation of this phenomenon *in vivo*, mathematical analysis affirmed this model for the effect of rebinding on ligand sensitivity. Cells have been shown to lose sensitivity *in vitro* to ligand-mediated extracellular signals when receptor clustering is disrupted and receptors are distributed more uniformly across the cell surface [11].

Anticipating the fact that FAME activity is spatially restricted to the area where substrates and catalyst meet (the surfaces of the lipid droplets in the reaction system), we decided to enhance localization of the other substrate (alcohol) to this microenvironment via rebinding. Additional alcohol-binding domains in the vicinity of the lipid droplets and FAME can be anticipated to

increase local alcohol concentration in the same way that receptor protein clustering enhances extracellular signal sensitivity by increasing local ligand concentration. We hypothesized that the best way to exploit this effect in the context of FAME activity was to mutate wild type FAME to append an additional alcohol-binding domain with high alcohol affinity.

1.8 LUSH

In the effort to select a prosthetic alcohol binding domain for the FAME fusion protein, we reviewed the known families of alcohol binding proteins. One might anticipate that human alcohol binding proteins, being naturally more studied than non-human alcohol binding proteins, would offer up an appropriate domain. However, they are generally either enzymes themselves, such as alcohol dehydrogenase, or transmembrane proteins, such as GABA receptors [41,49]. The former group was deemed unsuitable for our purposes because of the potential complications introduced by the catalytic properties of said enzymes. The latter group was deemed unsuitable because of the likelihood that either the presence of the soluble FAME domain or the differences between human and bacterial plasma membranes would interfere with the sensitive folding process attendant to transmembrane domains.

LUSH is a 125 amino acid protein found in the hair-like chemoreceptors that serve as the olfactory organs of *Drosophila melanogaster*. Because insects

have a dramatically different olfactory system, their chemoreceptors are not membrane-associated proteins [28,53]. Instead, insect olfactory chemoreceptors are soluble proteins found in the lymph inside porous hairs (Figure 1-7) on the surface of the animal's body. When airborne molecules dissolve through the pores in the hair into the lymph, and bind their complementary chemoreceptor, the resulting protein-ligand complex becomes complementary to transmembrane receptors found on nearby nerve endings. Binding of the receptor results in signal transduction within the nerve ending.

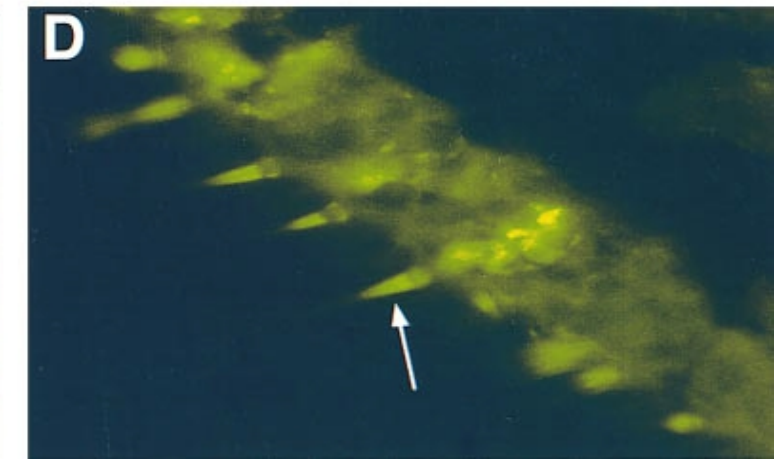

Figure 1-7. LUSH visualized *in vivo* via immunofluorescence. The LUSH is localized to chemosensory hairs [28].

Since 1998, LUSH has been known to be the *Drosophila melanogaster* chemoreceptor responsible for sensing some small alcohols, such as ethanol, propanol, and butanol. LUSH knockout flies display reduced ability to sense

alcohol, thereby losing some of the wild-type's natural avoidance response. Subsequently, LUSH was crystallized in concert with alcohol, showing a 6-helix bundle with a well-defined alcohol binding site within its center [1]. Of particular note is threonine 57, the side chain of which is shown experimentally to be crucial for alcohol binding [50], and computationally to be hydrogen bonded to the ligand's hydroxyl group. The LUSH structure model closely conforms with that of other insect chemoreceptors, such as that for the silkworm pheromone bombykol [29].

We have designed and recombinantly expressed a chimeric fusion protein consisting of the mature domain of the *S. aureus* FAME protein SAUSA300_2603 (also called SAL-1) connected via a short alpha helical linker [3] to the *D. melanogaster* LUSH protein. We have done so with the goal of rationally designing an esterase with a rebinding-derived improvement in its ability to catalyze the formation of fatty acid alkyl esters using small chain alcohols.

1.9 References

[1] L. Ader, D.N.M. Jones, H. Lin, Alcohol Binding to the Odorant Binding Protein LUSH: Multiple Factors Affecting Binding Affinities, Biochemistry 49(29) (2010) 6136–6142.

[2] E. Antonian, Recent advances in the purification, characterization and structure determination of lipases, Lipids. 23 (1988) 1101–1106.

[3] R. Arai, H. Ueda, A. Kitayama, N. Kamiya, Design of the linkers which effectively separate domains of a bifunctional fusion protein, Protein Eng. 14 (2001).

[4] A. Bajaj, P. Lohan, P.N. Jha, R. Mehrotra, Enzymatic Biodiesel production through lipase catalyzed transesterification : An Overview, J. Mol. Catal. B. Enzym. 62 (2010) 9–14.

[5] B. Cadieux, V. Vijayakumaran, M.A. Bernards, M.J. McGavin, D.E. Heinrichs, Role of Lipase from Community-Associated Methicillin-Resistant *Staphylococcus aureus* Strain USA300 in Hydrolyzing Triglycerides into Growth-Inhibitory Free Fatty Acids, J. Bacteriol. 196 (2014) 4044.

[6] B.R. Caré, H.A. Soula, Impact of receptor clustering on ligand binding, BMC Sys. Biol. 5:48 (2011).

[7] G. Carta, J.L. Gainer, A.H. Benton, Enzymatic Synthesis of Esters Using an Immobilized Lipase, (1990).

[8] N.R. Chamberlain, S.A. Brueggemann, Characterisation and expression of fatty acid modifying enzyme produced by *Staphylococcus epidermidis*, J. Med. Microbiol. 46 (1997) 693–697.

[9] R.C. Chang, S.J. Chou, J.F. Shaw, Synthesis of fatty acid esters by recombinant *Staphylococcus epidermidis* lipases in aqueous environment, J. Agric. Food Chem. 49 (2001) 2619–2622.

[10] R. Chang, J.C. Chen, J. Shaw, Studying the Active Site Pocket of *Staphylococcus hyicus* Lipase by Site-Directed Mutagenesis, Biochem. Biophys. Res. Commun. 10 (1996) 6–10.

[11] C.L. Chu, J.A. Buczek-Thomas, M. a Nugent, Heparan sulphate proteoglycans modulate fibroblast growth factor-2 binding through a lipid raft-mediated mechanism., Biochem. J. 379 (2004) 331–341.

[12] S.V. Iersel, L. Gamba, A. Rossi, S. Alberici, B. Dehue, J.V.D. Staiij, A. Flammini, “ALGAE-BASED BIOFUELS” AquaticBiofuels, Food and Agriculture Division of the United Nations. (2009) http://www.fao.org/bioenergy/aquaticbiofuels/documents/detail/en/?uid=20824

[13] G.A. Dunstan, J.K. Volkman, S.M. Barrett, C.D. Garland, Changes in the lipid composition and maximisation of the polyunsaturated fatty acid content of three microalgae grown in mass culture, J. appl. phyco. 5 (1993) 71–83.

[14] E.S. Dyet, F.A. Kapral, Partial Characterization of a Bactericidal System in Staphylococcal Abscesses, Infection and Immunity 30 (1980) 198–203.

[15] A.M. Farrell, T.J. Foster, K.T. Holland, Molecular analysis and expression of the lipase of *Staphylococcus epidermidis*., J. Gen. Microbiol. 139 (1993) 267–277.

[16] A.D. Ferrão-Gonzales, I.C. Véras, F. a L. Silva, H.M. Alvarez, V.H. Moreau, Thermodynamic analysis of the kinetics reactions of the production of FAME and FAEE using Novozyme 435 as catalyst, Fuel Process. Technol. 92 (2011) 1007–1011.

[17] N.S. Gandhi, S.B. Sawant, J.B. Joshi, Specificity of a lipase in ester synthesis : Effect of Alcohol, Biotechnol. Prog. 11 (1995) 282–287.

[18] H. Ghamgui, M. Karra-Chaâbouni, Y. Gargouri, 1-Butyl oleate synthesis by immobilized lipase from *Rhizopus oryzae*: A comparative study between n-hexane and solvent-free system, Enzyme Microb. Technol. 35 (2004) 355–363.

[19] M. Gopalakrishnan, K. Forsten-Williams, M. a Nugent, U.C. Täuber, Effects of Receptor Clustering on Ligand Dissociation Kinetics: Theory and Simulations, Biophys. J. 89 (2005) 3686–3700.

[20] H. Horchani, I. Aissa, S. Ouertani, Z. Zarai, Y. Gargouri, A. Sayari, Journal of Molecular Catalysis B : Enzymatic Staphylococcal lipases : Biotechnological applications, J. Mol. Catal. B, Enzym. 76 (2012) 125–132.

[21] H. Horchani, H. Mosbah, N. Ben Salem, Y. Gargouri, A. Sayari, Biochemical and molecular characterisation of a thermoactive, alkaline and detergent-stable lipase from a newly isolated *Staphylococcus aureus* strain, J. Mol. Catal. B Enzym. 56 (2009) 237–245.

[22] H. Horchani, S. Ouertani, Y. Gargouri, A. Sayari, The N-terminal His-tag and the recombination process affect the biochemical properties of *Staphylococcus aureus* lipase produced in Escherichia coli, J. Mol. Catal. B Enzym. 61 (2009) 194–201.

[23] C. Hu, N. Xiong, Y. Zhang, S. Rayner, S. Chen, Biochemical and Biophysical Research Communications Functional characterization of lipase in the pathogenesis of *Staphylococcus aureus*, Biochem. Biophys. Res. Commun. 419 (2012) 617–620.

[24] W.O.O. Hyuk, H. Kim, C. Lee, T. Oh, Biochemical Properties and Substrate Specificity of Lipase from *Staphylococcus aureus* B56, J. Microbiol. Biotechnol. 12 (2002) 25–30.

[25] J. V Karabinos, H.J. Ferlin, Bactericidal Activity of Certain Fatty Acids, J. Am. Oil Chem. Soc. 31 (1954) 228.

[26] J.G. Kenny, D. Ward, E. Josefsson, I.M. Jonsson, J. Hinds, H.H. Rees, J. a. Lindsay, A. Tarkowski, M.J. Horsburgh, The *Staphylococcus aureus* response to unsaturated long chain free fatty acids: Survival mechanisms and virulence implications, PLoS One. 4 (2009).

[27] E.K. Kim, W.H. Jang, Jung Ho Ko, Jong Seok Kang, Moon Jong Noh, O.J. Yoo, Lipase and its modulator from Pseudomonas sp. strain KFCC 10818: Proline-to-glutamine substitution at position 112 induces formation of enzymatically active lipase in the absence of the modulator, J. Bacteriol. 183 (2001) 5937–5941.

[28] M. Kim, A. Repp, D.P. Smith, LUSH Odorant-Binding Protein Mediates Chemosensory Responses to Alcohols in *Drosophila melanogaster*, Genetics 150 (1998) 711-721.

[29] S.W. Kruse, R. Zhao, D.P. Smith, D.N.M. Jones, Structure of a specific alcohol-binding site defined by the odorant binding protein LUSH from *Drosophila melanogaster*, Nat. Struct. Biol. 10 (2003) 694–700.

[30] V. Kukreja, M.B. Bera, Lipase from *Pseudomonas aeruginosa* MTCC 2488: Partial purification, characterization and calcium dependent thermostability, Indian J. Biotechnol. 4 (2005) 222–226.

[31] K.P. Lee, H.K. Kim, Enzymatic Transesterification reaction using *Staphylococcus haemolyticus* L62 lipase crosslinked on magnetic microparticles, Journal Mol. Catal. B, Enzym. 115 (2015) 76–82.

[32] N. Lenfant, T. Hotelier, Y. Bourne, P. Marchot, A. Chatonnet, Chemico-Biological Interactions Proteins with an alpha / beta hydrolase fold : Relationships between subfamilies in an ever-growing superfamily, Chem. Biol. Interact. 203 (2013) 266–268.

[33] J.P. Long, J. Hart, W. Albers, F. a. Kapral, The production of fatty acid modifying enzyme (FAME) and lipase by various staphylococcal species, J. Med. Microbiol. 37 (1992) 232–234.

[34] C.M. Longshaw, A.M. Farrell, J.D. Wright, K.T. Holland, Identification of a second lipase gene , gehD , in *Staphylococcus epidermidis* : comparison of sequence with those of other staphylococcal lipases, Microbiology 146 (2000) 1419–1427.

[35] T. Lu, J.Y. Park, K. Parnell, L.K. Fox, Characterization of fatty acid modifying enzyme activity in staphylococcal mastitis isolates and other bacteria, BMC Research Notes 5 (2012) 323.

[36] M. Mitta, M. Miyagi, I. Kato, S. Tsunasawa, Identification of the Catalytic Triad Residues of Porcine Liver Acylamino Acid-Releasing Enzyme, J. Biochem. 123 (1998) 924–931.

[37] J.E. Mortensen, T.R. Shryock, F. a. Kapral, Modification of bactericidal fatty acids by an enzyme of *Staphylococcus aureus*, J. Med. Microbiol. 36 (1992) 293–298.

[38] K. Nikoleit, R. Rosenstein, H.M. Verheij, F. Gotz, Comparative biochemical and molecular analysis of the *Staphylococcus hyicus*, *Staphylococcus*

aureus and a hybrid lipase. Indication for a C-terminal phospholipase domain, Eur. J. Biochem. 228 (1995) 732–738.

[39] B.-C. Oh, H.K. Kim, J.-K. Lee, S.-C. Kang, T.-K. Oh, *Staphylococcus haemolyticus* lipase : biochemical properties , substrate specificity and gene cloning, FEMS Microbiology Letters 179 (1999) 385-392.

[40] D.L. Ollis, E. Cheah, M. Cygler, B. Dijkstra, The α/β hydrolase fold, Protein Engineering 5 (1992) 197-211.

[41] S.M. Paul, Alcohol-sensitive GABA receptors and alcohol antagonists., Proc. Natl. Acad. Sci. U.S.A. 103 (2006) 8307–8308.

[42] R. Rosenstein; F. Götz, Staphylococcal lipases: Biochemical and molecular characterization, Biochimie. (2000) 1005–1014.

[43] S. Ramamurthi, A.R. McCurdy, Lipase-Catalyzed Esterification of Oleic Acid and Methanol in Hexane - A Kinetic Study, Jaocs. 71 (1994) 927–930.

[44] S. Ransac, M. Blaauw, B.W. Dijkstra, a T. Slotboom, J.W. Boots, H.M. Verheij, Crystallization and preliminary X-ray analysis of a lipase from *Staphylococcus hyicus*, J. Struct. Biol. 114 (1995) 153–155.

[45] J. Rollof, S.A. Hedstrom, P. Nilsson-Ehle, Positional specificity and substrate preference of purified *Staphylococcus aureus* lipase, Biochim. Biophys. Acta 921 (1987) 370–377.

[46] A.B. Salleh, R.N.Z.R.A. Rahman, M. Basri, New Lipases and Proteases, Nova Science Publishers, New York, 2006.

[47] J.W.F. a Simons, M.D. Van Kampen, I. Ubarretxena-Belandia, R.C. Cox, C.M. Alves Dos Santos, M.R. Egmond, H.M. Verheij, Identification of a calcium binding site in *Staphylococcus hyicus* lipase: Generation of calcium-independent variants, Biochemistry. 38 (1999) 2–10.

[48] J. Skjold-Jørgensen, J. Vind, A. Svendsen, M.J. Bjerrum, Altering the activation mechanism in *Thermomyces lanuginosus* lipase, Biochemistry. 53 (2014) 4152–4160.

[49] S. Svensson, P. Strömberg, T. Sandalova, J. Höög, Class II alcohol dehydrogenase (ADH2)--adding the structure., Chem. Biol. Interact. 130-132 (2001) 339–350.

[50] A.B. Thode, S.W. Kruse, J.C. Nix, D.N.M. Jones, The role of multiple hydrogen bonding groups in specific alcohol binding sites in proteins: Insights from structural studies of LUSH, J Mol Biol. 376 (2008) 1360–1376.

[51] R. Verger, “Interfacial activation” of lipases: Facts and artifacts, Trends Biotechnol. 15 (1997) 32–38.

[52] A.R.M. Yahya, W. a Anderson, M. Moo-young, C. a L. Sp, Ester synthesis in lipase- catalyzed reactions, Enzym. Microb. Biotechnol. 23 (1998) 438–450.

[53] J.J. Zhou, G.A. Zhang, W. Huang, M. a. Birkett, L.M. Field, J. a. Pickett, P. Pelosi, Revisiting the odorant-binding protein LUSH of *Drosophila melanogaster*: Evidence for odour recognition and discrimination, FEBS Lett. 558 (2004) 23–26.

[54] Fuel Comparison Chart, Alternative Fuels Data Center, US Department of Energy (2014) http://www.afdc.energy.gov/fuels/

Chapter II

Materials and Methods

2.1 Introduction

Although it has been known for some time that FAME (fatty acid modifying enzyme) activity is detectable in staphylococcal culture supernatant [7,8], it has not been conclusively attributed to a specific element of the staphylococcal proteome before now. As we later determined and discuss in chapter III, FAME activity is (unsurprisingly) attributable to a pair of highly similar lipase enzymes in the secretome of *Staphylococcus aureus*. We have determined this via size-exclusion fractionation of staphylococcal culture supernatant followed by para-nitrophenyl acetate (NPA) assaying of lipase activity and GC-MS analysis of FAME enzyme production. Additionally, FAME activity was gauged by observing the clearance of fatty acid droplets from solution (a decrease in turbidity) over time in solutions containing FAME-candidate proteins. Following identification and recombinant expression of FAME enzymes in *Escherichia coli*, we used PCR to engineer variants of one of the two FAME enzymes (SAUSA300_2603/SAL-1) chimerically linked to the *Drosophila melanogaster* alcohol-binding protein LUSH [11]. 8-anilino-1-naphthalene-sulfonic acid (ANS) fluorescence titration was used to compare the ethanol affinities of the two fusion variants to each other and to the wild type FAME.

2.2. Reagents

Butanol and para-nitrophenyl acetate were purchased from Acros Organics. Enzymes and enzyme buffers were purchased from New England Biolabs. 8-anilino-1-naphthalene-sulfonic acid was purchased from MP Biomedicals. All other reagents were purchased from Fisher Scientific.

2.3 Instrumentation

PCR and endonuclease reactions were performed using an MJ Research PTC-200 thermocycler. Sonication was done with a Fisher 550 Sonic Dismembrator. Culture supernatant was fractionated on an Amersham Biosciences AKTA FPLC system with an Amersham Biosciences HiLoad 26/60 Superdex size exclusion column. GC-MS was performed with an Agilent Saturn 2000 mass spectrometer system. UV-visible spectrophotometry was performed with a Thermo Scientific Nanodrop 2000c for DNA and protein concentration quantification, and a Varian Cary 50 Bio system for all other spectrophotometry needs. The fluorescence titration assay was done with a Tecan Infinite M200 plate reader. The dynamic light scattering measurement of oleic acid droplet radius was performed with a Wyatt Technologies DynaPro nanostar.

2.4 *Staphylococcus aureus* Cultures

The laboratory of Dr. Kelly Doran in the biology department of San Diego State University generously gave us access to their stock of *Staphylococcus aureus* strains, as well as facilities of the appropriate biosafety level in which to grow staphylococcal cells. On the basis of strain availability and previous literature, we chose the MRSA strains Newman, USA300, ISP 479C, and SA113 to use for this phase of the experimentation. Cells from glycerol stocks frozen at -80º Celsius were inoculated into 50 milliliters of liquid culture media. For this phase of the experiments, we used both Luria-Bertani (LB) culture broth (made as 1% Sodium Chloride, 1% tryptone, and 0.5% yeast extract) and 3% tryptic soy broth (TSB). Although we typically use LB media for cell culture, previous work related to FAME activity in staphylococcal culture supernatant was done with TSB; therefore we chose to test FAME activity under both conditions. In principle, the two media should support very similar behaviors and protein expression profiles in *S. aureus*, since they differ in the source of their digested proteins (yeast and milk for LB, soy for TSB), but those proteins are all processed into small peptides by trypsin digestion.

The inoculated cells were grown overnight in a shaker at 37º Celsius, and cell density was measured as light absorbance at 600 nanometers. culture supernatant was harvested by centrifugation of the culture at 3000 g for 30

minutes. The cell pellet was discarded and the supernatant was syringe filtered using a non-protein binding 0.45 micron nitrocellulose filter.

2.5 GC-MS Method of FAME Activity Assessment

Although more recently developed strategies, such as sodium hydroxide titration of residual fatty acid, have been successfully used to quantify organic-phase esterification, aqueous esterification assays are performed at very low reactant and product concentrations due to the low solubilities of fatty acids and fatty acid alkyl esters in water. The oldest assay for aqueous FAME activity, developed by Mortensen et. al. [8], consists of detecting radiolabeled fatty acid alkyl ester using a scintillation counter. However, Long et. al. [7] developed a simpler assay by measuring fatty acid alkyl esters in organic phase extracts of the reaction system on a GC-MS system. We opted for the latter approach. Briefly, the reaction systems consisted of 700 microliters of 100 millimolar sodium phosphate at pH 6.0, 250 microliters of filtered culture supernatant (diluted with phosphate buffer as necessary to ensure that each system corresponded to the same number of cells using the A600 measurements taken previously), and 50 microliters of substrate (5 mg/mL oleic acid dissolved in alcohol). Initially, 1-butanol was used as the alcohol substrate for identification of the FAMEs, but ethanol was used once the FAMEs had been recombinantly expressed. Oleic acid was used as the fatty acid substrate in all cases; it is the

fatty acid used in the assay as it is previously published, and other fatty acids are less well behaved in the reaction system with respect to their solubilities. The systems were allowed to incubate at 37º Celsius for 24 hours, and then immediately subjected to extraction of organic components twice with one volume of hexane. Hexane extracts were loaded onto an Agilent Saturn 2000 GC-FID-MS system and analyzed for the presence of fatty acid alkyl esters. Negligible amounts of fatty acid alkyl esters were found in the negative controls, where buffer was substituted for culture supernatant filtrate, and when the substrate alcohols were absent. Butyl oleate (maximum m/z = 338) was found to have been synthesized in the presence of culture supernatant filtrate from *S. aureus* cultures of the Newman and USA300 strains, but not in the presence of supernatant filtrates from ISP or SA113 cultures. Interestingly, both of the FAME-positive strains showed greater FAME activity when the cultures were grown in TSB than when they were grown in LB.

2.6 *S. aureus* Culture Fractionation and LC-MS Sequencing

Following confirmation of our ability to reproduce GC-MS detectable levels of FAME activity with *S. aureus* culture supernatant, we undertook an effort to isolate the protein responsible for fame activity. A UPC-900 and P-920 AKTA FPLC fitted with a GE HiLoad Superdex 200 26/60 size exclusion column. Filtered supernatant from USA300 S. aureus grown in TSB as described above

was concentrated using Amicon Ultra centrifugal filter units with a 10,000 dalton molecular weight cutoff. The concentrated supernatant was loaded onto the FPLC system and flowed through the column at a rate of 1.00 milliliter per minute, using the aforementioned pH 6.0 sodium phosphate buffer. Fractions were collected every 15 milliliters after the void volume. Due to the abundance of protein and media components in the concentrated supernatant, discrete peaks were not resolvable when the eluent was monitored for absorbance at 280 nanometers.

2.7 Cloning of NWMN_0624, NWMN_2434, SAUSA300_2518, SAUSA300_0320, and SAUSA300_2603

Three proteins found in the FAME-positive SEC eluent fraction were selected for recombinant expression and analysis. In the published genome of USA 300 *S. aureus* [4], the three proteins (and corresponding genes) are referred to as SAUSA300_2518, SAUSA300_0320, and SAUSA300_2603. These three are hereafter referred to as the “Isolated” proteins because they were selected as FAME candidates based on their isolation from *S. aureus* culture supernatant.

Cell cultures grown as described above were collected in 1 milliliter aliquots, centrifuged to pellet the cells (after which culture supernatant was

discarded), and used as a source of template DNA in PCR using the following recipe:

In 50 microliters:

1. Template DNA (a cell pellet or 1 microliter of DNA template solution)
2. 2 units of *Pfu* DNA polymerase (Pfusion from Fermentas or NEB)
3. 2 microliters of 25 millimolar dNTPs
4. 10 microliters of 5x Pfusion HF buffer (components are proprietary, 1.5 millimolar magnesium)
5. Oligonucleotide primers from IDT DNA, 2 microliters of 25 micromolar DNA each

And the following PCR program:

1. 98 °C for 30 seconds
2. T+3 °C for 30 seconds, where T = the melting temperature of the lower-melting DNA primer, as reported by IDT DNA
3. 72 °C for 90 seconds
4. Repeat steps 2 and 3 35 times
5. 72 °C for 10 minutes
6. Cool to 4 °C

Each primer pair was designed to anneal to the ends of the sequences for the mature forms of their corresponding proteins, adding an Nco1 endonuclease cut site to the 5' end of the gene and an Xho1 cut site to the 3' end. This was done

so that the expression product could be anticipated to be the mature form of the protein in each case.

SAUSA300_0320 5': GCGATCCGGCATATGGCGAATCAA

SAUSA300_0320 3': TGCGGGCCTCGAGTTAACTTGCTTT

SAUSA300_2603 5': CGGCGATGGATAAAGATGATCAAACG

SAUSA300_2603 3': AGGGCCCTCGAGTTATGCTTGCTT

SAUSA300_2518 5': CAACGTGTCGGCCACCCATGGAAACTTTAG

SAUSA300_2518 3':

GCGTACCCGGGCTCGAGTTATTAACCCCACATATTTAATAATAC

PCR product was purified using Zymogen or Macherey-Nagel DNA recovery kits according to the protocols in their manuals [3].

Production of PCR product was evaluated by loading 2 microliters of PCR product, brought to 1x loading dye concentration with 6x Fermentas DNA loading dye, into 1% agarose gels buffered with Tris-acetate-EDTA and containing 0.5-2 micrograms per milliliter ethidium bromide. Application of 115 volts for 45 minutes and examination under ultraviolet light showed unsatisfactory PCR results. Substitution of Newman *S. aureus* cells as a source of template DNA resolved this difficulty. The Newman homologs of the three proteins have identical primary sequences within the regions that we cloned.

We selected the pET bacterial expression system for this project [1], based on availability, high protein yield, and predicted compatibility with the

expression products. One common class of antibiotic is the β-lactam family, which are suicide inhibitors of the vital enzymes that remodel the peptidoglycans of the bacterial outer membrane. Members of the pET plasmid family feature β-lactamase genes, the protein products of which confer resistance to β-lactam antibiotics by hydrolyzing β-lactam antibiotics in the growth medium into non-bactericidal compounds. Additionally, pET vectors utilize the the T7 expression system with the *lac* operon for protein expression. The *lac* operon, found in nature as the portion of the genome responsible for bacterial response to local lactose availability, is notable for the strong *lac* repressor binding site that impairs expression of downstream genes in the absence of allolactose. Upon allolactose binding, the repressors dissociate from the repressor site, allowing protein expression. The promoter sequence for the downstream gene in a pET vector is tailored to complement T7 DNA polymerase, a high-output polymerase originally found in T7 bacteriophage. pET22b, specifically, includes a “signal sequence” between the start codon and the gene insert that (in *E. coli*) directs the nascent polypeptide through the inner membrane into the periplasmic space via the SecY transport pathway (Figure 2-1). Additionally, it includes six optional codons for a hexahistidine tag at the C-terminus of the protein product, intended for nickel affinity chromatography during purification.

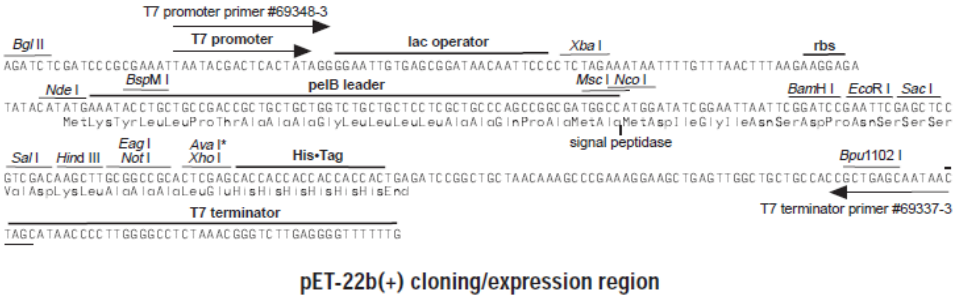

Figure 2-1. The expression region of the pET22b(+) plasmid. We used Nco1 and Xho1 as our restriction endonucleases for insertion of the gene constructs, effectively appending the pelB leader sequence to the 5' end of the genes. Note that a stop codon was incorporated into the 3' end of the PCR product, excluding the vector's hexahistidine tag sequence from the open reading frame [1].

Following amplification, the genes and a pET22b stock solution were cut by incubating them with restriction endonucleases:

In each 50 microliter sample:

1. 5 microliters 10x Fastdigest green buffer (Fermentas)
2. 1 microliter (20 units) each of Xho1 and Nco1(Fermentas, NEB)
3. 43 microliters PCR product or pET22b (1-2 micrograms DNA)

Each sample was incubated at 37 °C for 3 hours. In the case of the plasmid samples, 1 microliter of calf intestinal alkaline phosphatase (Fermentas, 20 units) was added after 2 hours to prevent re-closure of partially restricted plasmids. Re-

closure of partially restricted plasmids causes false positives in the initial transformation screening step.

Cut PCR product (insert) and pET22b (vector) were combined in varying (between 5:1 and 30:1) mole ratios and ligated:

In each 20 microliter sample:

1. 2 microliters 10x T4 DNA ligase buffer (NEB)
2. 1 microliter (400 units) T4 DNA ligase (NEB, Fermentas)
3. 2 microliters of cut vector
4. 2, 6, or 12 microliters of cut insert
5. Water to 20 microliters

Each sample was incubated at 25 °C for 3 hours and then transformed into competent Top10 *E. coli* cells; the cells were rendered chemically competent as described here.

Escherichia coli cells of the strains Top10 and BL21 were made chemically competent. Colonies were inoculated into 50 milliliters of LB media and grown at 37 °C for 8 hours. The cell cultures were centrifuged at 3000 g for 10 minutes and the supernatant discarded. The cell pellets were gently resuspended in 50 milliliters ice-cold 0.1 molar magnesium chloride and centrifuged again. The cell pellet was resuspended in 10 milliliters 0.1 molar calcium chloride, with 15% v/v glycerol. This stock solution was divided into 50 microliter aliquots and stored at -80 °C.

Top10 *E. coli* are a K12 (non-pathogenic family of laboratory *Escherichia coli* strains) strain optimized for plasmid copy number, making them ideal for replication of synthesized plasmids. The chemically competent Top10 cells were transformed with the ligation products described above. Two microliters of each ligation sample was added to its own competent cell aliquot. The tubes were allowed to sit on ice for 5 minutes and then heat shocked at 42 °C for 1 minute. Following another 5 minute recovery on ice, 200 microliters of LB media was added to each tube, and then the cells were allowed to recover at 37 °C for 45 minutes. Following this, 200 microliters of each cell culture was plated onto LB-agar dishes with 200 micrograms per milliliter ampicillin (a β-lactam antibiotic), and allowed to grow at 37 °C overnight. Colonies from these plates were picked and grown overnight again at 37 °C in 10 milliliters of liquid LB and 200 micrograms per milliliter ampicillin. Following this growth, the cell cultures were subject to plasmid purification using Zymogen or Macherey-Nagel plasmid recovery kits according to the protocols in their manuals [9]. The plasmid stock solutions were checked for insert DNA by using them as template DNA in another round of the PCR described above. Plasmid stocks that could template PCR product the same size (based on electrophoretic mobility in an agarose gel) as insert DNA were then submitted to Retrogen for sequencing and verified to be the appropriate DNA sequences.

In addition to the three genes mentioned above, we chose two other "Selected" genes from the *S. aureu*s (Newman strain) genome [2] based on their sequence features. Both NWMN_0624 and NWMN_2434 (the putative protein products) feature transport signal sequences in their N-terminal regions; we predicted that the FAME genes would contain this element due to the fact that FAME activity is found in culture supernatant rather than being confined to *S. aureus* cytoplasm. Additionally, we selected for genes that did not correspond to already-characterized proteins. Both NWMN_0624 and NWMN_2434 are not well studied but are putative hydrolases based on sequence alignments. *NWMN_0624* and *NWMN_2434* were amplified and transformed into plasmid vectors. *NWMN_2434* was ligated into pET22b as described above. *NWMN_0624* did not readily ligate into pET22b, but was instead ligated into pET21d, another pET vector [1]; pET21d lacks the pelB leader sequence, resulting in cytoplasmic expression of the gene insert rather than pET22b's periplasmic expression.

2.8 Recombinant Expression of FAME Proteins

Plasmids containing the genes for the mature forms of NWMN_0624, NWMN_2434, SAUSA300_0320, SAUSA300_2603, and SAUSA300_2518 were transformed into chemically competent BL21 (DE3) *E. coli* cells as described in 2.3.4. BL21 (DE3) is another K12 *E. coli* strain, with a lower plasmid copy

number (rendering them less suitable for plasmid production) than Top10, but one that expresses the T7 DNA polymerase, making it a superior strain for protein expression with the T7 expression system originally sourced from the T7 bacteriophage. After incubating at 37 °C on LB-agar-200 micrograms/mL ampicillin culture dishes, colonies were picked and separately inoculated into flasks of 50 mL liquid LB with 200 micrograms/mL ampicillin. Once the cells had multiplied to an optical density of 0.4-0.6 at a wavelength of 600 nm, the cell population was judged to be sufficiently large for induction of recombinant gene expression. At this point, 1 M Isopropyl β-D-1-thiogalactopyranoside (IPTG) stock solution was added at a ratio of 1:1000 to result in a 1 mM IPTG concentration of the cell culture. IPTG is an allolactose analog that binds lac repressor proteins, causing their dissociation from the *lac* repressor site, leading to recombinant protein expression. It is used in lieu of allolactose because it does not serve as a metabolic resource. Allolactose, the native protein ligand, is less suitable from an analytical standpoint because the availability of additional resources to an induced cell culture introduces an additional unwanted variable in comparison to a non-induced control culture.

After 3 additional hours of growth at 37 °C, the cell cultures were collected in 50 mL polypropylene conical tubes and centrifuged at 3000 g for 15 minutes. Cell pellets were resuspended in 10 mL of 50 mM Bis-Tris at pH 6.0. Resuspended pellets were then sonicated with 20 pulses lasting 15 seconds

each, separated by 30 second intervals on ice to prevent protein precipitation. After centrifugation at 3000 g for 30 minutes and separation of the cell debris pellet, expression of the proteins was verified with SDS-PAGE (Figure 2-2).

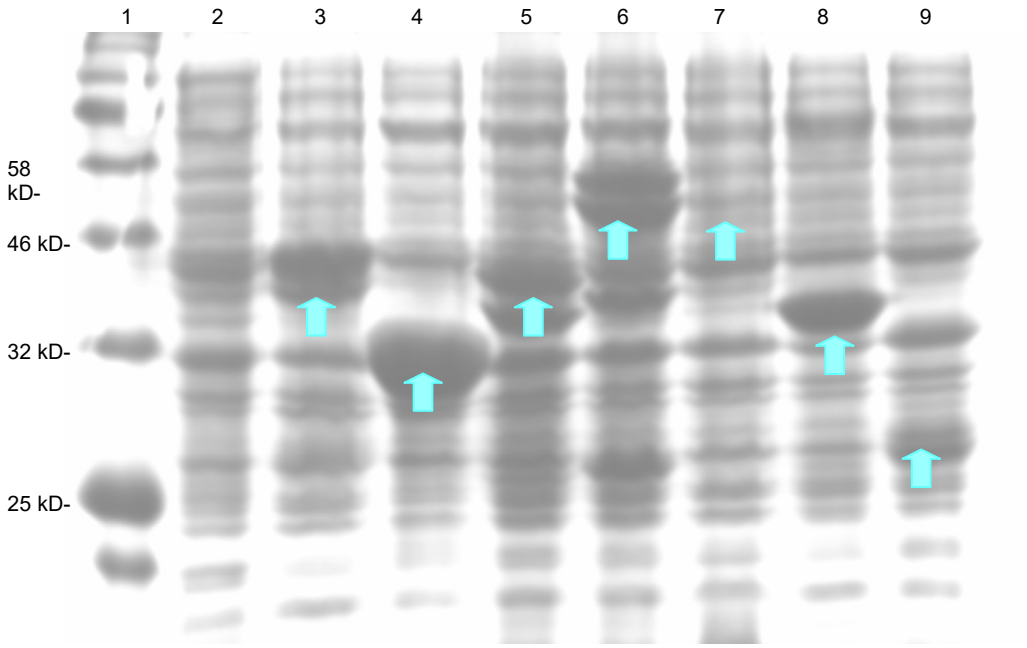

Figure 2-2. SDS-PAGE evaluation of recombinant protein expression. Lane 1: New England Biolabs molecular weight marker. Lane 2: non-induced *E. coli*. Lane 3: SAUSA300_0320. Lane 4: SAUSA300_2518. Lane 5: SAUSA300_2603. Lane 6: SAUSA300_2603-LUSH fusion. Lane 7: SAUSA300_2603-LUSH-T57A variant (low expression). Lane 8: SAUSA300_0641/NWMN_0624. Lane 9: SAUSA300_2473/NWMN_2434 (low expression).

2.9 Assaying of the "Selected" Proteins

In the earliest phase of our screening process for the recombinant proteins, NWMN_0624 and NWMN_2434 solutions from 2.3.5 were used in place of culture supernatant to prepare samples for the FAME assay described in 2.3.2:

1. 700 µL 100 mM sodium phosphate, pH 6.0
2. 250 µL filtered culture supernatant
3. 50 µL methanol containing 5 mg/mL palmitic(hexadecanoic) acid or 13.6 mg/mL caprylic(octanoic) acid

This system was incubated overnight at 37º C and extracted into one volume of hexane.

Initially, the hexane extract was assayed with a Hewlett Packard HP 6890 GC-FID. Although the FID showed peaks resembling the predicted butyl oleate, subsequent GC-MS analysis of these extracts using the Saturn 2000 revealed that the column eluent in question was trace free fatty acid (the intended substrate) rather than esters (the intended product).

2.10 NPA Assaying of Recombinant Isolated Proteins

Lipase activity is often assessed using 4-nitrophenol derivatives [10]. In its acidic form, 4-nitrophenol (also known as para-nitrophenol or p-nitrophenol) absorbs light at 405 nm with an extinction coefficient of 18000 M^{-1} cm^{-1}. Lipases

hydrolyze the ester bond in esters of p-nitrophenol and carboxylic acids, yielding free p-nitrophenol and causing a corresponding increase in A405, notable as a yellow coloration to the solution (Figure 2-3). Using the smallest and most soluble of these compounds, p-nitrophenyl acetate (NPA), we assayed the crude *E. coli* lysate for lipase activity.

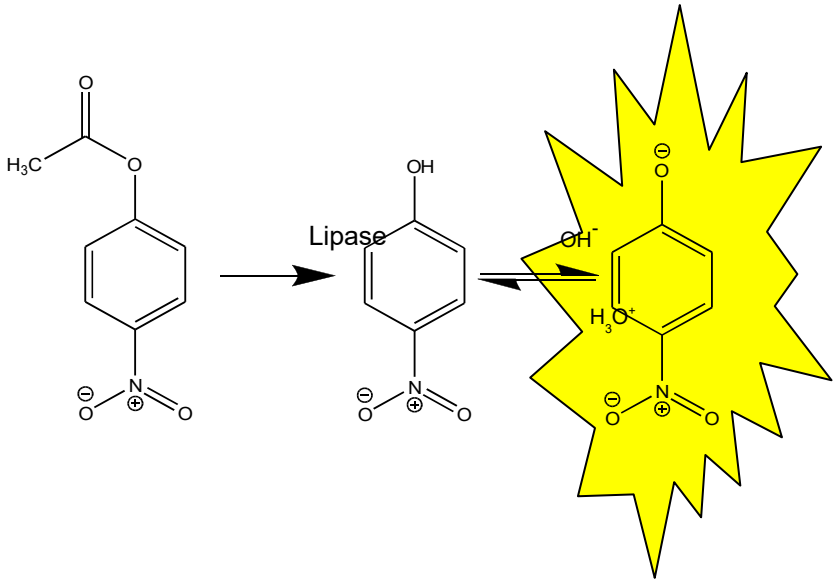

Figure 2-3. Nitrophenyl acetate assay for lipase activity. P-nitrophenyl acetate (left) is hydrolyzed by lipases to release p-nitrophenol, which equilibrates between its protonated and deprotonated forms. In the deprotonated state, p-nitrophenol absorbs strongly at λ = 405 nm.

The concentrated, sonicated, and centrifuged cell lysate supernatants of IPTG-induced recombinant *E. coli* clones described in section 2.3.5 above, and those expressing the engineered fusions described in sections 2.3.9 and 2.3.10 below, as well as lysate from non-recombinant BL21 *E. coli*, were each tested for

lipase activity. Each sample was added to a 1 mL cuvette, in which 990 microliters of supernatant was combined with 10 microliters of 5 mg/mL p-nitrophenyl acetate dissolved in acetonitrile (aqueous nitrophenyl acetate stock solutions are unreliable because the compound spontaneously hydrolyzes in contact with water), for a final working concentration of 50 µg/mL. After 10 minutes, we measured the absorbance of each sample at 405 nm and subtracted the absorbance of protein-free buffered (pH 6.0, 50 mM bis-tris) 50 µg/mL nitrophenyl acetate as a baseline to account for p-nitrophenol released into the sample via spontaneous hydrolysis.

2.11 Turbidity of Oleic Acid Suspensions

The pH 6.0 bis-tris buffered soluble protein fractions from 2.3.5 containing the three isolated proteins (SAUSA300_2518, SAUSA300_2603, and SAUSA300_0320) were screened for esterification based on their ability to clarify turbid oleic acid suspensions. Inclusion of 10% v/v ethanol and 250 micrograms per milliliter oleic acid in buffer or a soluble protein sample results in a visibly cloudy, colloidal solution that persists stably for >72 hours (Figure 2-4 A). Systematic exclusion of components from this system revealed that both ethanol and oleic acid are required for the formation of the light-scattering particles. In the absence of ethanol, the oleic acid partitions completely and remains a droplet floating on the surface of the buffer. In the absence of oleic acid, the

ethanol is fully miscible with the buffer and does not cloud the solution. This turbidity was quantified as optical density at 400 nm. Soluble protein fractions were incubated with 10% ethanol and 250 micrograms per milliliter oleic acid for 24 hours at 37°C. The samples were then centrifuged at 3000 g for 15 minutes to pellet and remove soluble proteins that had precipitated in that time. In the absence of SAUSA300_2603 or SAUSA300_0320, the solution remained cloudy. When cell sonicate from *E. coli* expressing either of those proteins was included in the system, however, the resulting solution was rendered clear.

In order to determine the actual morphology of these droplets, we used dynamic light scattering to measure the average radius of the particles, under the same buffer conditions as the GC-MS FAME assay: 50 mM bis-Tris, 250 µg/mL oleic acid, 0.5-40% ethanol v/v, pH 6.0.

We attempted to develop this system as an assay for quantification of FAME activity, noting a linear decrease in turbidity over time (Figure 2-4 B). It is worth noting, however, that a sufficiently large amount of other protein could be observed to cause non-specific co-precipitation of the oleic acid over time. As a result this technique is not suitably quantitative for most applications.

A

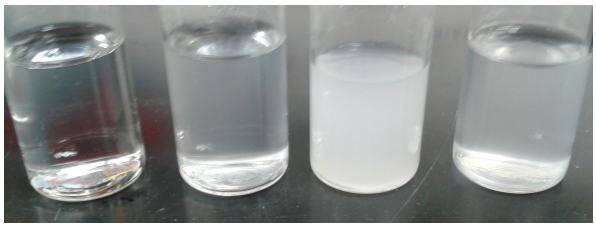

Oleic acid	-	+	+	+
Ethanol	+	-	+	+
Enzyme	+	+	-	+

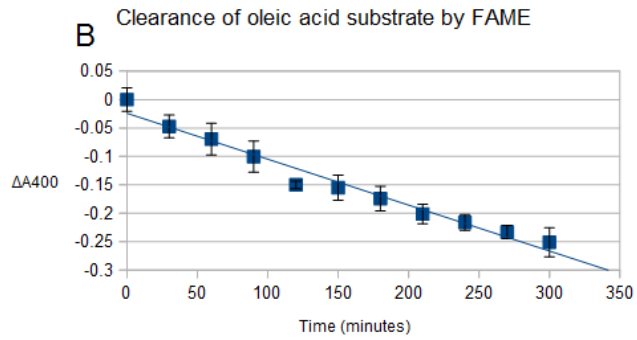

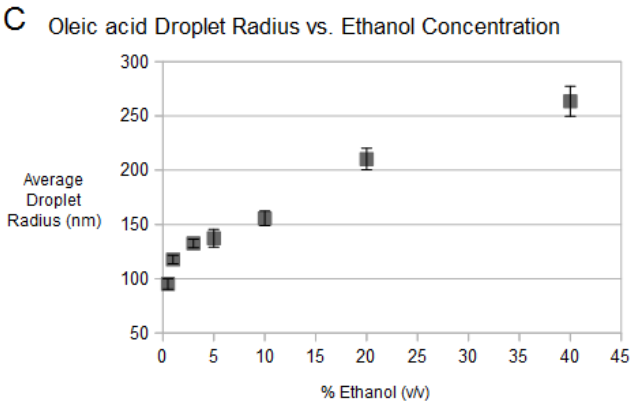

Figure 2-4. FAME activity reduces oleic acid droplet turbidity. Oleic acid forms a turbid suspension in buffer solution (A), but only in the presence of ethanol (vial 3). Purified FAME protein reduces this turbidity over time (vial 4), measured as light scattering at 400 nm (B). Dynamic light scattering measurement of oleic droplet radius as a function of ethanol concentration (C).

2.12 Design and Cloning of FAME-LUSH Fusion

In order to enhance the ability of one of the FAME enzymes (SAUSA300_2603) to catalyze fatty acid ethyl ester formation, we appended the *Drosophila melanogaster* LUSH alcohol-binding protein to its primary sequence. The gene sequence for the mature (without introns) primary sequence of LUSH was constructed with PCR using the aforementioned protocols and the following primers:

LUSHfoward1:ATGACAATGGAACAATTCTTGACCTCGCTAGACATGATCCGC
AGTGGCTGTGCG

LUSHfoward2:CGCAGTGGCTGTGCGCCGAAGTTTAAGCTCAAAACAGAAGA
TCTCGATCGGCTTC

LUSHfoward3:ATCTCGATCGGCTTCGCGTGGGTGATTTCAACTTTCCGCCAT
CGCAGGATCTTATG

LUSHfoward4:ATCGCAGGATCTTATGTGCTACACAAAGTGTGTGTCTTTGAT
GGCGGGCACTGTG

LUSHfoward5:ATGGCGGGCACTGTGAATAAAAACGGAGAATTCAACGCTCC
CAAGGCATTAGCAC

LUSHfoward6:CCAAGGCATTAGCACAACTTCCGCATCTGGTTCCACCCGAAA
TGATGGAGATGTCC

LUSHfoward7:AAATGATGGAGATGTCCAGGAAATCCGTTGAAGCTTGTCGG
GACACGCACAAGC

LUSHfoward8:GACACGCACAAGCAATTTAAGGAATCTTGCGAGAGAGTCTAC

CAGACGGCCAAGTGCTTC

LUSHreverse9:AGGCCACATGAATTGTCCATCTGCGTTTTCAGAGAAGCACTT

GGCCGTCTG

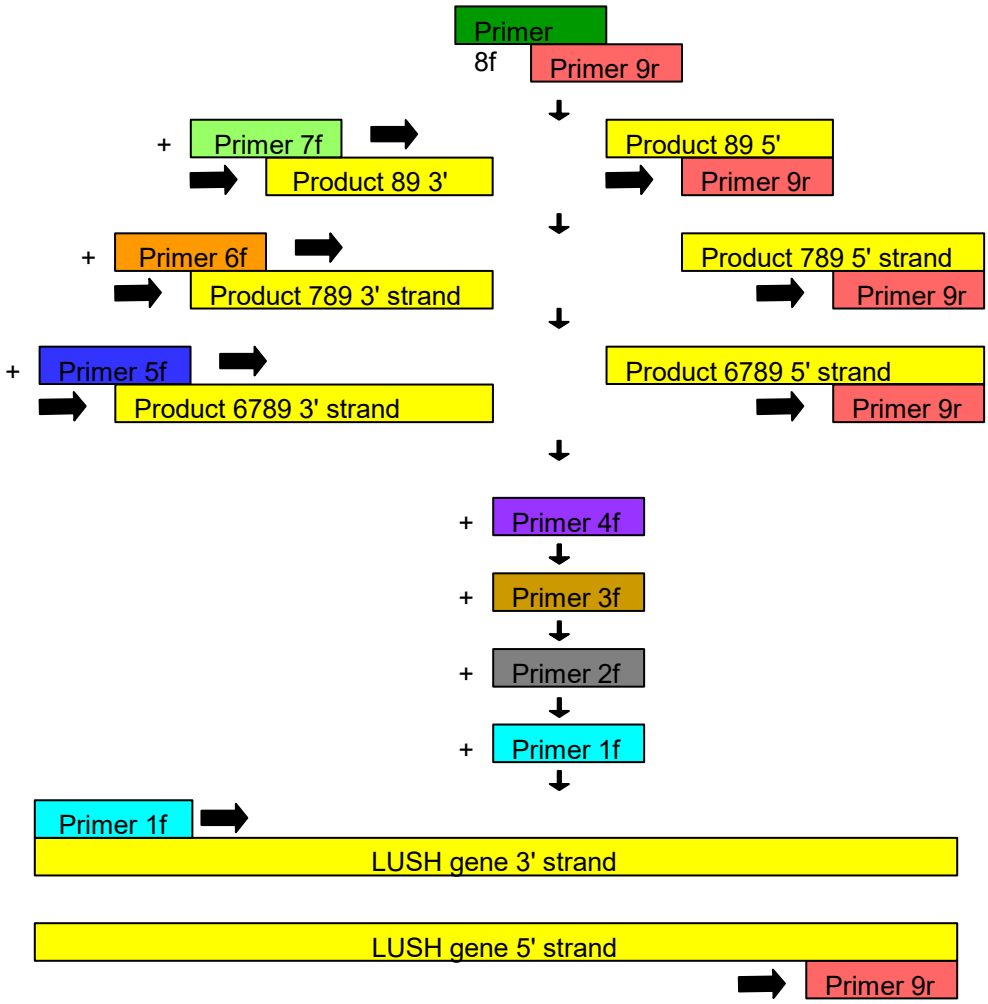

Figure 2-5. PCR scheme for construction of the LUSH gene. Each successive forward (f) primer adds several base pairs to the PCR product amplified by the previous forward primer. Horizontal arrows indicate direction of elongation (5' to 3').

Sequential annealing and elongation of these primers constructs the intron-free DNA sequence of a functional LUSH domain (Figure 2-5).

Following this, the PCR product was extracted from a 1% agarose gel using a razor blade and ethidium bromide as a visualizing agent. The largest molecular weight band (corresponding to the complete construct incorporating all 9 primers) was then subject to another round of PCR with the following primers:

LUSHforwardEcoR1:CCCACCACGAATTCGCAGAAGCAGCTGCTAAAGAAGCT GCTGCAAAAGCAATGACGATGG

LUSHreverseXho1:AAAAAAAAAAAAAGCGGCCGCTTAAGGCCACATGAACTG

The resulting PCR product codes for a short alpha-helical linker followed by LUSH, with an EcoR1 cut site near its 5' end and an Xho1 cut site near its 3' end.

In parallel with the design and construction of the LUSH gene, SAUSA300_2603's sequence was amplified with the following two primers:

SAUSA300_2603forward6xHisNco1:GGTTCCATGGATCACCACCACCACCACC ACAAGGATGATCAAACG

SAUSA300_2603reverseEcoR1:GAGCACCACAGAATTCTGCTTGCTTAGTATC AGTC

This PCR product is the sequence for SAUSA300_2603 with an N-terminal hexahistidine tag. The DNA sequence also includes an Nco1 cut site and an EcoR1 cut site. The PCR product was purified, cut with Nco1 and EcoR1, and ligated into pET-22b in the manner described above. After purification of this

plasmid construct from Top10 *E. coli*, the plasmid was cut with EcoR1 and Xho1 and ligated with similarly cut LUSH PCR product from the previous paragraph (LUSH). The resulting plasmid was verified to contain a gene coding for an N-terminal signal sequence, followed by a hexahistidine tag, followed by a FAME domain, followed by a helical linker, and finally ending in a LUSH domain. The fusion protein was expressed in BL21 *E. coli* as described for the wild-type FAME above.

2.13 Design and Cloning of FAME-LUSH Fusion T57A mutant

The T57A mutant, which lacks wild-type LUSH's ethanol affinity due to the loss of threonine 57's (as the 57th residue in the LUSH domain) hydrogen bond with the alcohol's hydroxyl group, was constructed similarly to the fusion described in 2.3.9 above. However, we used a slightly different set of primers in the construction of LUSH in order to incorporate the T57A mutation into the primary sequence of the LUSH domain.

LUSHfoward1:ATGACAATGGAACAATTCTTGACCTCGCTAGACATGATCCGC
AGTGGCTGTGCG

LUSHfoward2:CGCAGTGGCTGTGCGCCGAAGTTTAAGCTCAAAACAGAAGA
TCTCGATCGGCTTC

LUSHfoward3:ATCTCGATCGGCTTCGCGTGGGTGATTTCAACTTTCCGCCAT
CGCAGGATCTTATG

LUSHfoward4:ATCGCAGGATCTTATGTGCTACACAAAGTGTGTGTCTTTGATGGCGGGCACTGTG

LUSHreverse5:TGCTAATGCCTTGGGAGCGTTGAATTCTCCGTTTTTATTCACAGCGCCCGCCATC

LUSHreverse6:GGACATCTCCATCATTTCGGGTGGAACCAGATGCGGAAGTTGTGCTAATGCCTTGG

LUSHreverse7:GCTTGTGCGTGTCCCGACAAGCTTCAACGGATTTCCTGGACATCTCCATCATTTC

LUSHreverse8:GAAGCACTTGGCCGTCTGGTAGACTCTCTCGCAAGATTCCTTAAATTGCTTGTGCGTGTC

LUSHreverse9:AGGCCACATGAATTGTCCATCTGCGTTTTCAGAGAAGCACTTGGCCGTCTG

As with the wild type LUSH construct, the T57A mutant was amplified with the following two primers:

LUSHforwardEcoR1:CCCACCACGAATTCGCAGAAGCAGCTGCTAAAGAAGCTGCTGCAAAAGCAATGACGATGG

LUSHreverseXho1:AAAAAAAAAAAAAGCGGCCGCTTAAGGCCACATGAACTG

Allowing for ligation into pET22-b 3' of 2603 in the open reading frame for the expression system.

2.14 Purification of Recombinant FAME Constructs

Purification of 2603, 2603-LUSH, and 2603-LUSH-T57A was done in several stages. The recombinantly expressed FAME proteins in *E. coli* lysate, visualized via SDS-PAGE and coomassie staining (as described in section 2.3.6) show strong expression of the recombinant proteins as large bands on the polyacrylamide gels. However, much of the protein evidently remains in the pellet fraction of the sample after sonication and centrifugation of the buffer-resuspended cell culture. Because the FAME proteins are fully soluble in their native folds, we interpreted this to mean that the recombinant proteins were forming insoluble inclusion bodies during expression. The pET22b expression system contains a signal sequence that directs the nascent polypeptide into the cell periplasmic space via the “SecB” transport pathway [1]. Unfortunately, the throughput capacity of the SecB pathway is finite and in the case of high-expression systems such as the T7 expression system found in pET vectors this can create a “backlog” of nascent proteins that eventually misfold and remain in the cytoplasm.

We opted to overcome this limitation by denaturing and thus solubilizing the inclusion body proteins. We used a buffer (our wash buffer) consisting of 6 M guanidine hydrochloride and 100 mM sodium phosphate at pH 6.0 to resuspend the post-induction cell pellet instead of the guanidine-free buffer described at the end of section 2.3.6. Additionally, we included 0.2% (w/v) sodium azide in this

buffer as an anti-microbial agent to protect the samples and the FPLC system from colonization by opportunistic organisms. After resuspension of the cells, the solution was centrifuged as described above and the viscous supernatant was filtered with a 0.45 micron nitrocellulose syringe filter. A 5 mL GE HisTrap column [5], which features nickel-impregnated sepharose as its stationary phase was equilibrated with 10 volumes of wash buffer using a syringe pump, and then the denatured protein sample was loaded onto the column at 2 mL/minute. After protein loading, the column was washed with another 5 volumes of wash buffer. Finally, the column-bound protein was eluted with 2 volumes of elution buffer, which consisted of 6 M guanidine hydrochloride, 250 mM imidazole, 100 mM sodium phosphate, and 0.2% w/v sodium azide at pH 6.0. The imidazole in the elution buffer outcompetes the hexahistidine tags on the recombinant proteins for the nickel ions in the column stationary phase, allowing the proteins to elute in the mobile (buffer) phase. Between uses, the column was washed with 10-20 volumes of deionized water followed by 5-10 volumes of 20% v/v ethanol and stored at 4º Celsius.

The column eluent from this first chromatography phase was injected into a slide-a-lyzer dialysis cassette with a 10,000 dalton molecular weight cutoff membrane. The cassette was dialyzed in 3 successive 2-liter volumes of guanidine-free wash buffer over a period of 3 days to remove guanidine and imidazole from the sample. After dialysis, the sample was extracted from the

cassette and centrifuged to remove protein that had precipitated in the absence of guanidine hydrochloride.

We assembled a column system consisting of a 5 mL GE HiTrap Q Sepharose anion exchange column upstream of a 5 mL GE HiTrap SP cation exchange column [6]. Using a syringe pump, the columns were equilibrated with 10 volumes of the wash buffer for this step: 100 mM sodium phosphate and 0.2% w/v sodium azide at pH 6.0. The supernatant from the dialysis step was loaded onto the pair of columns using a syringe pump at 2 mL/minute, and then the cation exchange column was removed for installation in the AKTA FPLC system. On the FPLC system, the cation exchange column was washed with 5 volumes of wash buffer at 1 mL/minute. After column washing, elution buffer (wash buffer with an additional 1 M sodium chloride) was added to the mobile phase at a rate of 10% per minute. The fraction showing a strong 280 nm absorption peak was collected and concentrated using an Amicon Ultra 30,000 molecular weight cutoff centrifugal filter unit. After concentration to ~1 mg/mL the proteins were prepared for storage in buffered 50% glycerol and assayed for purity and concentration of the stock solutions using SDS-PAGE (Figure 2-6) and the nanodrop, then stored at -80º Celsius. The ion exchange columns were cleaned and stored as described for the nickel affinity column.

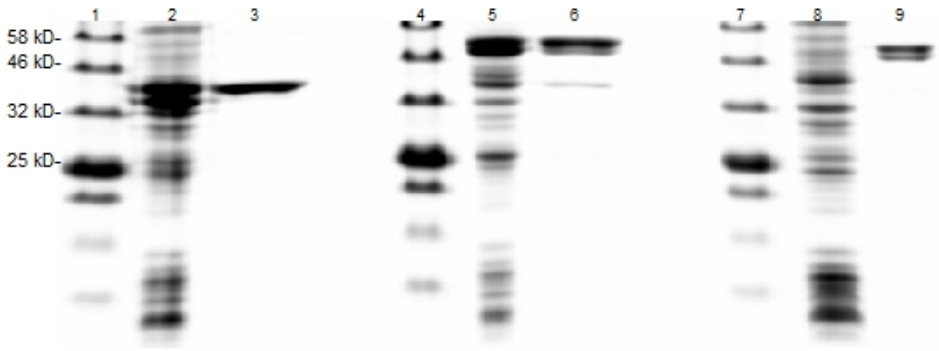

Figure 2-6. SDS-PAGE showing purified FAME constructs. Lanes 1,4,7: New England Biolabs molecular weight marker. Lane 2: *E. coli* cell lysate with wild type SAUSA300_2603/SAL-1 FAME. Lane 3: purified wild type FAME. Lane 5: *E. coli* lysate with FAME-LUSH fusion. Lane 6: purified FAME-LUSH fusion. Lane 8: *E. coli* lysate with FAME-LUSH-T57A variant (low expression is visible). Lane 9: purified FAME-LUSH-T57A variant.

2.15 ANS Fluorescence Titration of FAME and FAME-LUSH fusion

We used 8-anilino-1-naphthalene-sulfonic acid (ANS) to assay the differences in ethanol affinity between our three constructs: wild type FAME, FAME-LUSH fusion, and FAME-LUSH-T57A. Thode et. al. used ANS titration to show that their LUSH mutants had differing affinities for alcohol by noting that mutants which bind alcohol more strongly show a greater loss of fluorescence when alcohol is included in the solution [11]. ANS is a compound that associates non-specifically with accessible hydrophobic patches on protein surfaces, and gains fluorescence in doing so. In our assay, ANS absorbed 360 nm light and relaxed to emit light at a wavelength of 495 nm. Inclusion of ethanol in solution with ANS and protein creates competition between the ethanol and ANS for

access to the protein surface, resulting in a lower fluorescence signal (Figure 2-7).

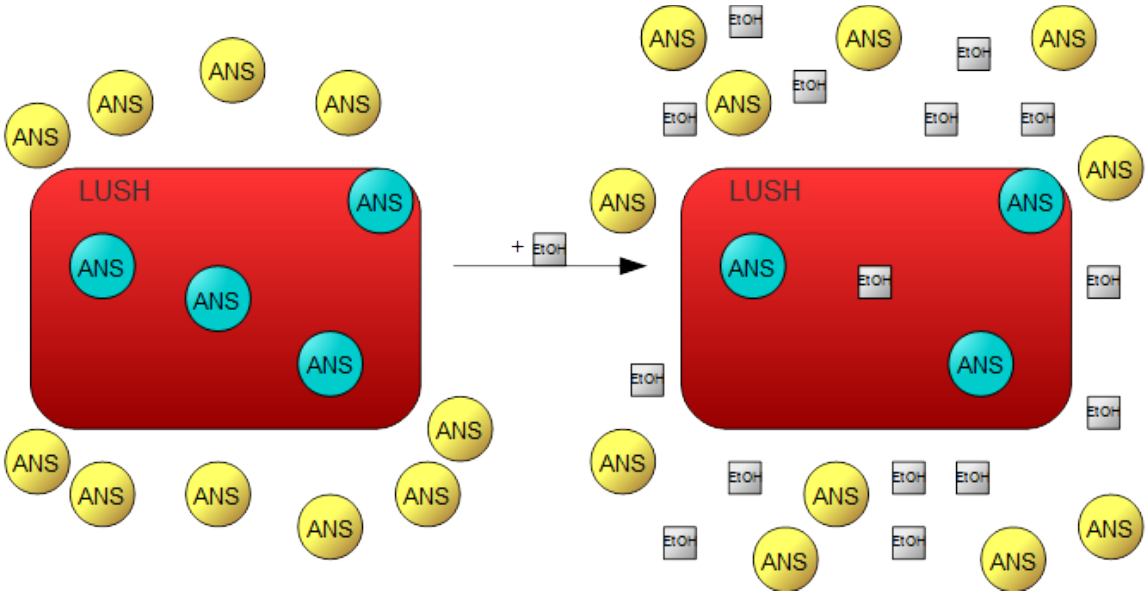

Figure 2-7. ANS fluorescence titration. ANS binding hydrophobic protein surfaces gains fluorescence (left). Addition of ethanol displaces ANS from protein surfaces with high ethanol affinity, leading to a decrease in the solution's fluorescence (right).

This effect is particularly pronounced for proteins that have specific ethanol-binding sites, because the stronger affinity of ethanol for protein at those sites allows for greater displacement of ANS and at lower ethanol concentrations.

In a 96-well polypropylene plate, we combined ANS, buffer, and proteins as follows:

1. FAME (2603), FAME-LUSH fusion, or FAME-LUSH-T57A to a working concentration of either 0.0 or 2.0 micromolar

2. ANS from 500 micromolar stock solution to a working concentration of between 0 and 60 micromolar

3. Ethanol to a working concentration of between 0% and 15% (v/v)

4. Bis-tris buffer to a working concentration of 50 millimolar, a pH of 6.0, and a total solution volume of 10 microliters.

The droplets were assayed for fluorescence in a Tecan Infinite M200 plate reader. ANS excitation was performed with 360 nm light, and emission of 495 nm was detected. Scans were performed in triplicate, and the readings for protein-free droplets were used as a baseline to subtract the fluorescence of unbound ANS.

2.16 GC-MS Assessment of FAME-LUSH Fusion

FAME activity for crude and purified FAME constructs (0320, 2603, 2603-LUSH, and 2603-LUSH-T57A) was done similarly to the process described in 2.3.2 for staphylococcal culture supernatant and 2.3.6 for recombinant NWMN_0624 and NWMN_2434. 700 microliters of pH 6.0 50 mM bis-tris buffer, 250 microliters of cell sonicate supernatant in the same buffer, and 50 microliters of ethanol containing 5 mg/mL oleic acid were incubated at 37º Celsius overnight. Two successive volumes of hexane were used to extract the organic components of the system and then pooled and run on the GC-MS system described above.

Purified FAME and FAME constructs were assayed similarly, with some adjustments:

1. A working concentration of 20 nM protein
2. Between 0.5% and 40% ethanol (v/v)
3. A working concentration of 250 µg/mL oleic acid, introduced to the solution pre-dissolved in the ethanol
4. 50 mM bis-tris at pH 6.0 to a volume of 3 mL

The reaction systems were incubated at 37º Celsius for 3 hours and then extracted into one volume of hexane, followed by GC-MS analysis. FAME activity was quantified as the ion count at telltale m/z values in the butyl oleate and ethyl oleate mass spectra (Figure 2-8).

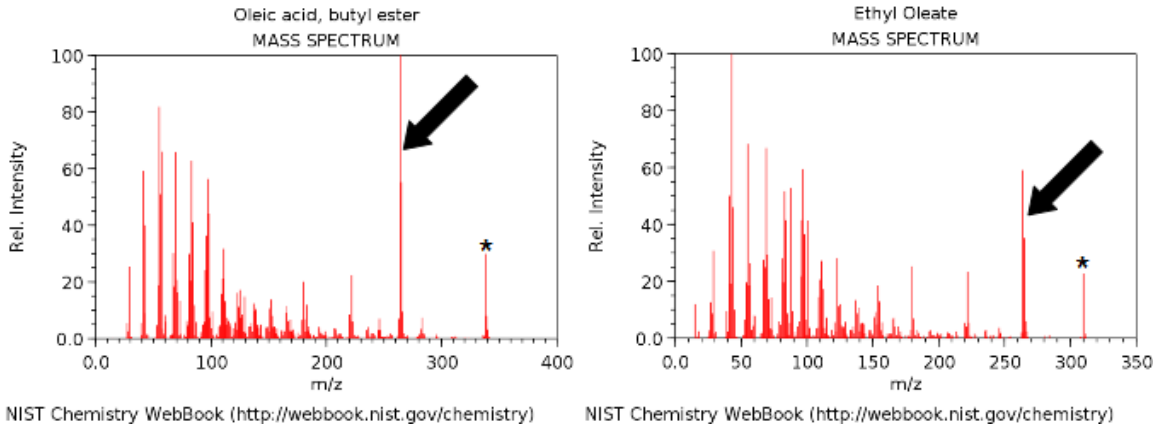

Figure 2-8. Mass spectra of butyl oleate and ethyl oleate. Molecular ions are marked with an asterisk, and m/z = 264 is indicated by arrows.

2.17 References

[1] pET System Manual, 10th edition. Novagen (2003).

[2] T. Baba, T. Bae, O. Schneewind, F. Takeuchi, K. Hiramatsu, Genome Sequence of *Staphylococcus aureus* Strain Newman and Comparative Analysis of Staphylococcal Genomes : Polymorphism and Evolution of Two Major Pathogenicity Islands, J. Bacteriol, 190 (2008) 300–310.

[3] Zymoclean™ Gel DNA Recovery Kit, Ver 1.2.0. Zymo Research (2016).

[4] B.A. Diep, S.R. Gill, R.F. Chang, T.H. Phan, J.H. Chen, M.G. Davidson, F. Lin, J. Lin, H.A. Carleton, E.F. Mongodin, G.F. Sensabaugh, F. Perdreau-Remington, Complete genome sequence of USA300, an epidemic clone of community-acquired meticillin-resistant *Staphylococcus aureus*, Lancet 367 (2006) 731–739.

[5] Instructions 71-5027-68 AK, HisTrap™ HP, 1 ml and 5 ml. GE Healthcare (2015).

[6] Instructions 71-7149-00 AP, HiTrap™ SP HP, 1 ml and 5 ml, HiTrap™ Q HP, 1 ml and 5 ml . GE Healthcare (2014).

[7] J.P. Long, J. Hart, W. Albers, F. a. Kapral, The production of fatty acid modifying enzyme (FAME) and lipase by various staphylococcal species, J. Med. Microbiol. 37 (1992) 232–234.

[8] J.E. Mortensen, T.R. Shryock, F. a. Kapral, Modification of bactericidal fatty acids by an enzyme of *Staphylococcus aureus*, J. Med. Microbiol. 36 (1992) 293–298.

[9] Zyppy™ Plasmid Miniprep Kit, Ver. 1.2.6. Zymo Research (2016).

[10] J. Skjold-Jørgensen, J. Vind, A. Svendsen, M.J. Bjerrum, Altering the activation mechanism in *Thermomyces lanuginosus* lipase, Biochemistry. 53 (2014) 4152–4160.

[11] A.B. Thode, S.W. Kruse, J.C. Nix, D.N.M. Jones, The role of multiple hydrogen bonding groups in specific alcohol binding sites in proteins:

Insights from structural studies of LUSH, J Mol Biol. 376 (2008) 1360–1376.

[12] pET-22b(+) Vector Map. Novagen (1998).

[13] S.E. Stein, P.J. Linstrom, W.G. Mallard, "Mass Spectra" NIST Chemistry WebBook, NIST Standard Reference Database Number 69, NIST Mass Spec Data Center, National Institute of Standards and Technology, Gaithersburg MD, http://webbook.nist.gov, (retrieved August 15, 2016).

Chapter III

Identification of Staphylococcal FAME

3.1 Introduction

This project's initial goal was the identification, study, and enhancement of the staphylococcal enzyme responsible for “FAME” activity [5,6,22,25], with the goal of exploring biochemical strategies for biofuel (fatty acid alkyl ester) production as an alternative to traditional alkaline catalysis of the esterification [9]. The first step, naturally, was the identification of the enzyme. Our first approach, the rational selection of FAME candidate proteins, was based on the assumption that the FAME enzyme would have telltale sequence features but be otherwise poorly characterized. This strategy proved to be naïve. Our second approach, isolating the source of *in vivo* FAME activity via chromatographic sample fractionation, led to identification of two *S. aureus* lipase proteins that act as FAMEs. These results were, in hindsight, predictable, given the known ability of many lipases to catalyze esterifications under the proper conditions [3,7,12,13,15,18]. In fact, at least one homologue of one of the isolated FAME proteins has been used to synthesize esters in a highly organic reaction medium [16].

3.2 NWMN_0624 and NWMN_2434 are Non-FAME Proteins

The proteins coded by the gene loci *NWMN_0624* and *NWMN_2434* in the Newman strain [1] of *Staphylococcus aureus* (which correspond to the loci *USA300_641* and *USA300_2473*, respectively, in the USA300 strain [10]) were our first two FAME candidate proteins. The first part of our rationale was that the protein responsible for *in vivo* fatty acid alkyl ester synthesis in staphylococcal lesions would have sequence similarity to esterases, based on the fact that ester hydrolysis and FAME activity both catalyze the transition between the same two states: that of a separate alcohol and carboxylic acid, and that of a single ester molecule [20,37]. This later proved to be sound reasoning. However, we erred in the second part of our rationale by hypothesizing that FAME was a previously uncharacterized protein; this will be further discussed in section 3.4. It was with both of the aforementioned considerations in mind that we selected NWMN_0624 and NWMN_2434 as our initial FAME candidate proteins. Cloning and recombinant expression of these two proteins using the pET22b yielded amounts of soluble protein visible on SDS-PAGE, and initial GC-FID results seemed promising in that they showed FID chromatogram peaks with retention times resembling that of the anticipated butyl oleate esterification product. However, subsequent analysis with GC-MS indicated that the peaks observed in the GC-FID chromatograms were not, in fact, butyl oleate ester. Given the apparent robustness of the Long et. al. assay, which directly measures reaction

product (esters), we concluded that neither NWMN_0624 nor NWMN_2434 are FAME proteins.

3.3 Square One: *Staphylococcus aureus* Culture Fractionation

After concluding that neither NWMN_0624 nor NWMN_2434 are FAME proteins, we decided to take a different approach to the isolation and identification of FAME. We acquired four *S. aureus* strains graciously provided by Dr. Kelly Doran at San Diego State University: Newman, USA300, ISP 479C, and SA113. After cultivation, centrifugation, and filtration of the cell culture supernatants, we repeated the Long. et. al. assay [22]. Our results showed varying degrees of FAME activity for the four strains, depending on both the strain identity and the growth media used (Figure 3-1). This both established the soundness of the assay itself, and that at least some of the strains in question expressed functional FAMEs under our growth conditions. For both USA300 and Newman strain *S. aureus* cultures, higher FAME activity was seen when the growth media was tryptic soy broth (TSB) as opposed to Luria Bertani media (LB).

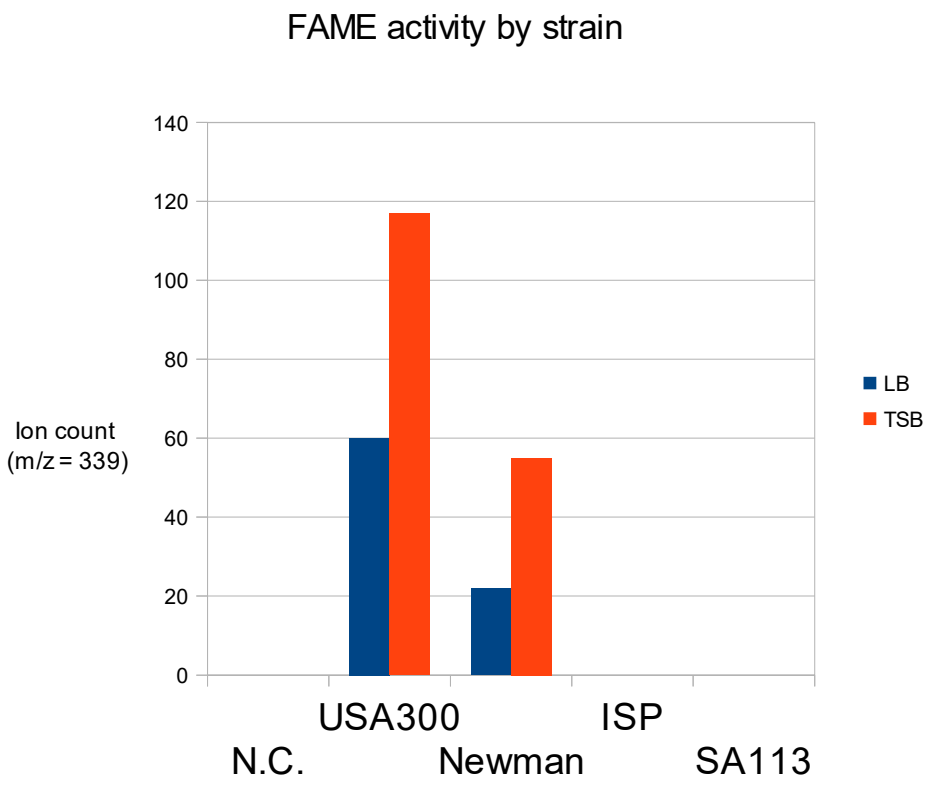

Figure 3-1. GC-MS determination of FAME activity in staphylococcal culture supernatants. Ion counts were measured at an m/z ratio of 339 amu, the mass of the butyl oleate molecular ion. In the case of sterile media filtrate in which no cells were cultured (N.C.), the ISP 479C staphylococcal strain, or the SA113 strain, no detectable amount of butyl oleate product was detected, whereas FAME activity was detected for the USA300 and Newman strains.

There are numerous possible explanations for this effect. Because crude supernatant was used to supply the bulk of the buffer system during the FAME assay, differences in ionic strength or pH between the two media may have impacted the ability of the FAMEs to catalyze esterification [4,5,29]. It would also

be unsurprising if the *S. aureus* cells' FAME protein expression patterns were affected by the availability of different nutrients in the media. Following this reasoning, it could not be concluded that the other two *S. aureus* strains, ISP 479C and SA113, lack genes coding for FAMEs. It may be the case that FAMEs are coded for within their respective genomes, but inter-strain proteomic differences result in negligible FAME expression or activation under our growth conditions.

Following verification of FAME activity in our *Staphylococcus aureus* cultures, the culture supernatant from the USA300 cells grown in TSB media (the supernatant showing the greatest amount of FAME activity) was fractionated on a GE HiLoad Superdex 200 26/60 size exclusion column, using pH 6.0, 100 mM sodium phosphate buffer as the mobile phase. The fractions were concentrated using centrifugal filter units after collection from the size exclusion column. Separate application of the Long assay to 15 mL fractions of the column eluent revealed a clear concentration of the FAME protein(s) in fraction E, the fifth 15-mL fraction collected after the column void volume. FAME activity was quantified at m/z values of 55 and 264 (Figure 3-2), which correspond to ions that are much more abundant than the molecular ion (m/z = 339) in the fragmentation spectrum of butyl oleate.

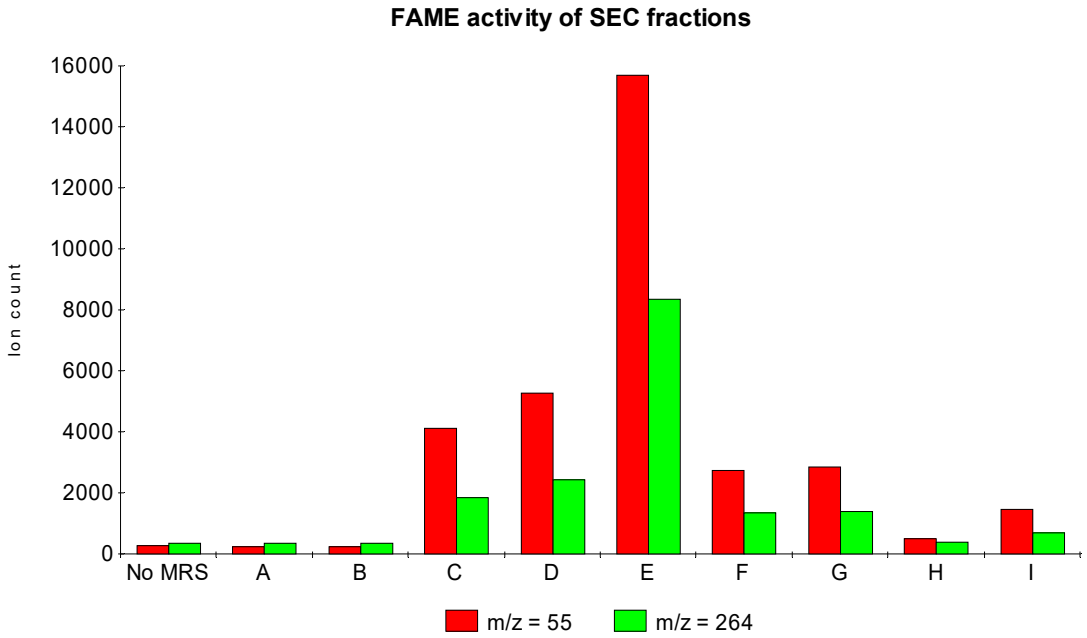

Figure 3-2. GC-MS determination of FAME activity in successive 15 mL size exclusion eluent fractions of staphylococcal culture supernatant. Ions were counted at two characteristic m/z values, 55 (a four-carbon fragment of the acyl chain) and 264 (the molecular fragment lacking the alkyl group).

We delivered this sample to the Biomolecular and Proteomics Mass Spectrometry facility at the University of California, San Diego. LC-MS analysis showed that the sample contained detectable amounts of numerous proteins including alpha-hemolysin and Panton-Valentine leukocidin (Table 3-1), but that 49% of the protein present consisted of two proteins flagged by sequence analysis as triacylglycerol lipases. In the USA300 genome these two proteins are coded by loci numbered 0320 and 2603 [10], and hereafter we will refer to them as SAUSA300_0320 and SAUSA300_2603.

Table 3-1. Protein contents of FAME-active supernatant fraction. LC-MS sequencing of the size exclusion column eluent fraction “E” from figure 3-2, arranged by peptide abundance. Only three proteins found I this fraction are lipases or potential lipases.

Protein	Genbank accession number	% of total peptides
SAUSA300_0320 lipase	87162130	32.6
SAUSA300_2603 lipase	87160182	16.8
α-hemolysin	87160380	16.8
Panton-Valentine leukocidin	87161953	10.4
1-phosphatidylinositol phosphodiesterase	87162123	5.5
Autolysin	87162026	4.5
Glycerophosphoryl diester phosphodiesterase	87160899	4.2
ABC transporter substrate binding protein	87161864	2.7
Sulfatase family protein	87161249	2.6
γ-hemolysin components A,B	87161385, 87160716	1.7
Leukotoxin	87162036	1.0
SAUSA300_2518 esterase/lipase	87161328	0.9
Leukocidin/hemolysin family protein	87160982	0.3

The two proteins have >50% amino acid sequence identity, and feature N-terminal secretion signal sequences. This conforms with their location in the culture medium, as the signal sequence serves to direct the nascent polypeptides out of the cell during protein translation [2,32]. The secreted forms

of the two highly similar proteins are further divided into two domains: an N-terminal inhibitory domain, and a C-terminal lipase domain [11,14,26]. The inhibitory domain serves to restrict the lipase domain, limiting lipase activity. *S. aureus* secretes protease (aureolysin) that hydrolyze the immature proteins, releasing mature lipases consisting solely of the lipase domain [4]. It is certainly possible that this regulatory step is the cause of the disparity in FAME activity between the four tested strains and two tested growth media; *S. aureus* cells expressing lipases but not their activating proteases would show little or no FAME activity. In addition to these two lipases, trace amounts (<1% of total protein) of a third protein, SAUSA300_2518, were detected in the sequenced sample. Sequence comparison indicated that this protein was in the broad hydrolase family, but it is smaller than SAUSA300_0320 or SAUSA300_2603, and does not align well with either of them.

Following examination of the sequencing results, we opted to recombinantly express these three proteins using *E. coli*, as we had with NWMN_0624 and NWMN_2434. Because the focus of our inquiry was the enzymatic activity of an active, mature protein, we chose to incorporate only the DNA sequence corresponding to the mature lipase domains of SAUSA300_0320 and SAUSA300_2603 into the pET22b plasmids used for recombinant expression in *E. coli*. Note that, as described in Materials and Methods, we used Nco1 as a restriction endonuclease for creating sticky ends to ligate the

recombinant genes into cut pET22b. This results in the inclusion of the pelB leader sequence in the open reading frame of the recombinant proteins, which directs them (as nascent polypeptides) to the periplasmic space during translation. The pelB leader sequence, however, is not the same as the lipases' wild-type N-terminal secretion signal sequence [2]; the latter is incompatible with our expression system, as *S. aureus* is gram-positive while *E. coli* is gram-negative. All three proteins expressed as determined by SDS-PAGE, showing bands at the appropriate molecular weights after coomassie staining.

3.4 Para-Nitrophenyl Acetate Hydrolysis Results

In addition to assaying recombinant proteins for FAME activity, we used nitrophenyl acetate (specifically, para-nitrophenyl acetate, abbreviated NPA) to test them for lipase activity (Figure 3-3). Lipases hydrolyze the ester bond in NPA to release para-nitrophenol, which in its acidic form absorbs light strongly at 405 nm, giving it a distinctive yellow color. As such, NPA serves as a simple colorimetric assay for lipase activity in a sample [34].

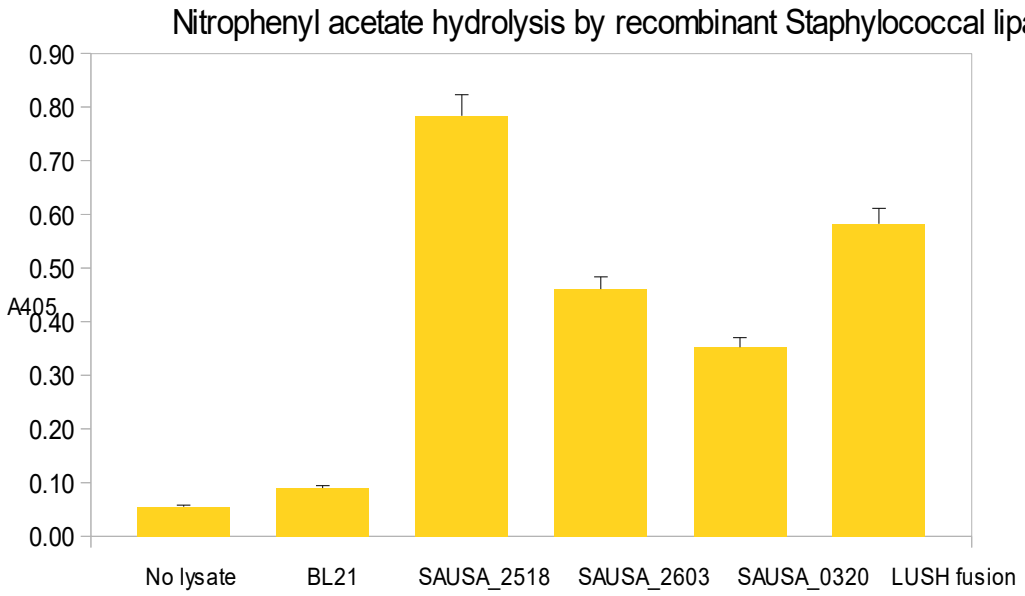

Figure 3-3. Nitrophenyl acetate hydrolysis by recombinant staphylococcal lipases. Absorbance measured at 450 nm indicates the evolution of p-nitrophenol, a lipolytic product. All three of the tested lipases, in addition to the 2603/LUSH fusion variant, catalyzed the formation of relatively similar amounts of p-nitrophenol. Lipases endogenous to the BL21 expression strain of *E. coli* are minimally active under these conditions (2nd bar). Lipase activity data for NWMN_0624 and NWMN_2434 are not shown.

It should be noted that NPA's ester bond decomposes spontaneously in aqueous solutions at a non-negligible rate. This means that negative control samples show an increase in absorbance at 405 nm over time; in our figures this baseline absorbance has been subtracted out to show only the NPA hydrolysis caused by agents other than water and buffer components. Another consideration in the use of the NPA assay is that only the acidic form (that is, the deprotonated conjugate base $C_6H_4NO_3^-$) absorbs light at 405 nm, which means

that the functional extinction coefficient is smaller at low pH values as most of the para-nitrophenol is protonated, but greater at high pH values as most of the para-nitrophenol is deprotonated. Literature suggests that staphylococcal lipases and FAMEs are mainly active at mildly acidic pH values [5,25], whereas *E. coli*'s endogenous lipases are evolutionarily optimized for higher pH values [38]. With these factors in mind, we performed the assay in pH 6.0 buffers, in which para-nitrophenol has strong effective absorbance but endogenous *E. coli* lipase activity appears negligible.

Qualitatively, the outcome of the NPA assay showed lipase activity for most of our recombinant proteins. Recombinant NWMN_0624 expressed as a functional lipase, despite the fact that it lacks FAME activity (at least, in the comparatively aqueous conditions of the Long et. al. assay). This is noteworthy in that it reveals the fact that FAME activity is not a general feature of staphylococcal lipases, consistent with previous literature suggesting that at least some staphylococcal strains show lipase activity but not FAME activity [5,22]. NWMN_2434 lacks both lipase activity and FAME activity, suggesting that it has some other role in the staphylococcal proteome; however, because that role lies outside of the scope of this project, it was not investigated further.

Testing the three recombinant proteins isolated from USA300 *S. aureus* supernatant, SAUSA300_0320, SAUSA300_2518, and SAUSA300_2603, for lipase activity using nitrophenyl acetate showed that all three catalyze NPA

hydrolysis under our experimental conditions. While this result was expected in the case of SAUSA300_0320 and SAUSA300_2603, it established that SAUSA300_2518 is indeed a lipase (or a lipase-like esterase) as predicted by sequence analysis. However, we ruled out SAUSA300_2518 as a FAME candidate protein, for two reasons. The first is that its DNA sequence lacks any secretion signal sequence [41], suggesting that it is normally a cytoplasmic esterase, whereas literature indicates that FAMEs are secreted proteins. Its presence in trace amounts (less than 1%) in some of the culture supernatant is likely due to small amounts of cell lysis during the handling, centrifugation, and filtration steps taken in the preparation of the sample.

3.5 SAUSA300_0320, SAUSA300_2603 and *in vitro* FAME Activity

The two remaining FAME candidate proteins, tested for FAME activity via the Long assay, showed the ability to catalyze the esterification of butanol or ethanol and oleic acid to form butyl oleate or ethyl oleate. This establishes their identities as the proteins responsible for FAME activity in staphylococcal supernatant (Table 3-2).

Table 3-2. Summary of recombinant staphylococcal protein enzymatic activities. Of the five staphylococcal proteins that we recombinantly expressed, four were lipases, as determined by NPA hydrolysis. Of those four, two were secreted proteins (based on sequence comparison) and were shown to exhibit FAME activity *in vitro*.

Protein	Lipase activity (NPA)	FAME activity (GC-MS)
USA300_0641(NWMN_624)	+	-
USA300_2473(NWMN_2434)	-	-
USA300_2518	+	ND
USA300_0320(SAL-2)	+	+
USA300_2603(SAL-1)	+	+
FAME-LUSH fusion	+	+
FAME-LUSH-T57A	+	+

As we discussed in section 3.1, it is unsurprising that the FAME proteins are lipases, as the two enzymatic functions they exhibit differ only in the direction of the reaction. In fact, Rosenstein et. al. designated the two proteins we identified as SAUSA300_2603 and SAUSA300_0320 as SAL-1 and SAL-2 (Staphylococcus aureus lipase), respectively, during investigation and review of secreted staphylococcal lipase family members [29]. The fact that there are two highly similar FAME proteins in the USA300 proteome is curious; it is unclear whether the two differ with respect to their substrate specificities, or with respect to how their activity levels are regulated. Cadieux et. al. offer evidence for the first explanation, showing that SAUSA300_0320/SAL-2 knockout *S. aureus* have inhibited growth in the presence of bactericidal long-chain triglycerides, despite

the availability of SAUSA300_2603/SAL-1 [5]. Interestingly, although they show a pH optimum of ~8.0 for SAL-2 lipase activity, and credit SAL-2 as *S. aureus*' primary source of triglyceride resistance via lipase activity, overall optimal FAME activity is seen at pH ~6.0, the optimal pH for SAL-1. We found that both lipases showed some lipase activity (using nitrophenyl acetate) and FAME activity at pH 6.0 when recombinantly expressed in *E. coli* and assayed separately. We decline to speculate about the possibility of a pH-based switch between lipase and FAME activity of SAUSA300_0320/SAL-2 *in vivo*.

Although previous work has shown at least some esterification by staphylococcal lipases, the family of proteins has predominantly been studied in their capacities as lipases, or of esterification in organic solvents [3,16,18,20,37]. Of note, however, is the work of Chang et. al., who have had success with aqueous esterification of alcohols and fatty acids using a lipase from *Staphylococcus epidermidis*, SEL-1 [7]. Sequence analysis shows that SEL-1 shows high similarity to SAUSA300_2603/SAL-1 (approximately 80%), suggesting that the two proteins are homologous. Of note, however, is the fact that SEL-1 did not show any discernible ability to esterify alcohols smaller than butanol. This is significant for commercial applications, as ethanol manufacturing is well-established (butanol is approaching equal cost-effectiveness, although its greater toxicity may be a concern).

As catalysts, the two enzymes act to lower the energy of the transition state between the reactant(s) and the product(s), allowing the reactant-product population to move toward equilibrium more quickly. In the absence of any apparent requirement for a supply of additional free energy (ATP, for example), the FAMEs can only drive the system toward equilibrium, meaning that they will function as lipases when alcohols and fatty acids are scarce in comparison to fatty acid alkyl esters, and as FAMEs when the reverse is true. Lipases have been used for some time now as catalysts for ester synthesis in highly organic media. The FAMEs are noteworthy for their apparent abilities to form fatty acid alkyl esters in the comparatively aqueous conditions that we have used, although they share this property with lipases isolated from *Candida rugosa* [13]. As we have shown with SAUSA300_0641, this does not appear to be a universal property of staphylococcal lipases. This is consistent with the original finding of Long et. al. that the FAME+ and lipase+ phenotypes correlate strongly but not perfectly across staphylococcal strains.

3.6 Features of SAUSA300_0320 and SAUSA300_2603

Based on primary sequence alone, SAUSA300_0320 and SAUSA300_2603 belong in a large family of closely-related staphylococcal lipases [4,23,29]. The functional differences between these lipase family members are not fully known; selectivity with respect to substrate acyl chain

length is at least one such distinction, as is thermal stability [17,19,31]. They do, however, share the globular α/β hydrolase fold, a beta sheet of variable size sandwiched between two sets of alpha helices [21,28]. The gene sequences for this family of staphylococcal lipases code for, reading from N-terminus to C-terminus, a secretion signal sequence, an inhibitory pre-protein domain, and a lipase domain. The signal sequence is recognized by member proteins of the staphylococcal translocation pathway, and serves to direct the nascent polypeptide into the medium surrounding the bacterium but is hydrolyzed in the process. The pre-protein domain, which impairs but does not fully abolish enzymatic activity, is removed by the metalloprotease aureolysin to release the mature form of the protein (the lipase domain). We initially used PCR to amplify both the sequences of both full-length immature FAME and the mature lipase domain alone. However, the immature form is of little interest with respect to biodiesel-related applications; its function *in vivo* appears to be purely inhibitory. Because the mature form of the FAMEs express and fold as recombinant *E. coli* proteins, only the mature lipase domain was studied further.

We used sequence alignment searches to find the protein most similar to the two FAMEs that had a crystal structure deposited in the Protein Data Bank. The closest match to both is the well-studied *Staphylococcus hyicus* phospholipase, SHyL, which with the FAMEs also share >50% amino acid sequence identity (Figure 3-4) [8,14,26,30,33].

```
2603(SAL-1) ---KDDQTNKVAKQGQYKNQDPIVLVHGFNGFTDDINPSVLAHYWGGNKMNIRQDLEENG
0320(SAL-2) KKVRPLKANQVQPLNKY----PVVFVHGFLGLVGDNAPALYPNYWGGNKFKVIEELRKQG
SHyL        ---------AVQNPENPKNKDPFVFVHGFTGFVGEVAAKG-ENHWGGTKANLRNHLRKAG

2603(SAL-1) YKAYEASISAFGSNYDRAVELYYYIKGGRVDYGAAHAAKYGHERYGKTYEGIYKDWKPGQ
0320(SAL-2) YNVHQASVSAFGSNYDRAVELYYYIKGGRVDYGAAHAAKYGHERYGKTYKGIMPNWEPGK
SHyL        YETYEASVSALASNHERAVELYYYLKGGRVDYGAAHSEKYGHERYGKTYEGVLKDWKPGH

2603(SAL-1) KVHLVGHSMGGQTIRQLEELLRNGNREEIEYQKKHGGEISPLFKGNHDNMISSITTLGTP
0320(SAL-2) KVHLVGHSMGGQTIRLMEEFLRNGNKEEIAYHKAHGGEISPLFTGGHNNMVASITTLATP
SHyL        PVHFIGHSMGGQTIRLLEHYLRFGDKAEIAYQQQHGGIISELFKGGQDNMVTSITTIATP

2603(SAL-1) HNGTHASDLAGNEALVRQIVFDIGKMFGNKNSRVDFGLAQWGLKQKPNESYIDYVKRVKQ
0320(SAL-2) HNGSQAADKFGNTEAVRKIMFALNRFMGNKYSNIDLGLTQWGFKQLPNESYIDYIKRVSK
SHyL        HNGTHASDDIGNTPTIRNILYSFAQ-MSSHLGTIDFGMDHWGFKRKDGESLTDYNKRIAE

2603(SAL-1) SNLWKSKDNGFYDLTREGATDLNRKTSLNPNIVYKTYTGEATHKALNSDRQKADLNMFFP
0320(SAL-2) SKIWTSDDNAAYDLTLDGSAKLNNMTSMNPNITYTTYTGVSSHTG-PLGYENPDLGTFFL
SHyL        SKIWDSEDTGLYDLTREGAEKINQKTELNPNIYYKTYTGVATHET-QLGKHIADLGMEFT

2603(SAL-1) FVITGNLIGKATEKEWRENDGLVSVISSQHPFNQAYTKATDK---IQKGIWQVTPTKHDW
0320(SAL-2) MATTSRIIGHDAREEWRKNDGVVPVISSLHPSNQPFVNVTNDEPATRRGIWQVKPIIQGW
SHyL        KILTGNYIGSVDDILWRPNDGLVSEISSQHPSDEKNISVDEN-SELHKGTWQVMPTMKGW

2603(SAL-1) DHVDFVGQDSSDTVRTREELQDFWHHLADDLVKTE----KLTDTKQA
0320(SAL-2) DHVDFIGVDFLDFKRKGAELANFYTGIINDLLRVEATESKGTQLKAS
SHyL        DHSDFIGNDALDTKHSAIELTNFYHSISDYLMRIE----KAESTKNA
```

Figure 3-4. Sequence alignment of FAMEs and *Staphylococcus hyicus* phospholipase [26]. High sequence identity is apparent. The Ser-His-Asp catalytic triad seen in the *S. hyicus* phospholipase crystal model, as well as their corresponding residues in the FAMEs, are highlighted in black. The four calcium-coordinating aspartic acid residues of the *S. hyicus* phospholipase are highlighted in gray.

Using Swissmodel, we mapped the amino acid sequences of the two FAMEs onto the backbone of the *S. hyicus* phospholipase in order to develop a pair of theoretical structural models [39] (Figure 3-5). The FAME amino acid sequences match the *S. hyicus* phospholipase fold well, showing a few features that the three proteins are likely to share *in vivo*. Tiesinga et. al. describe the

overall structure of the phospholipase as having “a heart-like shape” and use computational docking to show a putative substrate binding site.

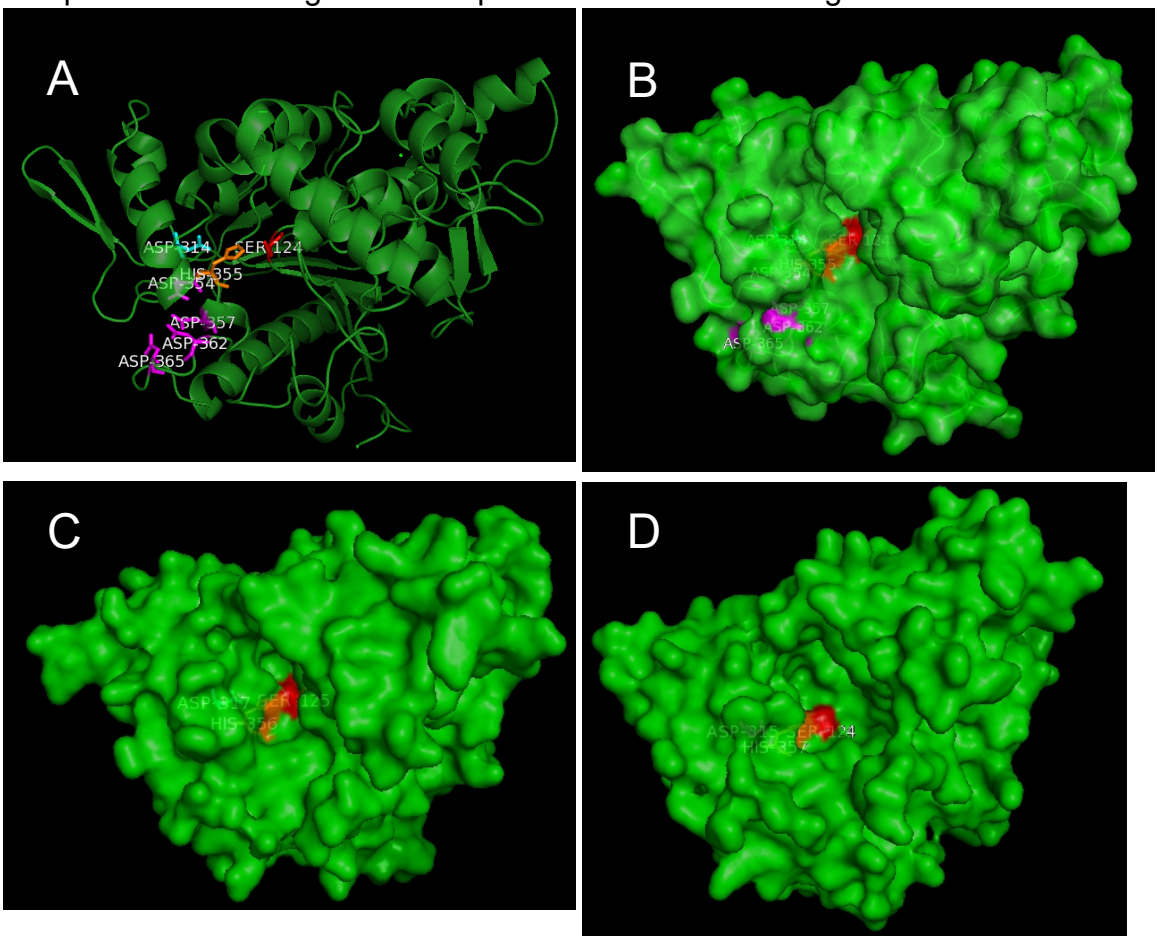

Figure 3-5. Structure comparison of FAMEs to *S. hyicus* phospholipase's crystal model. (A) In PyMOL [40], the backbone of SHyL, the *S. hyicus* phospholipase crystal model [30], showing the catalytic triad (red, orange, cyan) and the four calcium-coordinating aspartic acids (pink). (B) Surface map of ShyL showing the binding groove on the enzyme's face. (C,D) SAUSA300_2603/SAL-1 and SAUSA300_0320/SAL-2 primary sequences mapped onto the SHyL model.

One face of the protein is dominated by a deep groove containing many surface-exposed hydrophobic sidechains. The acyl chains of a hypothetical substrate fit neatly into these grooves, creating a favorable entropy of binding by burying the hydrophobic sidechains in the binding site. Situated in the center of the groove is a classic Ser-His-Asp catalytic triad characteristic of serine hydrolases, as well as an oxyanion hole that stabilizes the transition state in the hydrolysis [8,24,26,35]. As the acyl chains of a lipid substrate fit the hydrophobic groove, the ester groups linking them to the glycerol backbone are brought into close proximity to the catalytic serine, allowing the serine hydroxyl group to attack the ester carbon. This model suggests a hypothetical mechanism for ester synthesis; the hydrophobic groove of a FAME protein binds fatty acids and alcohols in the same manner that *S. hyicus* phospholipase binds phospholipid or triglyceride acyl chains, and the oxyanion hole stabilizes a transition state in which the alcohol group can serve as a nucleophilic attacker of the ester carbon, forming an ester bond. This binding scheme supports both double displacement and single displacement reaction mechanisms, as we will discuss in the next chapter. The model is also consistent with the fact that larger, more hydrophobic alcohols seem to more readily esterify to fatty acids in the FAME reaction [25]. A larger alcohol, such as cholesterol, would be expected to associate with the FAME's hydrophobic groove with a more favorable free energy of binding, as it would bury more hydrophobic surfaces than a small alcohol. This substrate preference

was our primary concern in the engineering of FAME mutants, as discussed in chapter IV.

Another shared feature of SAUSA300_0320, SAUSA300_2603, and *S. hyicus* phospholipase is the presence of a calcium binding site on the surface of the protein (as indicated by the *S. hyicus* crystal model) [33]. Calcium dependence is a not uncommon characteristic of enzymes in the broader lipase family [15,17,27,34]. In the case of the *S. hyicus* phospholipase, catalytic activity seems to be entirely contingent on calcium availability. However, the calcium binding site, discernible as a cluster of aspartic acid residues, is not in proximity to the hydrophobic groove and the active site; therefore the calcium ion cannot be directly involved in catalysis or stabilization of the oxyanion transition state. The *Thermomyces lanuginosus* lipase, another α/β hydrolase which shares a number of features with the staphylococcal lipases, also shows strong calcium dependence, and enzymatic assays of rationally designed mutants suggest that (at least in that case), the calcium ion serves to allosterically stabilize the active conformation of the enzyme [34]. The FAMEs that we isolated in USA300 *S. aureus* are functionally distinct from the *S. hyicus* phospholipase in this regard; they are not calcium-dependent for enzyme activity. We draw this conclusion from the fact that the Long et. al. assay that we have reproduced excludes calcium from the reaction system, and in fact the phosphate buffer originally used would precipitate inadvertent contaminating calcium. Horchani et. al. report

that SAL3, the likely homologue of SAUSA300_2603 (SAL-1) isolated from an unknown soil-isolated S. aureus strain, has its lipase activity enhanced substantially in the presence of 2 mM calcium chloride, and has much higher pH and temperature optima for lipase activity [17]. Chang et. al. have shown that *S. epidermidis* esterase activity with respect to large alcohols [7]. Whether calcium enhances *S. aureus* dual-enzyme FAME activity remains to be determined; although we did not evaluate that characteristic, it is highly likely that SAUSA300_2603/SAL-1 has its FAME activity enhanced by calcium as long as FAME activity is a function of the same active conformation that lipase activity is. Calcium-dependence of SAUSA300_0320/SAL-2 remains similarly unknown. In any case, comparison of the two *S. aureus* FAME proteins to the *S. hyicus* phospholipase furnished us with a starting point for rational protein design, with the goal of improving FAME activity with respect to the small alcohols (i.e. methanol or ethanol) that commonly serve as reagents in commercial biofuel production.

Members of the staphylococcal lipase family generally feature a flexible “lid” that serves to stabilize the proteins in solution by masking the hydrophobic groove when substrate is not available, and opening to admit substrate access when substrate is available. Because lipid substrates typically partition into hydrophobic structures such as droplets or cell membranes, the open and active enzyme conformation is spatially associated with said structures at the interface

between the hydrophobic structure and the aqueous surroundings. As a result, this effect has come to be known as “interfacial activation” [34,36]. Although the crystal structure model of the *S. hyicus* phospholipase does not directly betray the presence of a lid, that is likely to be simply because the lid is “open” in the crystallized form of the protein; the location of a putative lid is indicated by Tiesinga et. al. in their analysis [35]. The spatial localization of active FAME proteins and their substrates also came to be a major consideration in our rational design as described in chapter IV.

3.7 Conclusion

In retrospect, many of the aspects of our results closely match similar determinations that have come before; the staphylococcal lipase family has been extensively studied in its capacity as both lipases and esterification catalysts (Figure 3-6). Consequently, most of our results could have been predicted with very high confidence by existing literature. However, this project revealed that two, rather than one, of the secreted *S. aureus* lipases, are FAME proteins: USA300_2603/SAL-1 and USA300_0320/SAL-2. Curiously, although it has been shown that SAL-1 is not sufficient to protect *S. aureus* from the bactericidal effects of long-chain triglycerides in the absence of SAL-2 (even though the two are highly similar to each other) [4], SAL-1 is nonetheless capable of exhibiting FAME activity when supplied with the long chain oleic acid as an esterification

substrate. This suggests that FAME activity may show less substrate specificity than lipase activity. These two proteins are also highly homologous to the *S. epidermidis* lipase (and probable SAL-1 homologue) SEL-1 [7].

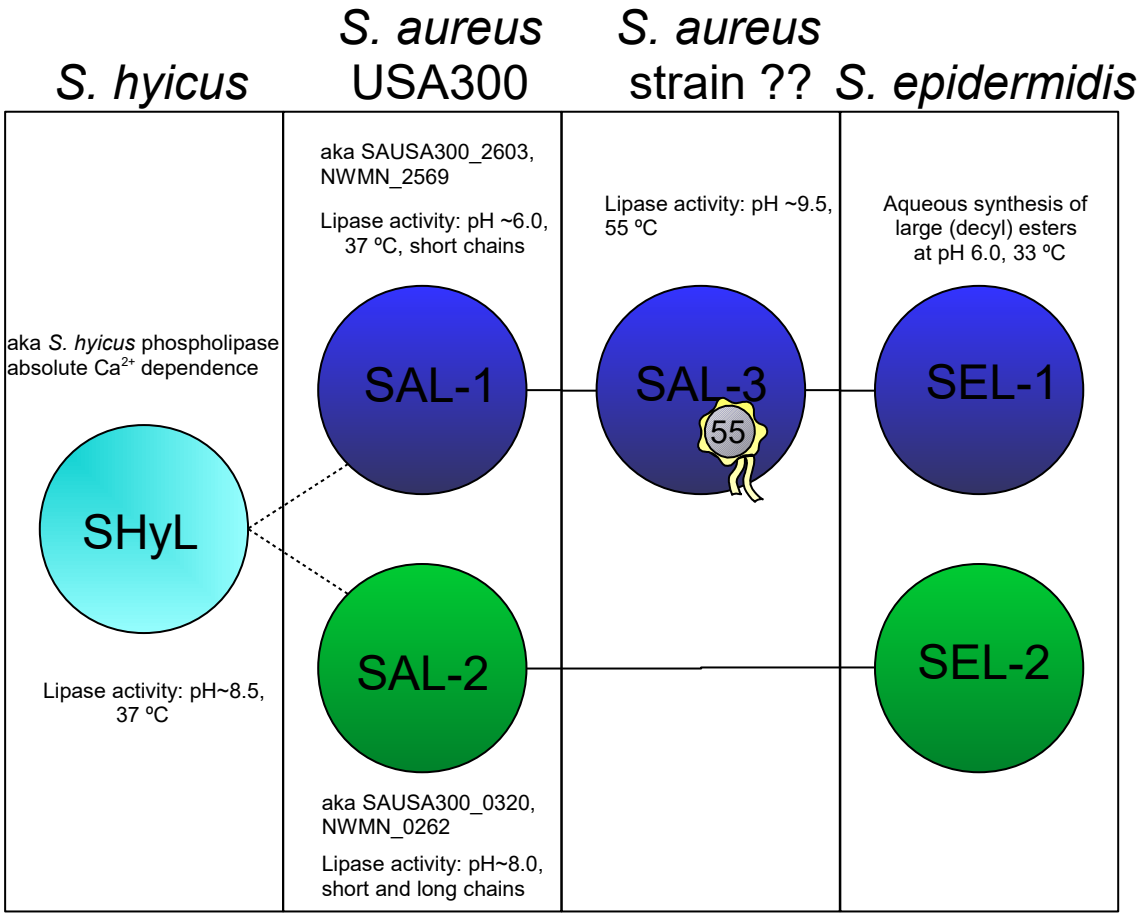

Figure 3-6. Physical properties and putative relationships of members of the secreted staphylococcal lipase family. As seen here with S. aureus (USA300 strain) and S. epidermidis, staphylococcal secreted lipases appear to exist as pairs in staphylococcal genomes. Family members have high sequence identity (>50%) both within pairs and across strains, but some functional differences [4,16,29.33].

Unlike most of the lipases that have been characterized as esterification catalysts, these staphylococcal lipases have been shown to function under aqueous conditions. We have shown that SAL-1 and SAL-2 are capable of using some of the smallest alcohols as esterification substrates; they are therefore at least partially functionally distinct from SEL-1. It is not unlikely that other staphylococcal lipases have similar properties.

3.8 References

[1] T. Baba, T. Bae, O. Schneewind, F. Takeuchi, K. Hiramatsu, Genome Sequence of *Staphylococcus aureus* Strain Newman and Comparative Analysis of Staphylococcal Genomes : Polymorphism and Evolution of Two Major Pathogenicity Islands, J. Bacteriol, 190 (2008) 300–310.

[2] T. Bae, O. Schneewind, The YSIRK-G / S Motif of Staphylococcal Protein A and Its Role in Efficiency of Signal Peptide Processing The YSIRK-G / S Motif of Staphylococcal Protein A and Its Role in Efficiency of Signal Peptide Processing, 185 (2003).

[3] A. Bajaj, P. Lohan, P.N. Jha, R. Mehrotra, Enzymatic Biodiesel production through lipase catalyzed transesterification : An Overview, J. Mol. Catal. B. Enzym. 62 (2010) 9–14.

[4] B. Cadieux, V. Vijayakumaran, M.A. Bernards, M.J. McGavin, D.E. Heinrichs, Role of Lipase from Community-Associated Methicillin-Resistant *Staphylococcus aureus* Strain USA300 in Hydrolyzing Triglycerides into Growth-Inhibitory Free Fatty Acids, J. Bacteriol. 196 (2014) 4044.

[5] N.R. Chamberlain, S.A. Brueggemann, Characterisation and expression of fatty acid modifying enzyme produced by *Staphylococcus epidermidis*, J. Med. Microbiol. 46 (1997) 693–697.

[6] N.R. Chamberlain, B. Imanoel, Genetic regulation of fatty acid modifying enzyme from Staphylococcus aureus, J. Med. Microbiol. 44 (1996) 125–129.

[7] R.C. Chang, S.J. Chou, J.F. Shaw, Synthesis of fatty acid esters by recombinant *Staphylococcus epidermidis* lipases in aqueous environment, J. Agric. Food Chem. 49 (2001) 2619–2622.

[8] R. Chang, J.C. Chen, J. Shaw, Studying the Active Site Pocket of *Staphylococcus hyicus* Lipase by Site-Directed Mutagenesis, Biochem. Biophys. Res. Commun. 10 (1996) 6–10.

[9] S.V. Iersel, L. Gamba, A. Rossi, S. Alberici, B. Dehue, J.V.D. Staiij, A. Flammini, “ALGAE-BASED BIOFUELS” AquaticBiofuels, Food and

Agriculture Division of the United Nations. (2009) http://www.fao.org/bioenergy/aquaticbiofuels/documents/detail/en/?uid=20824

[10] B.A. Diep, S.R. Gill, R.F. Chang, T.H. Phan, J.H. Chen, M.G. Davidson, F. Lin, J. Lin, H.A. Carleton, E.F. Mongodin, G.F. Sensabaugh, F. Perdreau-Remington, Complete genome sequence of USA300, an epidemic clone of community-acquired meticillin-resistant *Staphylococcus aureus*, Lancet 367 (2006) 731–739.

[11] A.M. Farrell, T.J. Foster, K.T. Holland, Molecular analysis and expression of the lipase of *Staphylococcus epidermidis*., J. Gen. Microbiol. 139 (1993) 267–277.

[12] A.D. Ferrão-Gonzales, I.C. Véras, F. a L. Silva, H.M. Alvarez, V.H. Moreau, Thermodynamic analysis of the kinetics reactions of the production of FAME and FAEE using Novozyme 435 as catalyst, Fuel Process. Technol. 92 (2011) 1007–1011.

[13] H. Fukuda, A. Kondo, H. Noda, Biodiesel fuel production by transesterification of oils, J. Biosci. Bioeng. 92 (2001) 405–416.

[14] F. Götz, F. Popp, E. Kom, K.H. Schleifer, Complete nucleotide sequence of the lipase gene from Staphylococcus hyicus cloned in Staphylococcus carnosus, Nucleic Acids Res. 13 (1985) 5895–5906.

[15] R. Gupta, N. Gupta, P. Rathi, Bacterial lipases: An overview of production, purification and biochemical properties, Appl. Microbiol. Biotechnol. 64 (2004) 763–781.

[16] H. Horchani, I. Aissa, S. Ouertani, Z. Zarai, Y. Gargouri, A. Sayari, Journal of Molecular Catalysis B : Enzymatic Staphylococcal lipases : Biotechnological applications, J. Mol. Catal. B, Enzym. 76 (2012) 125–132.

[17] H. Horchani, H. Mosbah, N. Ben Salem, Y. Gargouri, A. Sayari, Biochemical and molecular characterisation of a thermoactive, alkaline and detergent-stable lipase from a newly isolated *Staphylococcus aureus* strain, J. Mol. Catal. B Enzym. 56 (2009) 237–245.

[18] H. Horchani, S. Ouertani, Y. Gargouri, A. Sayari, The N-terminal His-tag and the recombination process affect the biochemical properties of

Staphylococcus aureus lipase produced in Escherichia coli, J. Mol. Catal. B Enzym. 61 (2009) 194–201.

[19] W.O.O. Hyuk, H. Kim, C. Lee, T. Oh, Biochemical Properties and Substrate Specificity of Lipase from *Staphylococcus aureus* B56, J. Microbiol. Biotechnol. 12 (2002) 25–30.

[20] K.P. Lee, H.K. Kim, Enzymatic Transesterification reaction using *Staphylococcus haemolyticus* L62 lipase crosslinked on magnetic microparticles, Journal Mol. Catal. B, Enzym. 115 (2015) 76–82.

[21] N. Lenfant, T. Hotelier, Y. Bourne, P. Marchot, A. Chatonnet, Chemico-Biological Interactions Proteins with an alpha / beta hydrolase fold : Relationships between subfamilies in an ever-growing superfamily, Chem. Biol. Interact. 203 (2013) 266–268.

[22] J.P. Long, J. Hart, W. Albers, F. a. Kapral, The production of fatty acid modifying enzyme (FAME) and lipase by various staphylococcal species, J. Med. Microbiol. 37 (1992) 232–234.

[23] C.M. Longshaw, A.M. Farrell, J.D. Wright, K.T. Holland, Identification of a second lipase gene , gehD , in *Staphylococcus epidermidis* : comparison of sequence with those of other staphylococcal lipases, Microbiology 146 (2000) 1419–1427.

[24] M. Mitta, M. Miyagi, I. Kato, S. Tsunasawa, Identification of the Catalytic Triad Residues of Porcine Liver Acylamino Acid-Releasing Enzyme, J. Biochem. 123 (1998) 924–931.

[25] J.E. Mortensen, T.R. Shryock, F. a. Kapral, Modification of bactericidal fatty acids by an enzyme of *Staphylococcus aureus*, J. Med. Microbiol. 36 (1992) 293–298.

[26] K. Nikoleit, R. Rosenstein, H.M. Verheij, F. Gotz, Comparative biochemical and molecular analysis of the *Staphylococcus hyicus*, *Staphylococcus aureus* and a hybrid lipase. Indication for a C-terminal phospholipase domain, Eur. J. Biochem. 228 (1995) 732–738.

[27] B.-C. Oh, H.K. Kim, J.-K. Lee, S.-C. Kang, T.-K. Oh, *Staphylococcus haemolyticus* lipase : biochemical properties , substrate specificity and gene cloning, FEMS Microbiology Letters 179 (1999) 385-392.

[28] D.L. Ollis, E. Cheah, M. Cygler, B. Dijkstra, The α/β hydrolase fold, Protein Engineering 5 (1992) 197-211.

[29] R. Rosenstein; F. Götz, Staphylococcal lipases: Biochemical and molecular characterization, Biochimie. (2000) 1005–1014.

[30] S. Ransac, M. Blaauw, B.W. Dijkstra, a T. Slotboom, J.W. Boots, H.M. Verheij, Crystallization and preliminary X-ray analysis of a lipase from *Staphylococcus hyicus*, J. Struct. Biol. 114 (1995) 153–155.

[31] J. Rollof, S.A. Hedstrom, P. Nilsson-Ehle, Positional specificity and substrate preference of purified *Staphylococcus aureus* lipase, Biochim. Biophys. Acta 921 (1987) 370–377.

[32] J. Rollof, S. Normark, In vivo processing of Staphylococcus aureus lipase, J. Bacteriol. 174 (1992) 1844–1847.

[33] J.W.F. a Simons, M.D. Van Kampen, I. Ubarretxena-Belandia, R.C. Cox, C.M. Alves Dos Santos, M.R. Egmond, H.M. Verheij, Identification of a calcium binding site in *Staphylococcus hyicus* lipase: Generation of calcium-independent variants, Biochemistry. 38 (1999) 2–10.

[34] J. Skjold-Jørgensen, J. Vind, A. Svendsen, M.J. Bjerrum, Altering the activation mechanism in *Thermomyces lanuginosus* lipase, Biochemistry. 53 (2014) 4152–4160.

[35] J.J.W. Tiesinga, G. Van Pouderoyen, M. Nardini, S. Ransac, B.W. Dijkstra, Structural Basis of Phospholipase Activity of Staphylococcus hyicus lipase, J. Mol. Biol. 371 (2007) 447–456.

[36] R. Verger, “Interfacial activation” of lipases: Facts and artifacts, Trends Biotechnol. 15 (1997) 32–38.

[37] A.R.M. Yahya, W.A. Anderson, M. Moo-Young, Ester synthesis in lipase-catalyzed reactions, Enzym. Microb. Biotechnol. 23 (1998) 438–450.

[38] G. Nantel, P. Proulx, Lipase Activity in *E. coli,* Biochim. Biophys. Acta. 316 (1973) 151-161.

[39] K. Arnold, L. Bordoli, J. Kopp, T. Schwede, The SWISS-MODEL Workspace: A web-based environment for protein structure homology modelling, Bioinformatics 22 (2006) 195-201.

[40] The PyMOL Molecular Graphics System, Version 1.8 Schrödinger, LLC.

[41] PSORTb v3.0: N.Y. Yu, J.R. Wagner, M.R. Laird, G. Melli, S. Rey, R. Lo, P. Dao, S.C. Sahinalp, M. Ester, L.J. Foster, F.S.L. Brinkman, PSORTb 3.0: Improved protein subcellular localization prediction with refined localization subcategories and predictive capabilities for all prokaryotes, Bioinformatics 26(13) (2010) 1608-1615.

Chapter IV

Design and Analysis of Staphylococcal FAME-LUSH fusions

4.1 Introduction

Our second goal in this project was the development (via rational design or random mutagenesis) of a FAME protein better suited to commercial biodiesel production [9]. Protein longevity is an important consideration for commercial enzyme utility; proteins that remain functional for longer periods of time are more cost-effective simply because they require replacement or replenishment less frequently. Thermal stability, the melting temperature of a protein and its ability to remain folded and functional at high temperatures, is a reliable predictor of protein longevity. Enhancement of thermal stability, therefore, is a common goal in the field of commercial enzyme design [15,23].

We were also aware of the fact that wild-type FAME (whatever protein it might be) preferentially esterified large alcohol substrates [19]. Because the most common alcohols used in biodiesel synthesis are small alcohols, such as methanol and ethanol, modifying wild-type FAME to enhance affinity for these substrates was another possible approach to FAME enhancement. Furthermore, a lipase capable of catalyzing esterification in an aqueous, low-alcohol solution is theoretically compatible with a bioreactor in which a feedstock organism (e.g. algae) produces lipids while the lipase concurrently esterifies them into biodiesel.

In most other cases of documented lipase-catalyzed esterification, the reaction is detectable at high levels of substrate and extremely hydrophobic conditions; water is often present in trace amounts or absent entirely [5,11,13,14,15,18]. High alcohol concentrations, organic solvents, and low water availability are all toxic to algae and therefore incompatible with algal bioreactors. The advantage of high-substrate, low-water, organic esterification systems is that substrate availability is not the rate-limiting parameter of the reaction, because even an enzyme with low affinity for substrate can be expected to approach saturation. In the aqueous system we have employed, alcohol availability is rate-limiting, due to the low binding affinity of FAME for small alcohols. Modification of wild-type FAME to improve its binding affinity for small alcohols is therefore a possible approach to improve lipase-catalyzed aqueous esterification; a FAME that works in a low-alcohol system is more “algae-friendly.”

These goals were established well before the actual identity of the FAME(s) was determined, and as such we were not yet aware of the specific challenges that would be encountered in this FAME improvement phase. Nevertheless, several possible strategies were anticipated to be effective. Random mutagenesis, followed by experimental screening of the resulting mutant library, can be used to find useful protein variants in many instances [25]. In the case of FAME, which has been hypothesized to afford *S. aureus* strains a selective advantage by increasing their resistance to bactericidal free fatty acids

in their growth environment. This suggested using the approach of screening a FAME mutant library by transforming it into *E. coli* and then screening the bacteria by plating the cells onto solid media containing bactericidal fatty acids and small alcohol substrate with which to esterify them [20,24] (Figure 4-1).

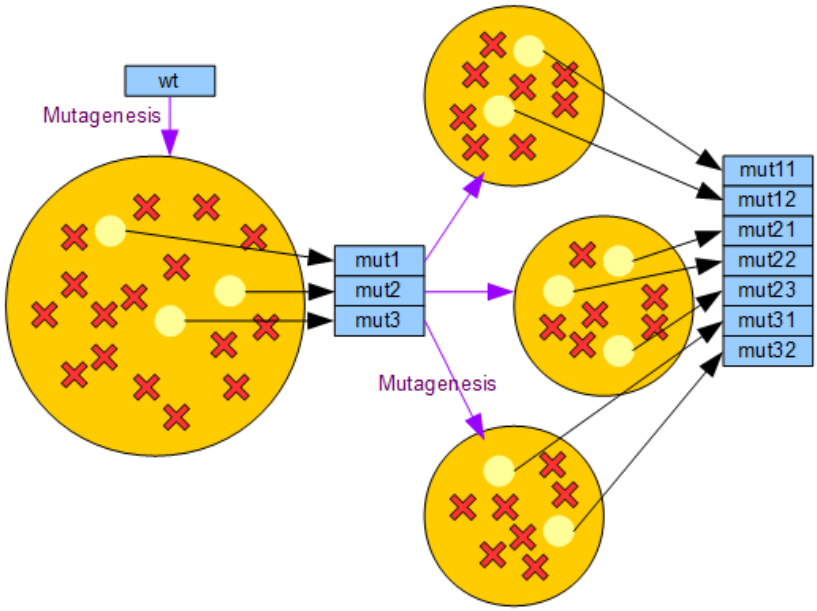

Figure 4-1. Schematic of mutant library screening of a hypothetical mutagenized FAME library. Random mutagenesis of FAME genes, followed by transformation into E. coli plated onto media containing bactericidal FAME substrates. Cells transformed with improved FAME mutants will multiply to form colonies. If necessary, multiple rounds of screening with more stringently selective media can be used.

Transformants capable of growing in fatty acid-rich media could be screened on media with successively greater amounts of free fatty acid. PCR amplification of the most fatty acid-resistant clones would reveal which FAME mutants have optimal affinity for small alcohol esterification substrates.

The prospect of using rational protein design, on the other hand, presented a different challenge; specifically, the goal of improving FAME affinity for small alcohols. In chapter III we hypothesized that wild-type FAME's affinity for large alcohols was entropy-driven, given that large alcohol binding buries more hydrophobic surface area and leaves less exposed to the aqueous solution. A decrease in the size of the binding pocket could increase the amount of hydrophobic surface contact between substrate and protein, improving the thermodynamic favorability of binding. However, the fold of the FAMEs, as predicted by the crystal model of the closely related *S. hyicus* lipase, shows that the amino acids forming the hydrophobic binding groove are recessed deeply toward the core of the protein. Rational design for improving thermostability offers many more options than rational design for substrate affinity [7,26], because stability is more likely to be impacted (and potentially enhanced) by mutations far from the substrate binding site. Rational redesign of core amino acid residues is perilous; perturbation of the protein core is much more likely to cause dramatic destabilization of the overall protein fold.

In lieu of redesigning the amino acids of the FAME protein(s), we took a cue from an observation made during routine troubleshooting of the Long et. al. assay [19]. Under our experimental conditions, in which pH 6.0 low-salt buffer is incubated with protein, 250 μg/mL (885 μM) oleic acid, and up to 40% v/v ethanol (although we used 5% v/v butanol during initial screening). In the

absence of alcohol, oleic acid is not miscible with the buffer; it forms small droplets floating on the surface of the aqueous phase. The alcohol-buffer mixture, however, allows oleic acid to form a milky, turbid suspension of microscopic oleic acid droplets, dramatically increasing the available surface area of the fatty acid substrate. As discussed in chapter II, we attempted to use this turbidity as a measure of esterification, reasoning that the morphology or number of lipid droplets would be affected by the depletion of substrate and the accumulation of ester. We did not successfully develop a reliable quantitative measure of FAME activity in crude cell lysate by monitoring changes in turbidity, as co-precipitation of other proteins with the fatty acid confounded measurement of catalysis-driven loss of light scattering. Furthermore, although all of our FAME assay samples were incubated at 37°C (*S. aureus* colonizes human tissue and therefore its enzymes generally function well near human body temperature [6,19]), we did attempt multiple sample incubation strategies, and noted a marked visible difference between samples that had been shaken during incubation and those that had been incubated without shaking.

Lipases, as discussed in chapter III, necessarily function only when their lipid substrates are present; unlike soluble substrates, lipids are typically sequestered in an aqueous system, either as lipid droplets, micelles or membranes. Lipases catalyzing esterification are similarly constrained; in our case, esterification of alcohol and fatty acid can only occur in the space at the

surface of the oleic acid droplets. The lack of homogeneity in the system, therefore, serves to localize the esterification events to a subset of total solution volume. This explains why homogenization via shaking impaired catalysis: the enzymes were prevented from co-localizing to the lipid droplets via thermodynamically favorable interactions (interfacial activation may play a role in this, as mentioned in chapter III [12,13,14,29,30]) (Figure 4-2).

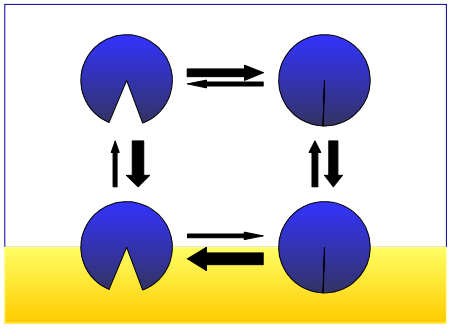

Figure 4-2. Interfacial activation. A lipase/esterase that exhibits interfacial activation exists in an ensemble of four states. It can be active or inactive, but can also exist at or within the lipid interface, or far away from it. The favorable energy of binding substrate, combined with the favorable energy of activating at the lipid interface, push the equilibrium of the ensemble toward the bound/active state, resulting in strong co-localization of protein to lipid.

Similarly, only enzyme and ethanol molecules within the space immediately around the oleic acid droplets can participate in the esterification reactions. The overall ethanol concentration in the system, therefore, does not necessarily fully reflect the ethanol concentration in the microenvironments around the oleic acid droplets where the local ethanol concentration is a determinant of the rate of esterification. Homogenization of the sample prevents co-localization of the ethanol to the oleic acid and FAMEs; the difference in esterification between

shaken and unshaken suggests that the ethanol concentration in the immediate microenvironment is greater than the overall ethanol concentration in the sample, and that this effect has a non-negligible effect on catalysis.

This suggested an alternative approach to improving catalysis without redesign of the lipase domain of the FAME(s). Spacial clustering of binding sites affects ligand (or substrate) concentration in the vicinity of the cluster by increasing the likelihood that a ligand molecule, having dissociated away from the binding site, will encounter another binding site before it diffuses far. As diffusion away from the location of the binding sites is kinetically hindered by this phenomenon, the equilibrium state of the system will feature a ligand concentration in the vicinity of the binding sites that is greater than the ligand concentration elsewhere in the system. This phenomenon called rebinding [4]. It has been shown experimentally that cell surface receptor binding can be modulated by regulating receptor localization; Gopalakrishnan et. al. and Chu et. al. have both shown that the mammalian ligand FGF-2 binding to cell surface receptors is dependent on the clustering of multiple receptors on lipid rafts on the cell membrane [12,33]. It is likely, therefore, that rebinding affects cell sensitivity to signal molecules *in vivo* when the receptors are permitted to adopt their natural, clustered arrangement. Computational predictions show that the rebinding effect may not universally improve ligand residency and may be reduced at very high binding site clustering [12], but is contingent on a number of

factors. We reasoned that clustering of ethanol binding sites near the oleic acid droplets would enhance the existing co-localization effect, increasing the residence time of ethanol in the binding site of FAME by increasing the ethanol concentration local to the oleic acid and proteins. As the FAMEs are soluble proteins, incorporation into lipid rafts was not a reasonable option. Immobilization of staphylococcal lipases on polymer surfaces is a very popular strategy for lipase optimization, and has been shown to improve protein stability and longevity, and gain in activity is often seen as well [5,11,13,18]; the reasons for this are unclear, but rebinding may play a role. In the case of immobilized lipases, however, it is difficult to attribute changes in function to a single factor because linkage to the underlying substrate can have thermodynamic (stabilizing or destabilizing) effects on the fold of the protein. We opted to search for a soluble alcohol-binding protein that could be covalently tethered to FAME, which would hypothetically cause improved rebinding (and attendant increase in local concentration) of ethanol in the microenvironment of the oleic acid droplet surfaces.

4.2 Alcohol Binding Proteins

We sought an alcohol-binding protein that could be linked to FAME (for this phase of the project we focused exclusively on SAUSA300_2603, also called SAL-1). Several criteria had to be met by our selected protein. Because of the

system in which we planned to use it, a soluble (non-transmembrane, non-fibrous) protein was preferred. Because we planned to use *E. coli* as our recombinant expression system, the selected protein would have to express in *E. coli*. We also chose to exclude any other enzymes from consideration, in order to avoid some other enzymatic depletion of ethanol during incubation of the samples. Finally, we hoped to select a protein that binds ethanol with much more affinity than FAME (i.e. a low k_d) in order to gain the greatest rebinding effect. These criteria specified a soluble, easily expressed ethanol-binding receptor protein.

Human alcohol-binding proteins are naturally of greater interest, and therefore many have been studied [21,27] (Figure 4-3 A). However, human transmembrane alcohol-binding proteins were already ruled out, as there are unique pitfalls associated with recombinant expression of transmembrane proteins (we discuss this further in the next chapter), particularly very large ones. Alcohol dehydrogenase, for example, is a well-characterized human protein, soluble, and binds alcohol, but is an enzyme in it's own right. This renders it unsuitable for our purpose.

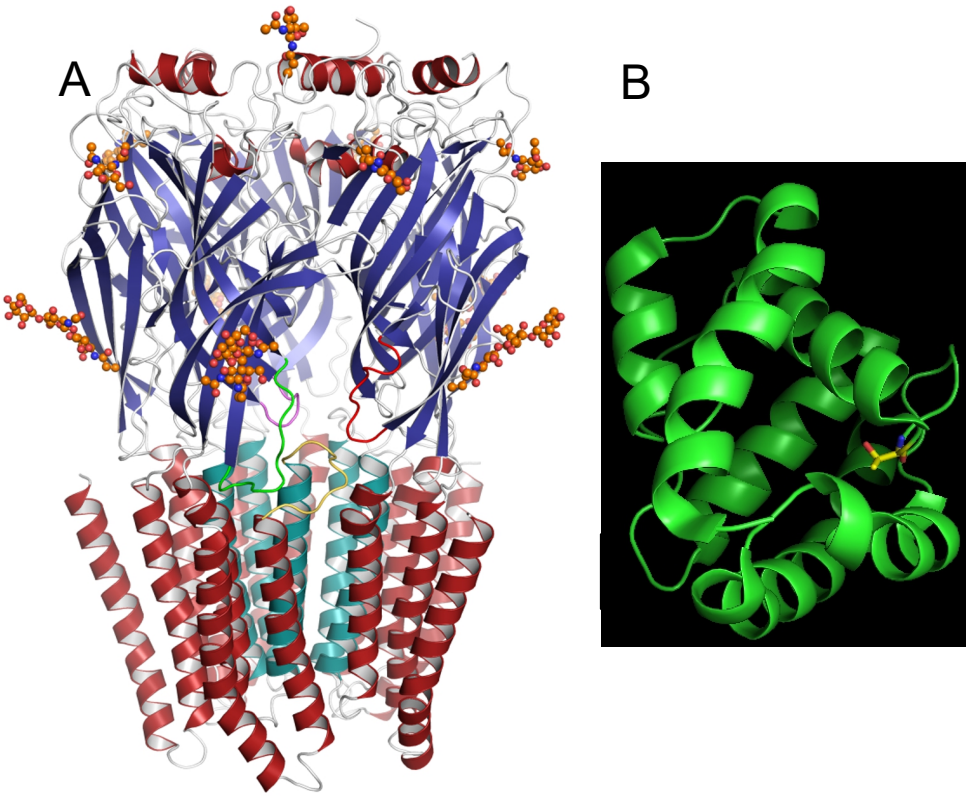

Figure 4-3. Crystal models of alcohol-binding proteins. Human $GABA_A$ receptor (A), an alcohol receptor, exists a transmembrane pentamer [35]. *Drosophila melanogaster* LUSH, visualized with PyMOL [36] (B) is a soluble, 14 kD monomer [17]. One of the two is more readily expressed in *E. coli*.

Fortuitously, however, vertebrate and arthropod chemosensory systems have evolved along very different paths. Insects' chemosensory apparatus analogous to the human sense of smell is not linked to their respiratory systems, but is instead housed in hairs situated along their bodies. The receptor proteins that a fly of the species *Drosophila melanogaster* uses to “smell” airborne compounds in its surroundings include soluble receptors such as the alcohol-

binding protein LUSH [1,17,34]. LUSH is a 14 kD protein named for the behavior of LUSH-knockout flies, which lose the wild-type's aversion response to alcohol-rich solutions. There is at least one crystal model for LUSH in the Protein Data Bank, and its alcohol binding site has been identified (Figure 4-3 B). Thode et. al. have used selective mutagenesis to show that threonine 57 is a key residue for alcohol binding, forming a hydrogen bond with the ligand's alcohol group [28]. Recombinant LUSH expresses well in *E. coli*, although the *Drosophila* form of the gene contains introns. We chose LUSH as our supplemental alcohol-binding domain because it met the criteria outlined above.

4.3 FAME-LUSH Design

Chapter II describes the specifics of our design strategy for the FAME-LUSH fusion. We chose to focus on SAUSA300_2603/SAL-1 [23] as our FAME of choice for this phase of the project. As mentioned in section 4.2, the gene coding for LUSH contains introns, which are incompatible with recombinant expression in *E. coli*. In lieu of seeking cDNA for the LUSH gene, we opted to synthesize it using PCR and a set of nine oligonucleotide primers. With further PCR amplification, we incorporated codons for an alpha-helical linker described by Arai et. al., with the primary sequence AEAAAKEAAAKA, to create space between the two protein domains and allow them to fold independently [2]. The

final open reading frame coded for the following protein (n-terminus to c-terminus): pelB leader sequence-6xHis tag-SAL-1-LUSH (Figure 4-4).

Figure 4-4. Open reading frame of the gene for the FAME-LUSH fusion variant. The pelB leader sequence, included in stock pET22b(+), directs the nascent polypeptide to the periplasmic space during translation. The 6xH hexahistidine tag aids in purification via nickel affinity chromatography, and the alpha-helical linker serves to separate the two globular domains for independent folding.

4.4 FAME-LUSH-T57A

Our hypothesis predicted that the FAME-LUSH fusion would show an improved rate of esterification due to enhanced ethanol rebinding by virtue of the LUSH domain. However, it was also possible that the presence of the LUSH domain in the fusion protein might have some inadvertent stabilizing or destabilizing effect on the FAME domain. As we discussed in sections 3.6 and 4.1, stability plays a role in catalytic esterification by lipases; it impacts both the overall longevity of the enzymes and the propensity to take on the active conformation. In order to reject the possibility that the LUSH domain impacts the FAME domain's stability or fold simply by virtue of its presence, we also constructed a FAME-LUSH-T57A variant, in which the 57th amino acid of the LUSH domain is mutated from a threonine to an alanine. Thode et. al. [28] showed that T57A LUSH lacks discernible ethanol-binding ability, but retains the thermostability of the wild type. This is due to the fact that the alanine cannot

form the energetically favorable hydrogen bond that the wild-type threonine forms with the alcohol ligand in wild type LUSH. Our FAME-LUSH-T57A variant, therefore, was predicted to have the same properties as FAME-LUSH (wild type) with the exception that it lacks the LUSH domain's ethanol-binding ability.

4.5 FAME-LUSH Fusion Purification

As we discussed in section 2.14, purification of the three recombinant proteins used in our quantitative FAME activity assays involved multiple chromatographic steps. In the case of each, codons for a hexahistidine tag were incorporated into the open reading frame of the recombinant genes, 3' of the pelB leader sequence and 5' of the codons corresponding to the FAME domain. Initially we planned to purify the recombinant proteins via nickel affinity chromatography of *E. coli* cell sonicate supernatant. However, the histidine-tagged recombinant proteins did not bind the nickel column as strongly as hoped, generally eluting from the column near 25 mM imidazole. As a result, many other endogenous *E. coli* proteins co-purified with the FAME constructs during this step, even if the chromatography was performed under denaturing conditions in order to recover inclusion body proteins.

In order to overcome this obstacle, after dialysis to refold the post-nickel column samples, we passed the solution through two successive ion exchange columns and eluted purified FAME constructs using a salt gradient. At this point,

SDS-PAGE visualization of the proteins made it clear that the protein “backlog” created by the pelB leader sequence resulted in a significant amount of scarring at the N-terminus of the proteins, caused by incomplete proteolysis of the pelB amino acids. This is visible as a double-banding effect on the coomassie stained PAGE gel. Future users of pET22b and the pelB leader sequence beware!

4.6 FAME-LUSH Ethanol Binding and Fluorescence Spectroscopy

The fluorescent compound 8-anilino-1-naphthalene-sulfonic acid (ANS) associates non-specifically with solvent-exposed hydrophobic surfaces on proteins. ANS gains fluorescence (with absorption near 360 nm and emission near 495 nm) when bound to proteins; the fluorescence signal of a protein-ANS solution can therefore serve as an indicator of the amount of hydrophobic surface exposed by a protein. ANS is used to show destabilization or unfolding in a protein population as hydrophobic core residues become exposed, or the availability of a protein's hydrophobic binding sites . In the case of LUSH, titration of LUSH-ANS with alcohol has been used to show a decrease in ANS fluorescence as alcohol outcompetes and displaces the ANS molecules in the LUSH alcohol binding site [28].

We incubated purified FAME and its fusion variants with ethanol and ANS in droplets in a 96-well plate, monitoring ANS fluorescence. As expected, ANS fluorescence was greater at higher ANS concentrations, displaying a classic

binding curve. In the presence of ethanol, however, ANS fluorescence was suppressed in a dose-dependent fashion. Protein-free droplets showed negligible background fluorescence, indicating that direct interaction between ethanol and ANS does not contribute meaningfully to the fluorescence signal of protein-bound ANS samples.

All three variants (FAME, FAME-LUSH, FAME-LUSH-T57A) showed loss of fluorescence upon ethanol binding, but the FAME-LUSH fusion showed a greater loss of fluorescence compared to wild-type FAME, indicating a greater binding affinity for ethanol (Figure 4-5). The T57A mutant fusion protein showed a smaller loss of fluorescence than the other FAME-LUSH fusion, verifying that the T57A mutation abolishes specific ethanol binding. It does, however, show greater loss of fluorescence than wild type FAME; this is to be expected, because the addition of the LUSH domain adds additional hydrophobic surfaces to the protein, increasing both baseline (in the absence of ethanol) fluorescence and the possibility of weak hydrophobic interactions between ethanol and protein when the latter is present. The T57A mutant actually loses a slightly smaller percentage of it's maximum fluorescence when incubated with alcohol, meaning that the T57A LUSH mutant domain actually has less overall alcohol affinity than the FAME domain.

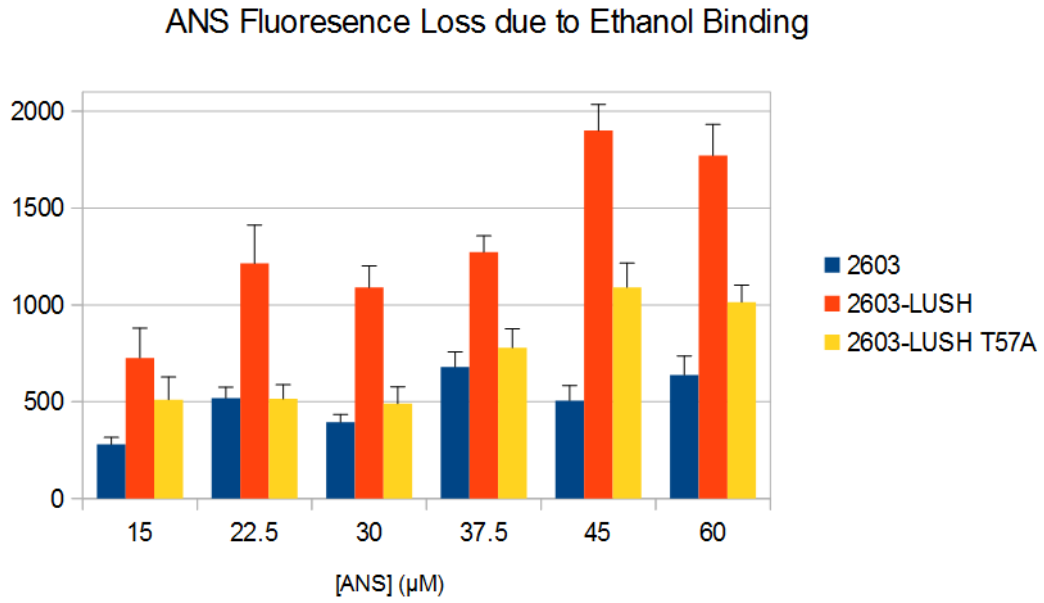

Figure 4-5. Loss of ANS fluorescence due to ethanol binding. At 15, 30, 45, and 60 μM ANS, the difference in fluorescence between 0% ethanol and 15% ethanol (v/v) is indicated by the corresponding y-axis values. A greater loss in fluorescence indicates more association between protein and ethanol.

4.7 FAME Activity of FAME-LUSH Fusions

We used the Long et. al. assay to evaluate FAME activity for our three purified constructs. Because we were interested in FAME activity with respect to ethanol, however, we used ethanol as our alcohol, and varied the ethanol concentration from 0.5% to 40% v/v, or 171 mM to 6.85 M. This range was constrained by the fact that below 0.5% ethanol, the oleic acid did not form a turbid, colloidal suspension of microscopic droplets, and remained in large visible

droplets floating on the surface of the buffer. Similarly, above 40% ethanol the oleic acid goes into solution entirely, producing a clear, homogeneous sample. Because we were interested in examining the effect of enhanced co-localization, meaningful results would not be derived from comparison of kinetic data between colloidal and non-colloidal reaction conditions. Thode et. al. reported the k_d of LUSH-ethanol binding to be ~107 mM [28], only slightly higher than our minimum of 0.5% v/v (86 mM). The reactions were allowed to proceed for 3 hours, during which the reaction rate was constant based, rather than 24. The molecular ions for butyl oleate and ethyl oleate have m/z= 338-339 and 310-311, respectively. Initially, we evaluated relative FAME activity by counting molecular ions, but later opted to detect at m/z = 264, a characteristic ion formed by oleate esters. At m/z = 264, small molecular weight contaminants and solvents are not detected, but the signal (ion count) is much higher than for the molecular ion, allowing more sensitive detection. The one drawback of using m/z = 264 is that it is also a part of the fragmentation pattern of unreacted oleic acid, which is present in the hexane extract. Although oleic acid has a longer retention time, trace amounts co-elute with the alkyl esters, and are discernible when the m/z signal is close to the lower detection threshold; this is the cause of the small signal seen in the negative controls of figure 3 in appendix I.

Mass spectrometric comparison of the esterification data shows that, compared to wild type FAME and FAME-LUSH-T57A, FAME-LUSH catalysis

proceeds at a greater rate at low ethanol concentrations, where ethanol availability is (apparently) rate-limiting (Figure 4-6 A). At higher ethanol concentrations (≥20% v/v), differences in the rate of catalysis diminish greatly as ethanol availability ceases to be the rate-limiting factor in the reaction. This is consistent with our hypothesis that the presence of an alcohol-binding LUSH domain enhances the availability of ethanol to the FAME domain.

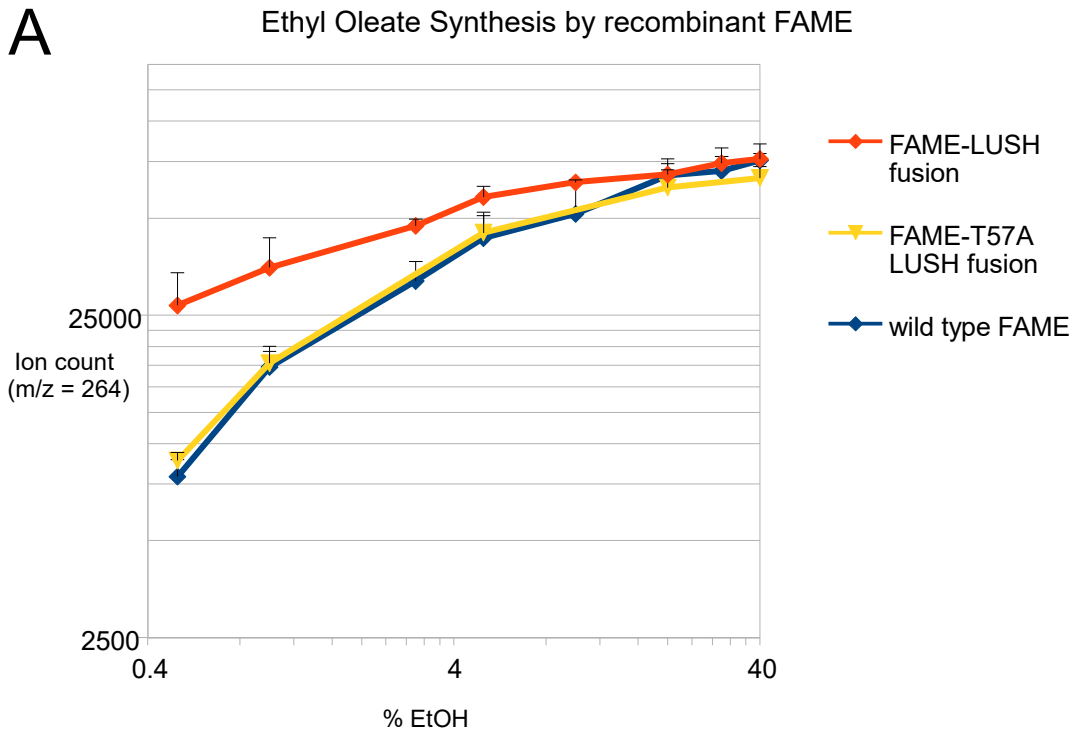

Figure 4-6. GC-MS determination of ester synthesis as a function of ethanol concentration. (A) Although the variants all have similar activities at higher ethanol levels, the 2603 FAME-LUSH fusion catalyzes esterification at a greater rate at low alcohol concentrations. The LUSH point mutant T57A, which has been demonstrated to not bind ethanol, mimics the wild-type FAME's catalytic ability.

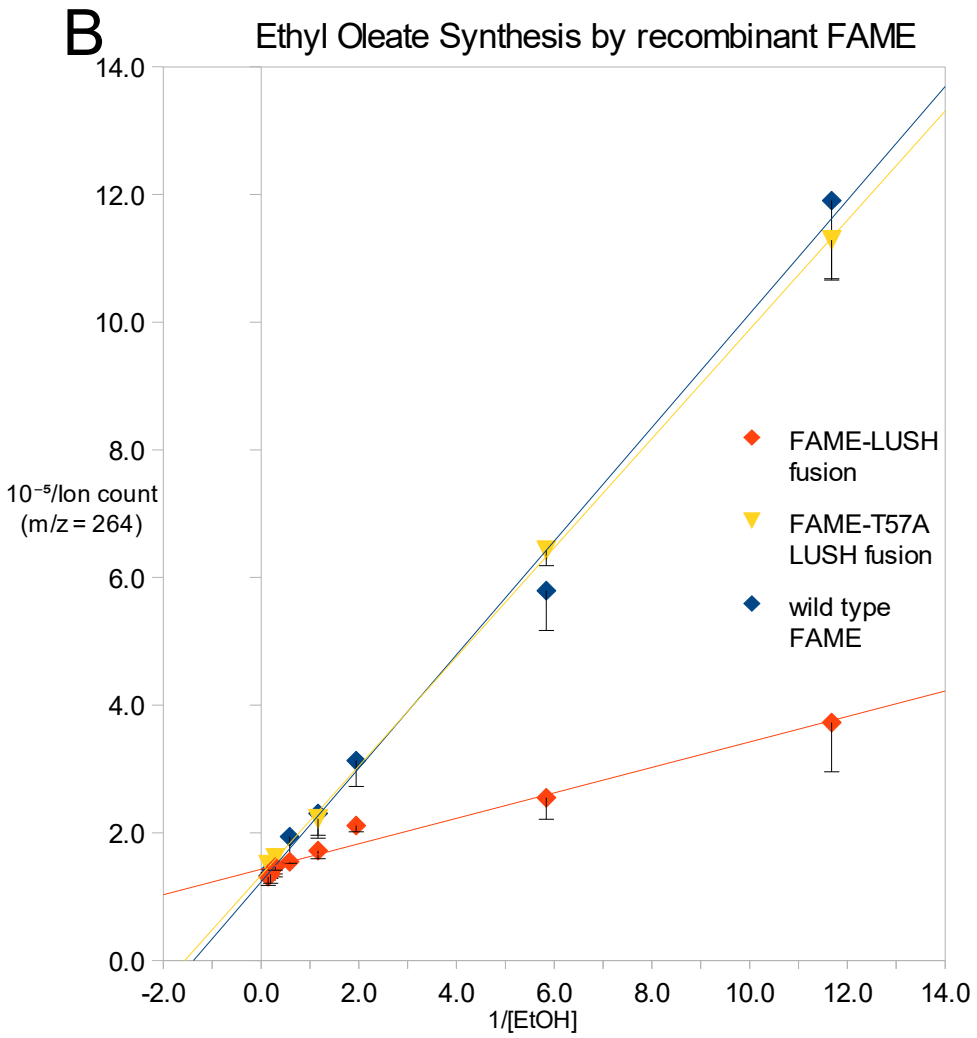

Figure 4-6, continued. (B) A Lineweaver-Burk double reciprocal plot shows similar $1/V_{max}$ for all three enzymes but greater effective $1/K_M$ (and therefore a lower effective K_M) for the 2603 FAME enzyme fused to the wild-type LUSH protein.

Because the FAME-LUSH-T57A variant shows enzymatic activity comparable to that of wild type FAME at low and high ethanol concentrations, we conclude that it is the alcohol-binding function of the LUSH domain that is responsible for this

effect, as opposed to some other influence it might have on the FAME domain (i.e altered stability).

4.8 Kinetic Data Interpretation

Unsurprisingly, double reciprocal Lineweaver-Burk plot of this data shows similar V_{max} values for the three constructs. However, the double reciprocal regression line for FAME-LUSH has a much shallower slope, and therefore a more negative x-intercept (Figure 4-6 B). In Michaelis-Menten theory, the x-intercept in a Lineweaver-Burk plot corresponds to $-1/K_M$. Visual inspection of the regression line assigned by our spreadsheet software shows a significantly more negative $-1/K_M$ value for the FAME-LUSH fusion, and hence a smaller value of K_M. Analysis of the raw data with GraphPad Prism 7, however, shows a more modest 3.46-fold decrease in effective K_M compared to wild type FAME and the T57A fusion mutant (Table 4-1).

Table 4-1. Effective K_M values for FAME and FAME-LUSH fusion constructs with respect to ethanol, as determined by GraphPad Prism 7. The LUSH fusion shows a lower effective K_M, meaning that the local concentration of ethanol around the FAME domain active site is greater than when the LUSH domain is absent. The FAME-LUSH-T57A mutant lacks this property, indicating that it is a consequence of ethanol binding by LUSH.

Variant	K_M (mM)
wt FAME	622 ±59
FAME-LUSH	180 ±21
FAME-LUSH-T57A	616 ±75

Note, however, that we have not modified any of the terms that make up the actual K_M value for the FAME domain: k_{on}, k_{cat}, and k_{off}. The rebinding effect instead increases the local concentration of substrate near the enzyme active site, which increases the rate of substrate binding without altering the actual kinetic constant for substrate binding (k_{on}). Because $k_{off}/k_{on} = k_d$, the ~3-fold decrease in effective K_M should correspond to a ~3-fold decrease in k_d. we can compare this with the result of Gopalakrishnan et. al., who report an effective ~5.75-fold decrease in the dissociation rate effective k_d for HSPG-FGF-2 as a result of HSPG receptor clustering into groups of 5-10 molecules per cluster *in vivo*[12], and Chu et. al., who similarly showed a 5-fold loss of binding when clustering is impaired [33]. In our case, many of the substrate concentrations tested are so high that an actual threefold increase in concentration is physically impossible, but as shown in Figure 4-6 B, at concentrations >500 mM V_0 for the fusion is statistically indistinguishable from V_0 for the wild type, indicating that rebinding does not meaningfully impact substrate concentration at those concentrations. Our calculated difference between the wild type FAME's K_M and the effective K_M of the fusion is therefore determined predominantly by the V_0s observed at lower (85-500 mM) concentrations.

It is worth noting that many lipase-catalyzed hydrolysis and transesterification have been shown to conform to the Ping Pong Bi Bi kinetic model [10,22,31], because a double displacement occurs during classical

hydrolysis as described in section 1.3. Several groups have shown some precedent for this deviation from classic Ping Pong Bi Bi behavior as a consequence of alcohol inhibition [3,8,10,16,29], but we observed no such effect at our ethanol concentrations. A two-step transesterification mechanism would involve the alcohol substrate acting as the nucleophile attacking the transitional enzyme-fatty acid covalent complex, making the alcohol the second substrate (substrate B) [3]. With respect to substrate B (but not substrate A), the kinetics and Lineweaver-Burk plot of such mechanisms are similar to single-substrate kinetics, meaning that both V_o is a function of substrate B concentration and V_{max} is a function of [EA*] (the concentration of enzyme already covalently complexed to substrate A), whereas K_M itself is an intrinsic property of the enzyme under the given reaction conditions. In our data, the change in V_{max} seems to be small, negligible in comparison to the change in K_M (though again, the change in apparent K_M is really only a change in effective ethanol concentration in the microenvironment near the enzyme).

Aside from Ping Pong Bi Bi kinetics, there is at least one other possible model that conforms to our data. It is generally accepted that in the first step of the catalyzed reaction, the catalytic serine's hydroxyl group serves as the nucleophile attacking the carbon in substrate A (a fatty acid or triglyceride), creating a covalently bound enzyme-acyl chain complex. At this point, in the Ping Pong Bi Bi mechanism, the leaving group can dissociate away and substrate B

(alcohol or water) can bind the complex and participate in the second displacement. Looking at the structure of a triglyceride in the SHyL binding groove, it is apparent that the triglyceride occupies most or all of the available space in the binding groove. This eliminates the possibility of the alcohol binding to the enzyme before the first attack and the dissociation of the leaving group. However, if substrate A is a fatty acid rather than a triglyceride, the enzyme can simultaneously bind both substrates prior to either displacement taking place. The possibility of this “ternary complex” allows for a non-Ping Pong kinetic model, one that our data does not reject. In the case of this ternary complex model, it is even possible for the alcohol hydroxyl to act as the first and only nucleophilic attacker, leaving the catalytic serine out of the process entirely. The possibility of such a mechanism depends on how well the serine is positioned with respect to the target carbon, and how well the other amino acid sidechains in the vicinity of the active site might stabilize a nucleophilic alcohol. There is precedent for this general process in the mechanism of aspartyl proteases, which hydrolyze amide bonds without direct covalent interaction with either substrate [32].

4.9 Conclusion

The original goal of this phase of the project was to engineer a FAME variant with superior affinity for small alcohols (i.e. ethanol), with the intent of

enhancing the rate of esterification in systems where the binding of alcohol by the enzyme was a rate-limiting factor for the reaction. The FAME-LUSH fusion does so, with an effective K_M of 180 ±21 mM, threefold lower than the wild type FAME's K_M of 622 ±59 mM. As we discussed above, this measurement is not a consequence of the FAME domain's ethanol affinity (which is unchanged, as k_{on} and k_{off} are unchanged), but of co-localization of ethanol, which makes the ethanol concentration higher near catalysis than in the bulk solution as a whole. The rebinding phenomenon is, to an extent, non-Michaelian, in that the effect of the enhanced co-localization is itself concentration dependent; Comparing V_0 for the FAME-LUSH fusion to that of wild type FAME shows that, at the lowest tested ethanol concentration, 86 mM, V_0 for the former is comparable to that of the latter when the substrate concentration is ~6-fold higher. At 250 mM ethanol, fusion shows only a ~2-fold greater localization of ethanol than that of the wild type. It is likely that this ~500 mM “ceiling” is the result of LUSH domain saturation; above that concentration, not enough LUSH binding sites are free to contribute to rebinding. This seems to be a high value considering the relatively low (20 nM) enzyme concentration. However, as the lipase binds fatty acid strongly, due to both standard enzyme-substrate affinity and interfacial activation, the enzyme becomes concentrated into the volume at or within the droplets. If the enzyme localizes into the droplets, it is potentially concentrated by 3-4 orders of magnitude as this is the volume ratio of oleic acid to aqueous

solution (using the droplet radii shown in figure 2.4 C, and the working concentration of 250 μg/mL oleic acid). If the enzyme mainly localizes to the lipid-aqueous interface, the effect is even stronger, as strong localization into the space immediately around the droplets (within 2-4 nm of the surfaces, as these are the predicted tumbling diameters of the enzymes) would increase the enzyme concentration by roughly 5 orders of magnitude.

As discussed here, the fusion's rebinding effect and consequent co-localization is only meaningful at ethanol concentrations low enough to render ethanol binding a rate-limiting factor. In the organic, ethanol-rich solvent systems which are frequently used in the study of industrial lipase applications, this advantage disappears. As a result the rebinding effect and its attendant increase in effective K_M occupies a narrow niche in terms of its potential application. A hypothetical bioreactor in which algae are used as a source of lipids or fatty acids, and staphylococcal lipases are used concurrently to convert those fatty acids into alkyl esters, would necessarily contain very low concentrations of alcohol, as algae cannot tolerate higher amounts.

In their review of biotechnological applications of staphylococcal lipases, Horchani et. al. note the advantages of immobilizing lipases on solid support, noting that covalent linkage to supports increases both recoverability and thermostability [14]. These effects improve the reusability and longevity of the lipases. They also note, however, an improvement in specific activity. This may

be a consequence of immobilization's aforementioned enhancement of thermal stability, but it may also be a rebinding co-localization effect at work. In this case, lipase immobilization would appear to be a more robust application of the strategies we have employed here. Unlike immobilization, our strategy does not confer additional longevity to the enzymes. Note, also, that the activity assay was performed with equimolar amounts of enzyme, and the fusion proteins are ~1/3rd larger than wild type FAME, meaning that the actual cost per gram of protein, in terms of the resources required to make them, diminishes the fusion's advantage.

4.10 References

[1] L. Ader, D.N.M. Jones, H. Lin, Alcohol Binding to the Odorant Binding Protein LUSH: Multiple Factors Affecting Binding Affinities, Biochemistry 49(29) (2010) 6136–6142.

[2] R. Arai, H. Ueda, A. Kitayama, N. Kamiya, Design of the linkers which effectively separate domains of a bifunctional fusion protein, Protein Eng. 14 (2001).

[3] S. Al-Zuhair, F.W. Ling, L.S. Jun, Proposed Kinetic Mechanism of the Production of Biodiesel From Palm Oil Using Lipase, P. Biochem. 42 (2007) 951-960.

[4] B.R. Caré, H.A. Soula, Impact of receptor clustering on ligand binding, BMC Sys. Biol. 5:48 (2011).

[5] G. Carta, J.L. Gainer, A.H. Benton, Enzymatic Synthesis of Esters Using an Immobilized Lipase, (1990).

[6] N.R. Chamberlain, S.A. Brueggemann, Characterisation and expression of fatty acid modifying enzyme produced by *Staphylococcus epidermidis*, J. Med. Microbiol. 46 (1997) 693–697.

[7] R. Chang, S. Chou, J. Shaw, Site-Directed Mutagenesis of a Highly Active *Staphylococcus epidermidis* Lipase Fragment Identifies Residues Essential for Catalysis, JAOCS 77:10 (2000) 1021-1026.

[8] B. Cheirsilp, A. H-kittikun, S. Limkatanyu, Impact of transesterification mechanisms on the kinetic modeling of biodiesel production by immobilized lipase, Biochem. Eng. J. 42 (2008) 261–269.

[9] S.V. Iersel, L. Gamba, A. Rossi, S. Alberici, B. Dehue, J.V.D. Staiij, A. Flammini, “ALGAE-BASED BIOFUELS” AquaticBiofuels, Food and Agriculture Division of the United Nations. (2009) http://www.fao.org/bioenergy/aquaticbiofuels/documents/detail/en/?uid=20824

[10] S.N. Fedosov, X. Xu, Enzymatic synthesis of biodiesel from fatty acids . Kinetics of the reaction measured by fluorescent response of Nile Red, Biochem. Eng. J. 56 (2011) 172–183.

[11] N.S. Gandhi, S.B. Sawant, J.B. Joshi, Specificity of a lipase in ester synthesis : Effect of Alcohol, Biotechnol. Prog. 11 (1995) 282–287.

[12] M. Gopalakrishnan, K. Forsten-Williams, M. a Nugent, U.C. Täuber, Effects of Receptor Clustering on Ligand Dissociation Kinetics: Theory and Simulations, Biophys. J. 89 (2005) 3686–3700.

[13] R. Gupta, N. Gupta, P. Rathi, Bacterial lipases: An overview of production, purification and biochemical properties, Appl. Microbiol. Biotechnol. 64 (2004) 763–781.

[14] H. Horchani, I. Aissa, S. Ouertani, Z. Zarai, Y. Gargouri, A. Sayari, Journal of Molecular Catalysis B : Enzymatic Staphylococcal lipases : Biotechnological applications, J. Mol. Catal. B, Enzym. 76 (2012) 125–132.

[15] H. Horchani, H. Mosbah, N. Ben Salem, Y. Gargouri, A. Sayari, Biochemical and molecular characterisation of a thermoactive, alkaline and detergent-stable lipase from a newly isolated *Staphylococcus aureus* strain, J. Mol. Catal. B Enzym. 56 (2009) 237–245.

[16] A.E.M. Janssen, A.M. Vaidya, P.J. Hailing, Substrate specificity and kinetics of *Candida rugosa* lipase in organic media, Enz. Microb. Tech. 18 (1996) 340–346.

[17] S.W. Kruse, R. Zhao, D.P. Smith, D.N.M. Jones, Structure of a specific alcohol-binding site defined by the odorant binding protein LUSH from *Drosophila melanogaster*., Nat. Struct. Biol. 10 (2003) 694–700.

[18] K.P. Lee, H.K. Kim, Enzymatic Transesterification reaction using *Staphylococcus haemolyticus* L62 lipase crosslinked on magnetic microparticles, Journal Mol. Catal. B, Enzym. 115 (2015) 76–82.

[19] J.P. Long, J. Hart, W. Albers, F. a. Kapral, The production of fatty acid modifying enzyme (FAME) and lipase by various staphylococcal species, J. Med. Microbiol. 37 (1992) 232–234.

[20] C.M. Longshaw, A.M. Farrell, J.D. Wright, K.T. Holland, Identification of a second lipase gene , gehD , in *Staphylococcus epidermidis* : comparison of sequence with those of other staphylococcal lipases, Microbiology 146 (2000) 1419–1427.

[21] S.M. Paul, Alcohol-sensitive GABA receptors and alcohol antagonists., Proc. Natl. Acad. Sci. U.S.A. 103 (2006) 8307–8308.

[22] M. Pilarek, K.W. Szewczyk, Kinetic model of 1,3-specific triacylglycerols alcoholysis catalyzed by lipases, J. Biotech.127 (2007) 736–744.

[23] R. Rosenstein; F. Götz, Staphylococcal lipases: Biochemical and molecular characterization, Biochimie. (2000) 1005–1014.

[24] M.Y. a. Samad, C.N. a. Razak, A.B. Salleh, W.M. Zin Wan Yunus, K. Ampon, M. Basri, A plate assay for primary screening of lipase activity, J. Microbiol. Methods. 9 (1989) 51–56.

[25] G. Sandoval, A. Marty, Screening methods for synthetic activity of lipases, Enzyme Microb. Technol. 40 (2007) 390–393.

[26] J. Skjold-Jørgensen, J. Vind, A. Svendsen, M.J. Bjerrum, Altering the activation mechanism in *Thermomyces lanuginosus* lipase, Biochemistry. 53 (2014) 4152–4160.

[27] S. Svensson, P. Strömberg, T. Sandalova, J. Höög, Class II alcohol dehydrogenase (ADH2)--adding the structure., Chem. Biol. Interact. 130-132 (2001) 339–350.

[28] A.B. Thode, S.W. Kruse, J.C. Nix, D.N.M. Jones, The role of multiple hydrogen bonding groups in specific alcohol binding sites in proteins: Insights from structural studies of LUSH, J Mol Biol. 376 (2008) 1360–1376.

[29] J.B.A. Van Tol, J.A. Jongejan, J.A. Duke, H.T. Kierkels, E.F.T. Gelade, F. Mosterd, W.J.J. Van Der Tweel, J. Kamphuis, Thermodynamic and Kinetic Parameters of Lipase-Catalyzed Ester Hydrolysis in Biphasic Systems with Varying Organic Solvents, Biotech. And Bioeng. 48 (1995) 179–189.

[30] R. Verger, “Interfacial activation” of lipases: Facts and artifacts, Trends Biotechnol. 15 (1997) 32–38.

[31] M. Yusoff, J. Brask, P. Munk, Z. Guo, Journal of Molecular Catalysis B : Enzymatic Kinetic model of biodiesel production catalyzed by free liquid lipase from *Thermomyces lanuginosus*, Journal Mol. Catal. B, Enzym. 133 (2016) 55–64.

[32] P.B. Szecsi,The Aspartic Proteases. Scand. J. Clin. Lab. In vest Suppl. 210 (1992) 5-22.

[33] C.L. Chu, J.A. Buczek-Thomas, M. a Nugent, Heparan sulphate proteoglycans modulate fibroblast growth factor-2 binding through a lipid raft-mediated mechanism., Biochem. J. 379 (2004) 331–341.

[34] M. Kim, A. Repp, D.P. Smith, LUSH Odorant-Binding Protein Mediates Chemosensory Responses to Alcohols in *Drosophila melanogaster*, Genetics 150 (1998) 711-721.

[35] P.S. Miller, A.R. Aricescu, Crystal structure of a human $GABA_A$ receptor, Nature 512 (2014) 270-275.

[36] The PyMOL Molecular Graphics System, Version 1.8 Schrödinger, LLC.

Chapter V

Outer Membrane Phospholipase A

5.1 OMPLA

As discussed in chapter I, our general goal in the FAME project was to explore possible catalytic utility of lipases and esterases with respect to biofuel production [5]. One known lipase (in the phospholipase subcategory) is *Escherichia coli*'s outer membrane phospholipase A, or OMPLA [1,2,15]. OMPLA is a transmembrane β-barrel protein [17] (Figure 5-1) that naturally hydrolyzes phospholipid ester bonds between the fatty acid chains and the glycerol backbone.

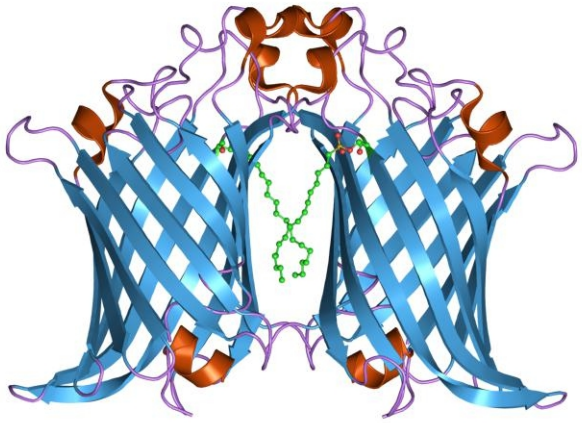

Figure 5-1. The crystal model of OMPLA in the active dimeric form. Lysophospholipid substrates are shown in green [24].

As such, we initially hoped to study OMPLA in an effort to adapt it for esterification or industrial lipid hydrolysis [9](for example, the hydrolysis of lipids supplied by algae). This chapter describes the steps taken in the OMPLA project, which was ultimately abandoned as staphylococcal FAME became a more promising subject for study.

OMPLA is a constitutively expressed *E. coli* protein, known for several decades, that is naturally found in the outer bacterial membrane. It appears to serve as a tool for remodeling the outer membrane by hydrolyzing diacyl phospholipids into monoacyl “lysophospholipids,” (Figure 5-2) thereby changing the shape and physical properties of the fluid mosaic. Strictly speaking, a phospholipase A hydrolyzes either the ester bond at the either the first (A1) or second (A2) carbon of the glycerol backbone; OMPLA is technically a phospholipase B as it is competent as both A1 and A2 phospholipase activity. OMPLA activity is dependent on the availability of its cofactor, ionic calcium. This is a common feature of many lipases and phospholipases, although calcium is not directly involved in the hydrolysis, in which a protein sidechain, as part of a catalytic triad [14], acts as a nucleophilic attacker in an sn2 mechanism. OMPLA is functional as a transient homodimer; its active site is formed at the interface between the two monomer units when their β-barrels align side by side. The assembled OMPLA complex shows little specificity with respect to the fatty acid side chain or head group identity of the phospholipid substrate molecule.

Additionally, as a protein that is normally expressed by *E. coli*, OMPLA was anticipated to be compatible with recombinant expression in *E. coli*; it lacks codons that are rare in *E. coli* and is amenable to folding in the context of the *E. coli* outer plasma membrane. For these reasons we considered OMPLA to be an appealing starting point for exploring the adaptation of a model lipase to work with non-native substrates.

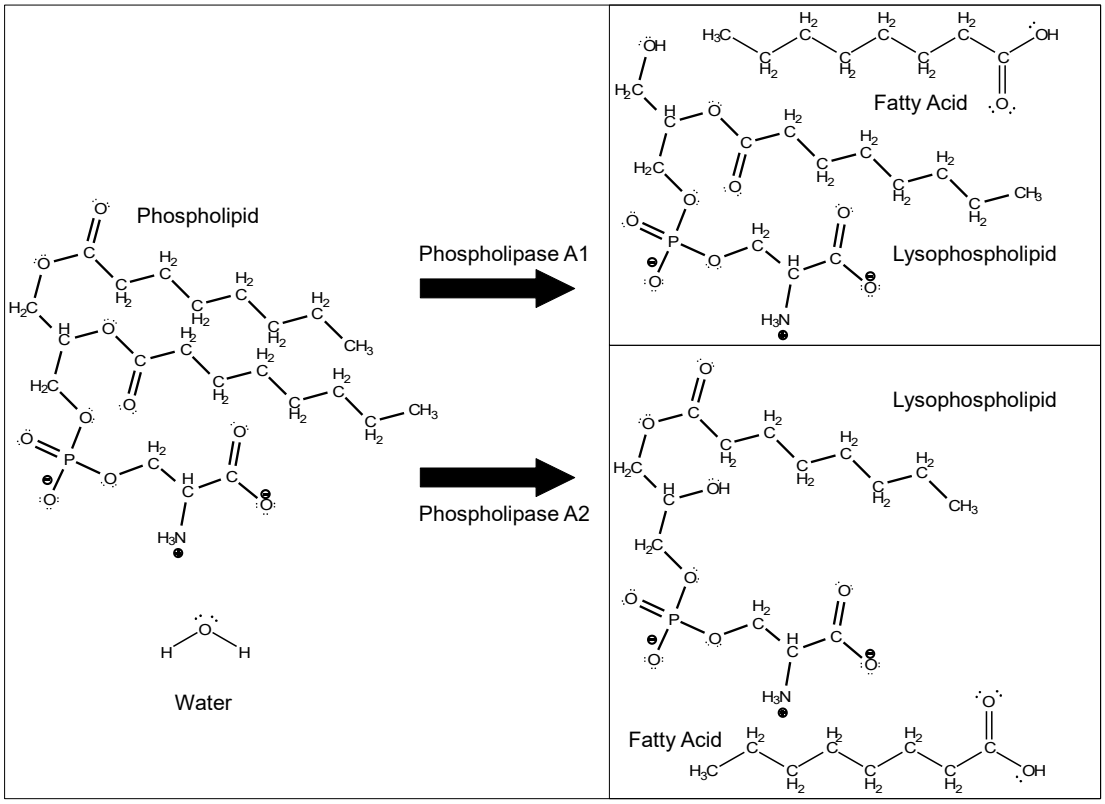

Figure 5-2. Phospholipase A1/A2/B catalyzed reactions. A phospholipase A hydrolyzes an acyl ester bond on a phospholipid, releasing a free fatty acid and a monoacyl species called a lysophospholipid. The positional specificity of the reaction dictates whether the enzyme is classed as an A1, A2, or B (A1+A2 activity) phospholipase.

5.2 Mutating OMPLA

Because OMPLA activity is regulated at the level of dimer formation, rather than protein expression or substrate availability, we intended to enhance OMPLA activity by covalently linking two OMPLA primary sequences as a single protein transcript. Compared to wild-type OMPLA, a successfully expressed and folded OMPLA-OMPLA fusion would favor the active dimer form as the entropy gained by dissociation of the two monomer units is dramatically reduced, while the entropy gain for burying the sidechains at the dimer interface remains unchanged.

5.3 Assessing OMPLA

Ultimately, evaluation of OMPLA, any potential engineered OMPLA variants, or their respective merits, must involve quantitatively assessing their lipase and phospholipase activities. The various strategies for quantitative assessment of phospholipase activity represent workarounds for the fact that the substrate phospholipid and the product fatty acids and lysophospholipids are not easily distinguished by simple spectrometric assays [19]. None of the aforementioned compounds have visible spectra and the infrared spectra of the system changes very little as hydrolysis progresses. *In vitro* assays such as nitrophenyl acetate or *in vivo* assays such as culture plate screening [4,10,18] for lipase activity, as described in section 2.10, would be unreliable if used in

conjunction with whole cells as the assay would necessarily be at a pH compatible with *E. coli* lipase activity. Among the oldest methods for measuring phospholipase activity are lipid phase extraction followed by thin layer chromatography and visualization with charring [1,2] (Figure 5-3) or detection of ^{14}C in fractionated lipids [15].

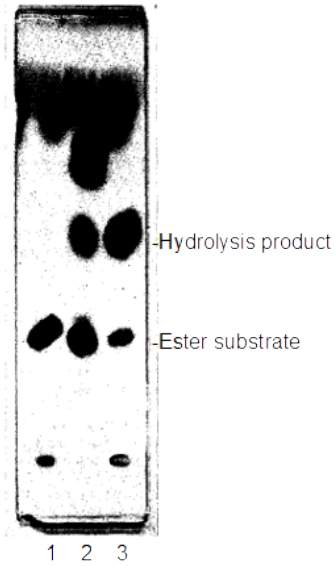

Figure 5-3. Example of thin layer chromatography: analysis of lipase activity. Lane 1: substrate, no lipase. Lane 2: standards. Lane 3: substrate and lipase. Modified from [1].

A newer method employs BODIPY fluorescent labels to detect phospholipase A/B activity [12,13,20]. A bis-BODIPY FL labeled phosphatidylcholine (POPC) molecule contains one fluorophore group covalently bound to the end of each of the two acyl chains [8]. Each of the fluorophores exhibits fluorescence with an

excitation wavelength of 488 nm and an emission wavelength of 530 nm. However, the close proximity of the fluorophores to each other allows for fluorescence resonance energy transfer (FRET) which causes the two fluorophores to effectively quench each other. Hydrolysis of the ester linkage between an acyl chain and the glycerol backbone of the labeled phospholipid releases a BODIPY labeled fatty acid (Figure 5-4), a loss of intramolecular fluorescence quenching, and a consequent gain of fluorescence emission at 530 nm. We originally intended to quantitatively measure OMPLA constructs against each other using bis-BODIPY substrates.

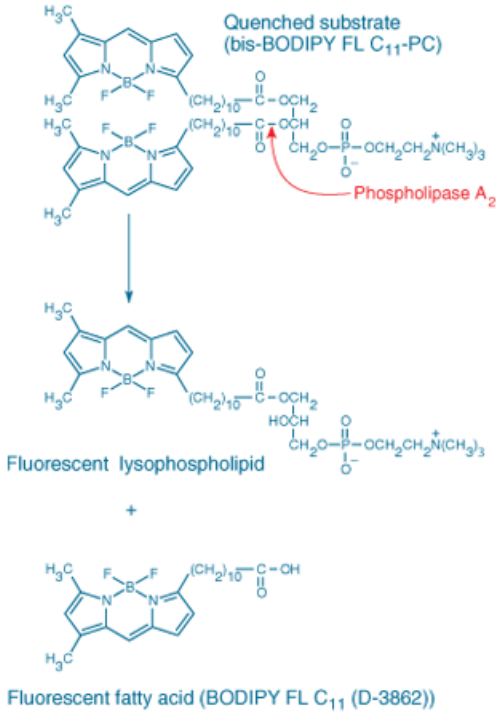

Figure 5-4. bis-BODIPY labeled phosphatidylcholine. Phospholipase activity releases one (or both) BODIPY fluorophores, resulting in loss of intramolecular quenching and an increase in fluorescence [25].

5.4 Reagents

Enzymes and enzyme buffers were purchased from both Fermentas and New England Biolabs. The gila monster venom phospholipase A was a generous gift from Robert Applegate. All other reagents were purchased from Fisher Scientific.

5.5 Instrumentation

We used many of the instruments described in section 2.3. PCR and endonuclease reactions were performed using an MJ Research PTC-200 thermocycler. Sonication was done with a Fisher 550 Sonic Dismembrator. UV-visible spectrophotometry was performed with a Varian Cary 50 Bio system. Fluorescence of the BODIPY dye was measured with a Horiba FluoroMax-3 fluorimeter.

5.6 Cloning of OMPLA for Recombinant Expression

Our goal in the first phase of the OMPLA project was to clone an *E. coli* population modified for enhanced OMPLA expression, for use as a control to evaluate the properties of OMPLA variants (such as the OMPLA-OMPLA fusion described in 5.1.2). The gene *plb*, which codes for wild type OMPLA is a part of *E. coli*'s genomic DNA. In order to enhance OMPLA expression for study we

opted to use the T7 recombinant expression system, via inclusion of the OMPLA gene sequence in a pET21a+ plasmid [22] (Figure 5-5). The properties of the pET expression system are discussed in section 2.8, as are the rationales for using it.

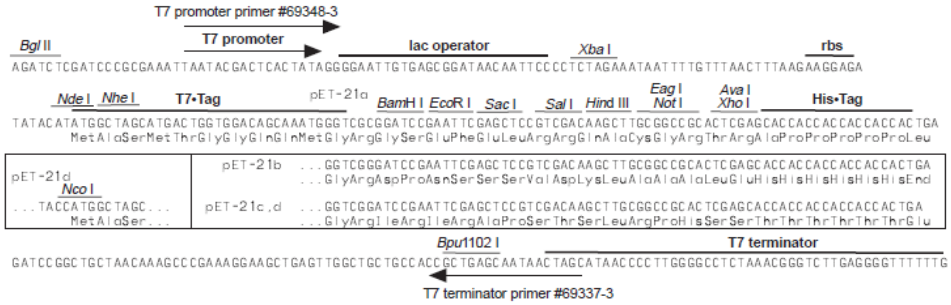

pET-21a-d(+) cloning/expression region

Figure 5-5. The expression region of the pET21a(+) plasmid. We used Nde1 and EcoR1 as our restriction endonucleases for insertion of the gene constructs, effectively appending the pelB leader sequence to the 5' end of the genes. As a result, the gene was positioned near the ribosome binding sequence, but did not include the vector's native T7 Tag or hexahistidine tag.

To re-iterate, the pET system uses the *lac* repressor sequence and the T7 expression system engineered from the T7 RNA polymerase and T7 promoter sequence originally found in the T7 bacteriophage. Lactose analogues such as Isopropyl β-D-1-thiogalactopyranoside (IPTG) bind the lac repressor proteins that prohibit gene expression, causing them to dissociate away from the repressor sites and making the T7 promoter site available to T7 RNA polymerase, resulting in recombinant gene expression. Therefore an E. coli bacterium harboring

pET21a-*plb* expresses OMPLA at low levels constitutively due to its genomic copy of *plb* and at high levels under IPTG induction due to the T7/*lac* repressor controlled *plb* genes in its supply of pET21a plasmids.

A frozen stock of BL21 K12 *E. coli* was inoculated into 25 mL of antibiotic-free liquid Luria-Bertani media and grown to stationary phase (after the absorbance of 600 nm light exceeds ~2.0). Genomic DNA was extracted [3] and used in the following :

In 50 microliters:

1. 1 microliter of BL21 *E. coli* genomic DNA
2. 2 units of *Pfu* DNA polymerase
3. 2 microliters of 25 millimolar dNTPs
4. 10 microliters of 5x Pfusion HF buffer
5. Oligonucleotide primers from IDT DNA, 2 microliters of 25 micromolar DNA each:

Primer 1: ATCAATCCATCCACATATGCGGACTCTGCAGGGC

Primer 2: CGCCGCCGCGGGAGAATTCTCATCAAAACAAATC

And the following PCR program:

1. 98 °C for 30 seconds
2. 69 °C for 30 seconds
3. 72 °C for 90 seconds
4. Repeat steps 2 and 3 30 times

5. 72 °C for 10 minutes

6. Cool to 4 °C

The PCR product was purified [6], cut, and ligated into pET21a+ plasmids (as described in section 2.7) using the restriction endonucleases Nde1 for the 5' end of the OMPLA gene and EcoR1 for the 3' end of the OMPLA gene, as well as for the respective cut sites on pET21a+. Successful transformation and amplification of the constructed plasmid in Top10 *E. coli* was verified using agarose gel electrophoresis and ethidium bromide staining. Recombinant plasmid was purified from Top10 *E. coli* [18] and transformed into BL21 *E. coli*. Expression of wild-type OMPLA in BL21 *E. coli*, as described in section 2.8, was verified using SDS-PAGE (Figure 5-6). The gene for the OMPLA-OMPLA dimer was a generous gift from Dr. Mario Navarro and Melissa Lokensgard.

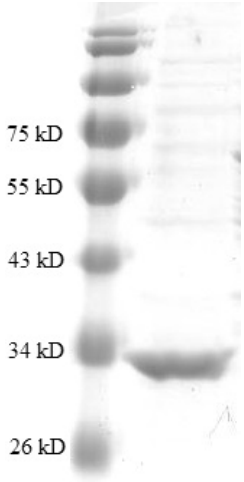

Figure 5-6. SDS-PAGE evaluation of recombinant OMPLA expression. Left lane: New England Biolabs molecular weight marker. Right lane: OMPLA from cell lysate.

5.7 Recombinant OMPLA Denaturation and Refolding

The first real hurdle in the OMPLA project was the challenge posed by the formation of protein inclusion bodies in cells expression recombinant OMPLA. As mentioned in section 2.14, the systems that transport nascent polypeptides from the cytoplasm through the inner bacterial cell membrane have a limited capacity. As a result, overexpression of proteins destined for the periplasmic space, the outer membrane, or secretion into the extracellular environment can potentially overwhelm the transport pathway, resulting in a population of recombinant proteins trapped in the cytoplasm where they are unable to fold properly. These misfolded proteins eventually aggregate into insoluble inclusion bodies in the cytoplasm [7,11,17].

In order to develop a protein sample in which the recombinant OMPLA is fully folded, we slightly modified the method of Dekker et. al. [17]. After protein expression induction for 3 hours at 37º Celsius, 25 mL of cell culture was centrifuged at 3000 g for 1 minutes. The cell pellet was resuspended in 10 mL of 50 mM tris at pH 8.0 with 40 mM ethylene diamine tetraacetate (EDTA). The resuspended pellet was sonicated with 10 pulses lasting 15 seconds each, separated by 30 second intervals on ice to prevent soluble protein precipitation. The solution was then centrifuged again for 15 minutes at 3000g, and the supernatant containing soluble *E. coli* proteins was discarded. The pellet,

consisting of cell debris and protein inclusion bodies, was then resuspended in 10 mL of a second buffer containing 20 mM tris, 2 mM EDTA, 10 mM Triton X-100, 100 mM glycine, and 8 M urea at pH 8.3. This sample was loaded into a 12 mL slide-a-lyzer dialysis cassette with a 3,000 dalton molecular weight cutoff. The sample was dialyzed into 1 L of buffer containing 20 mM tris, 2 mM EDTA, 10 mM Triton X-100, at pH 8.3 at 4º Celsius for 72 hours. The liter of buffer was replaced with fresh buffer every 24 hours. Following dialysis the protein-detergent solution was removed from the cassette and centrifuged at 3000 g for 15 minutes. SDS-PAGE verified that much of the OMPLA remained in the soluble supernatant fraction of the sample.

5.8 bis-BODIPY Fluorescence Assay for Phospholipase Activity

Purchased bis-BODIPY FL labeled phospholipids were dissolved at a concentration of 0.5 mg/mL in chloroform with 0.1%Triton X-100. The solution was evaporated down in air to form micelles, and then resuspended in 20 mM tris with 2 mM EDTA and a final working concentration of 0.5 mg/mL bis-BODIPY FL phospholipid and 0.1% Triton X-100 at pH 8.3.

A Horiba FluoroMax-3 fluorimeter was used to measure fluorescence of 1 mL samples containing 20 mM tris, 2 mM EDTA, 0 or 10 mM Triton X-100, and 0 or 5 µg/mL bis-BODIPY FL-labeled POPC incubated at 25º C for 1 hour. Excitation was at 488 nm and the emission spectrum of each sample was

scanned from 495 nm to 540 nm. As a positive control for phospholipase activity, we also incubated the BODIPY dye with phospholipase A from gila monster venom for up to 15 minutes.

5.9 Results: OMPLA Expression in *E. coli*

As an endogenous *E. coli* protein, OMPLA's wild-type sequence (the gene *plb*) lacks the rare codons that might otherwise complicate recombinant expression in *E. coli*; this would be a consideration in the case of recombinant expression of foreign genes. OMPLA expresses in the pET21a+ vector expression system, but SDS-PAGE is deceptive in this respect. OMPLA appears to be relegated to inclusion bodies upon overexpression. This first complication is adressed above in section 5.2.4. Urea denaturation followed by dialysis-driven refolding of recombinant OMPLA into Triton X-100 micelles has been shown to be an effective workaround for this problem.

5.10 Fluorescence Assay Complications

The fluorescence assay was originally intended to serve as a metric for the phospholipase activity of wild-type OMPLA and subsequent OMPLA variants. The bis-BODIPY FL phosphatidylcholine substrate, added to the Triton micelle sample, should show a gain of BODIPY fluorescence emission (Figure 5-7) at approximately 530 nm as phospholipase activity frees fluorophores from their

parent phospholipids, reducing the fluorophore-fluorophore quenching effect. Our data shows a gain of fluorescence emission near 530 nm as expected upon incubation of the BODIPY substrate with refolded OMPLA (Figure 5-8).

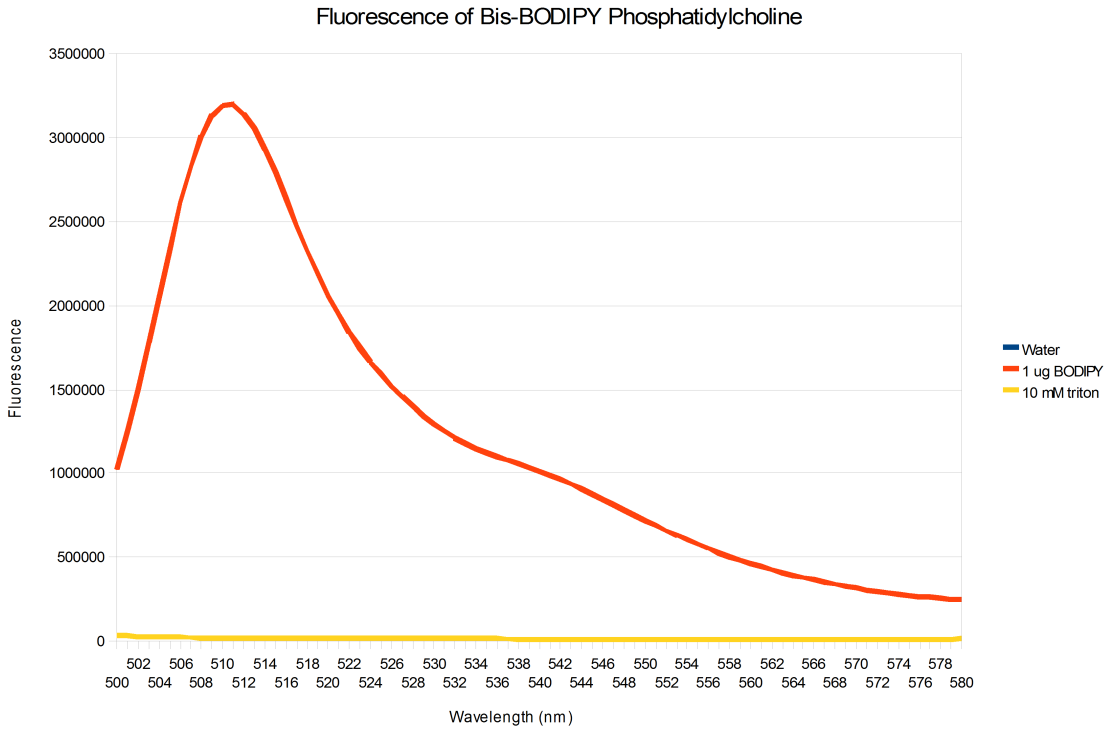

Figure 5-7. bis-BODIPY phosphatidylcholine fluorescence. Baseline buffered BODIPY fluorophore fluorescence (upon excitation at 488 nm) is shown. Neither water alone nor Triton X-100 show any detectable fluorescence under these conditions.

Incubation of the substrate with 20 mM tris, 2 mM EDTA shows no such increase in fluorescence. However, we also observed an increase in fluorescence emission when the BODIPY substrate was incubated with our negative control buffer, containing 20 mM tris, 2 mM EDTA, and 10 mM Triton X-100. An

unexpected increase in fluorescent emission at 530 nm upon addition of enzyme-free buffer presented a problem.

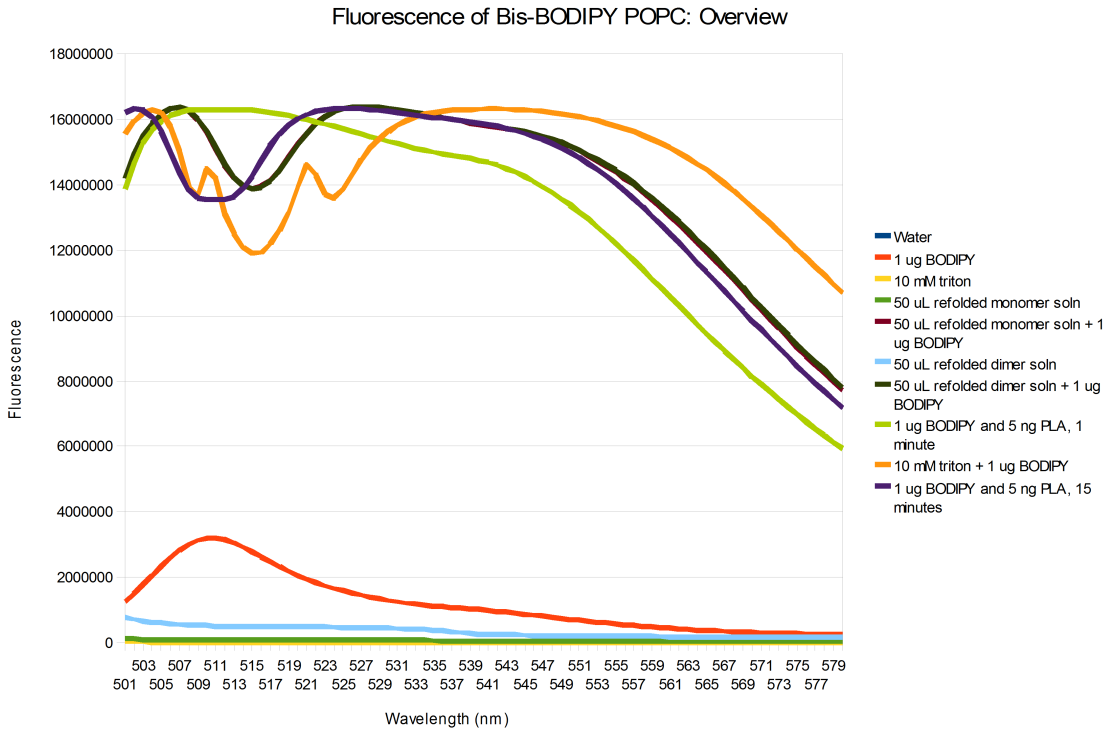

Figure 5-8. Gain in bis-BODIPY phosphatidylcholine fluorescence. BODIPY fluorescence increases greatly from baseline fluorescence (red) upon the addition of gila monster venom phospholipase in a time-dependent fashion (yellow-green, purple). It also increases upon the addition of refolded OMPLA and OMPLA-OMPLA dimer (maroon, dark green). However, both refolded OMPLA variants contain Triton X-100, which is sufficient to cause a comparable increase in fluorescence (orange).

There are at least two possible explanations for this result. One possibility is that the fluorophores are subject to oxidation when mixed with a much larger amount of Triton X-100 due to the contamination of the latter by oxidizing by-

products [21]. Any BODIPY fluorophores damaged by oxidization would be unable to quench their sister fluorophores within the labeled phosphatidylcholine molecule. Therefore, since it decreases quenching and increases fluorescence emission at 530 nm, oxidation (or any other damage to the fluorophores) is experimentally indistinguishable from phospholipase activity in this assay.

The second possibility is that the increase in fluorescent emission is the result of loss of intermolecular quenching, rather than intramolecular quenching. In concentrated bis-BODIPY FL phosphatidylcholine, each fluorophore will have its fluorescence quenched in part by its sister fluorophore within the same molecule (intermolecular quenching), and to a lesser extent by the fluorophores in nearby bis-BODIPY FL phosphatidylcholine molecules (intermolecular quenching). In the idealized form of the phospholipase assay, phospholipase activity is measurable as it reduces the former quenching effect. An overall decrease in BODIPY fluorophore concentration, however, causes the latter effect as the average distance between fluorophore pairs increases. The degree to which loss of intermolecular quenching affects the overall fluorescence signal is questionable, and it may well be negligible. It should be noted that while dilution in 10 mM Triton X-100 buffer caused the substrate stock solution to gain fluorescence, dilution to the same molar concentration with Triton-free buffer did not. At first glance, this would seem to contraindicate the hypothesis that intermolecular quenching is being lost via dilution. However, in the case of

micelle-borne molecules, molar concentration can be deceptive. The actual distances between molecules on the surfaces of micelles depend on the distributions of those molecules on the two-dimensional micelle surfaces rather than within the three-dimensional bulk solution. Therefore, in two bis-BODIPY FL phosphatidylcholine solutions of equal molar concentration, the fluorescently labeled molecules may be separated by greater or lesser average intermolecular distances depending on the amount of micelle-forming detergent.

5.11 Termination of the OMPLA Project

These initial hurdles in the OMPLA project are not insurmountable. The possibility that the false positive fluorescence gain in our BODIPY-based assay is attributable to oxidative degradation could be rejected or verified simply by using Triton X-100 from other sources. Alternatively, titrating bis-BODIPY FL phosphatidylcholine with Triton X-100 to oxidatively abolish fluorescence entirely would show that oxidizing contaminants are the cause of the apparent change in fluorescence. If the oxidation hypothesis is true, the fluorescence signal at 530 nm would first increase and then decrease as Triton concentration, as oxidative damage to the bis-BODIPY phosphatidylcholine first produces a population of mono-BODIPY phosphatidylcholine and then depletes the number of functional fluorophores to near zero. Although previous work employed Triton X-100 as the

detergent of choice for refolding recombinant OMPLA from inclusion bodies, exploration of other detergents such as Tween 20 is also possible.

If intermolecular fluorescence quenching does contribute to the background fluorescence problem seen at 530 nm, and oxidative damage to the fluorophores does not meaningfully contribute to the observed fluorescence gain, it is possible to treat the signal as background fluorescence. However, under our experimental conditions the majority of the fluorescence signal would appear to result from this effect, raising issues regarding the signal-to-noise ratio that would be associated with the resulting background-subtracted data. This approach would allow for partial comparative quantitation of the phospholipase activities of OMPLA and OMPLA variants. However the interference of significant intermolecular quenching means that the rate at which the fluorescence signal changes over time will not be linear with respect to the rate of catalysis, as phospholipase activity will affect both intermolecular and intramolecular quenching. As a result, the presence of significant intermolecular quenching confounds the derivation of kinetic data with this assay.

In summation, our initial difficulties in this OMPLA project were by no means impassable obstacles. However, soon after these difficulties came to light, the investigations that prompted FAME research described in the previous four chapters came to be seen as a far more promising avenue of inquiry. This reasoning was based in part on the existing history of FAME-catalyzed

esterification, and the fact that FAME was known to be a soluble (rather than transmembrane) protein.

5.12 References

[1] A.J. Aarsman, L.L.M. van Deenen, H. van den Bosch, Studies on lysophospholipases, Bioorg. Chem. 5 (1976) 241–253.

[2] O. Doi, S. Nojima, Lipase Activity of Detergent-resistant Phospholipase A in *Escherichia coli*, Biochimica et Biphysica Acta, 369 (1974) 64–69.

[3] H.R. Cheng, N. Jiang, Extremely rapid extraction of DNA from bacteria and yeasts, Biotechnol. Lett. 28 (2006) 55–59.

[4] G.L. Chrisope, C.W. Fox, R.T. Marshall, Lecithin agar for detection of microbial phospholipases, Appl. Environ. Microbiol. 31 (1976) 784–786.

[5] S.V. Iersel, L. Gamba, A. Rossi, S. Alberici, B. Dehue, J.V.D. Staiij, A. Flammini, "ALGAE-BASED BIOFUELS" AquaticBiofuels, Food and Agriculture Division of the United Nations. (2009) http://www.fao.org/bioenergy/aquaticbiofuels/documents/detail/en/?uid=20824

[6] Zymoclean™ Gel DNA Recovery Kit, Ver 1.2.0. Zymo Research (2016).

[7] N. Dekker, K. Merck, J. Tommassen, H.M. Verheij, *In vitro* folding of *Escherichia coli* outer-membrane phospholipase A, Eur. J. Biochem. 232 (1995) 214–219.

[8] J. Goedhart, H. Röhrig, M. a. Hink, A. Van Hoek, a. J.W.G. Visser, T. Bisseling, T.W.J. Gadella, Nod Factors Integrate Spontaneously in Biomembranes and Transfer Rapidly Between Membranes and to Root hairs, but Transbilayer Flip-Flop Does not Occur, Biochemistry. 38 (1999) 10898–10907.

[9] R. Gupta, N. Gupta, P. Rathi, Bacterial lipases: An overview of production, purification and biochemical properties, Appl. Microbiol. Biotechnol. 64 (2004) 763–781.

[10] E.K. Kim, W.H. Jang, Jung Ho Ko, Jong Seok Kang, Moon Jong Noh, O.J. Yoo, Lipase and its modulator from *Pseudomonas* sp. strain KFCC 10818: Proline-to-glutamine substitution at position 112 induces formation of

enzymatically active lipase in the absence of the modulator, J. Bacteriol. 183 (2001) 5937–5941.

[11] a Lohia, a N. Chatterjee, J. Das, Lysis of *Vibrio cholerae* cells: direct isolation of the outer membrane from whole cells by treatment with urea., J. Gen. Microbiol. 130 (1984) 2027–2033.

[12] T. Meshulam, H. Herscovitz, D. Casavant, J. Bernardo, R. Roman, R.P. Haugland, G.S. Strohmeier, R.D. Diamond, E.R. Simons, Flow cytometric kinetic measurements of neutrophil phospholipase A activation, J. Biol. Chem. 267 (1992) 21465–21470.

[13] L.J. Mitnaul, J. Tian, C. Burton, M.-H. Lam, Y. Zhu, S.H. Olson, J.E. Schneeweis, P. Zuck, S. Pandit, M. Anderson, M.M. Maletic, S.T. Waddell, S.D. Wright, C.P. Sparrow, E.G. Lund, Fluorogenic substrates for high-throughput measurements of endothelial lipase activity, J. Lipid Res. 48 (2007) 472–482.

[14] M. Mitta, M. Miyagi, I. Kato, S. Tsunasawa, Identification of the Catalytic Triad Residues of Porcine Liver Acylamino Acid-Releasing Enzyme, J. Biochem. 123 (1998) 924–931.

[15] O. Doi, M. Ohki, S. Jima, Two Kinds of Phospholipase A and Lysophospholipase in *Escherichia coli*, Biochimica et Biophysica Acta 260 (1972) 244–258.

[16] Zyppy™ Plasmid Miniprep Kit, Ver. 1.2.6. Zymo Research (2016).

[17] A.K. Patra, R. Mukhopadhyay, R. Mukhija, A. Krishnan, L.C. Garg, A.K. Panda, Optimization of Inclusion Body Solubilization and Renaturation of Recombinant Human Growth Hormone from *Escherichia coli*, 192 (2000) 182–192.

[18] M.Y.A. Samad, C.N.A. Razak, A.B. Salleh, W.M. Zin Wan Yunus, K. Ampon, M. Basri, A plate assay for primary screening of lipase activity, J. Microbiol. Methods. 9 (1989) 51–56.

[19] G. Sandoval, A. Marty, Screening methods for synthetic activity of lipases, Enzyme Microb. Technol. 40 (2007) 390–393.

[20] F.H.C. Tsao, D. Shanmuganayagam, D.K. Zachman, M. Khosravi, J.D. Folts, K.C. Meyer, A continuous fluorescence assay for the determination of calcium-dependent secretory phospholipase A2 activity in serum, Clin. Chim. Acta. 379 (2007) 119–126.

[21] B.A. Cooke, R.J.B. King, H.J. Van der Molen, Hormones and Their Actions Part I, Elsevier, Amsterdam, (1998) 114-115.

[22] pET System Manual, 10th edition. Novagen (2003).

[23] pET-21a-d(+) Vectors Map. Novagen (1998).

[24] H.J. Snijder, I. Ubarretxena-Belandia, M. Blaauw, K.H. Kalk, H.M. Verheij, M.R. Egmond, Structural evidence for dimerization regulated activity of an integral membrane phospholipase, Nature 401 (1999) 717-721.

[25] Fatty Acid Analogs and Phospholipids - Section 13.2, https://www.thermofisher.com/us/en/home/references/molecular-probes-the-handbook/probes-for-lipids-and-membranes/fatty-acid-analogs-and-phospholipids.html, (Retrieved August 16, 2016)

Appendix I: Manuscript in Review

The following section is a copy of the manuscript, now in review for publication, that covers much of the work and results described in chapters I-IV. Some of the figures form the previous chapters are shown again in this one.

A Secreted *Staphylococcus aureus* Lipase Engineered for Enhanced Alcohol Affinity for Fatty Acid Esterification

Abstract

Presently the production and use of biodiesel is not cost-effective in comparison to traditional fossil fuels. Naturally occurring enzymes, such as lipases and esterases, can potentially be engineered to lower the cost of certain steps in the biodiesel synthesis process that would otherwise be more costly. However, these enzymes have evolved to perform biologically relevant functions, and not necessarily to manufacture biodiesel under commercially viable conditions. To this end, we have identified, cloned, expressed, purified, and characterized two proteins from the staphylococcal lipase family that are capable of catalyzing the formation of fatty acid alkyl esters. In an effort to explore strategies for improving these fatty acid modifying enzymes (FAMEs), we have engineered a chimeric fusion protein that significantly increases the esterification of free fatty acid with ethanol. The fusion protein, which consists of a

staphylococcal FAME fused to a *Drosophila* ethanol binding protein, demonstrably improves the rate of catalysis by providing an additional substrate binding site and concomitant increase in the local concentration of substrate. This results in greater overall substrate (ethanol) residence in proximity to the catalytic domain, and a faster rate of catalysis, without the necessity of altering the amino acid sequence of the FAME protein.

Abbreviations: FAME, fatty acid modifying enzyme; MRSA, methicillin-resistant *Staphylococcus aureus*; ANS, 8-anilino-1-naphthalene-sulfonic acid; SAL1, 2, 3, Staphylococcus aureus lipase 1, 2, and 3; TSB, tryptic soy broth; LB, Luria-Bertani media.

A.1. Introduction

Biodiesel (composed of fatty acid alkyl esters) is appealing as an alternative fuel due to its compatibility with much of today's energy infrastructure. It can be used directly in diesel engines, whereas pure ethanol or ethanol-rich fuels typically require modifications to fuel injection technology or specialized internal combustion engines. Other energy sources, such as gas-electric hybrids and fully electric engines, are on the rise in the field of consumer vehicles, but it is not likely that we will see widespread use of these engines in certain sectors,

such as aviation or the military, due to the lower energy density of batteries relative to liquid hydrocarbon fuels. Therefore the enhancement of biodiesel production merits investigation. Biodiesel is typically synthesized by heating a mixture of triglycerides (*e.g.,* waste vegetable oils) with small-chain alcohols (*i.e.,* methanol or ethanol) at high pH. The necessity for heat energy and alkaline catalysts add to biodiesel production costs and thus reduces its economic viability as a fuel source. Additionally, unwanted side products are produced in the presence of water, and many potential sources of feedstock oil, such as plant oils and algal oil, are difficult to completely dehydrate without the investment of additional energy [46]. Enzymes in the lipase/esterase family offer an appealing alternative as these proteins can potentially be engineered to catalyze the synthesis of fatty acid alkyl esters at lower temperatures and at neutral pH values in aqueous environments [2], [16].

Enzymes in the lipase/esterase family are already in use in manufacturing where they are used to synthesize organic molecules with high specificity, greatly reducing the costs associated with separating a desired product from unwanted side products that are produced using traditional non-enzymatic means [43]. Lipases can, under proper conditions (most commonly in organic solvents), catalyze the formation of esters by stabilizing the transition state between the esterified and hydrolyzed states of the substrate molecules. The fact that lipases can be employed in the synthesis of esters is not surprising since the catalysis of

the formation of a lipid ester bond is the reverse of the hydrolysis of a lipid ester bond. The ‘direction’ of such a reaction depends in large part on the relative concentration of substrates and product. This form of catalysis has been observed to occur with certain fungal and bacterial enzymes [5], [15], [17], [27], [28], and [37], including staphylococcal enzymes [9] and [21]. Within this report fatty acid modifying enzymes, such as lipases/esterases, are referred to as FAMEs.

A particularly interesting example of FAME-catalyzed ester synthesis has been observed when certain strains of *Staphylococcus aureus* infect human hosts [13], [30], [31], and [32]. Fatty acid esters have been detected in host abscesses, as well as in liquid cultures in cases where a staphylococcal infection occurred at the interface between human tissue and synthetic material such as catheters and other medical devices [7]. Additionally, this phenomenon has been observed in populations of the closely related *Staphylococcus epidermis* [14]. It was formerly hypothesized that the accumulation of free fatty acids was a byproduct of bacterial catabolism of host tissue [4], but more recent work suggests that bactericidal fatty acids are released by host organisms as a measure of defense against bacterial infection [6], [23], and [24]. Previous research has demonstrated that staphylococcal populations are adversely affected by the presence of free fatty acids in their environment [8] and [11]. Elimination of these free fatty acids by conversion to esters is therefore a

potentially beneficial adaptation for the bacteria. Genomic and proteomic analysis of staphylococcal strains indicates that the ability to esterify free fatty acids strongly correlates to virulence [8]. If this FAME activity has a biological role, then *S. aureus* strains exhibiting FAME activity must express at least one enzyme that is evolved to produce biodiesel-like esters in aqueous conditions. An *S. aureus* lipase has previously been used to synthesize esters in organic solvent (*i.e.,* hexane) [21]. However, because staphylococcal FAME activity has been observed *in vivo*, there remained the question of which *S. aureus* lipases were responsible for FAME activity in aqueous conditions, and how many distinct lipase proteins participate in the process. Moreover, the possibility of identifying the lipase capable of ester synthesis under aqueous conditions, where hydrolysis of an ester group would be predicted to be thermodynamically favored over the synthesis of an ester group, provided an opportunity to explore different avenues for *in vitro* ester synthesis. Aqueous catalysis of ester formation may obviate the use of organic solvents to extract fatty acids from their biological source. For the research reported herein, we describe how two highly similar lipases, which function as fatty acid modifying enzymes (secreted by *S. aureus*), were isolated, identified, recombinantly expressed, and shown to catalyze fatty acid alkyl ester production under aqueous laboratory conditions.

Additionally, we have taken steps to address the practical consequences of wild-type *S. aureus* FAMEs' evident low affinity for small alcohol substrates. It

has been suggested, based on computational models [18], that clustering of ligand binding sites can reduce diffusion of ligand (or substrate) away from a protein/enzyme by increasing the likelihood of rebinding [17]. Cells exploit this phenomenon by clustering surface receptors to enhance or modulate their sensitivity to extracellular signals [10]. We have improved the ability of one of the *S. aureus* enzymes to employ small alcohols as substrates (without modifying its active site) by appending the gene for an alcohol-binding protein to 3' end of the FAME gene. This results in the expression of a chimeric fusion protein in which the alcohol binding protein is fused to the C-terminus of the FAME protein. We hypothesize that the presence of this small alcohol-binding domain (*i.e.,* the *Drosophila* LUSH protein) can increase the effective affinity of the protein for small alcohols. LUSH is a 14 kD soluble protein found in *Drosophila melanogaster* chemosensory hairs. Kim et. al. determined that LUSH is required for *Drosophila*'s normal avoidance response to alcohol-rich materials [25]. Based on structural and *in vitro* assays, LUSH has been determined to be the alcohol-binding element of the detection pathway as it contains a well-characterized alcohol binding site [1], [26], [41], and [44]. The addition of an alcohol binding domain with much greater alcohol-binding affinity than that of FAME in proximity to the esterase enhances the rate of alcohol rebinding to the enzyme by increasing the substrate's local concentration in proximity to the active site. GC-MS analysis indicates that the addition of the LUSH alcohol-binding domain

improves the catalytic ability of engineered staphylococcal FAME, especially at low ethanol concentrations. Computational analysis of GC-MS data shows a lower effective ethanol binding constant for the FAME-LUSH fusion protein. Fluorescence spectroscopy using 8-anilino-1-naphthalene-sulfonic acid (ANS) and ethanol was used to affirm that the ethanol-binding capability of LUSH was not abolished by its covalent linkage to the lipase, and a T57A LUSH domain mutation was used to affirm that ethanol binds LUSH's native ethanol binding site in the fusion protein.

A.2. Experimental

2.1 Reagents

Butanol and nitrophenyl acetate were purchased from Acros Organics. DNA oligonucleotide primers for cloning and PCR were purchased from Integrated DNA Technologies. Anilino-1-naphthalene-sulfonic acid (ANS) was purchased from MP Biomedicals. The enzymes and associated buffers that were used for standard recombinant DNA methods were purchased from New England Biolabs. All other chemicals and reagents were purchased from Fisher Scientific.

2.2. Identification of FAME-positive Strains

Tryptic soy broth (TSB) and Luria-Bertani (LB) media were used separately for overnight cultures (at 37º C) for the following four *Staphylococcus aureus* strains: Newman, USA300, ISP 479C, and SA113. Culture supernatants were collected by centrifugation at 3900 g for 20 minutes. The culture supernatant was filtered using a 0.2 µm syringe filter and normalized to the concentration of the pre-filtration media (as measured by A_{600} measurements). Catalytic activity for these supernatants was assayed using the method described by Long et. al. [30]. In brief, one volume of supernatant was combined with 3 volumes of 50 mM sodium phosphate at pH 6.0, 5% butanol (v/v), and 250 µg/mL oleic acid at 37 ºC for 24 hours. The resulting butyl oleate ester was extracted into hexane and detected at m/z = 339 (the mass of butyl oleate) on an Agilent Saturn gas chromatography-mass spectrometer.

2.3. Identification of FAME Protein(s)

To isolate the FAME(s), the supernatant from the USA300 TSB culture was filtered through a 0.2 µm filter, concentrated using a 15 kD MWCO centrifugal filter unit, and separated into successive 15 mL fractions using an Amersham Biosciences AKTA FPLC system and an Amersham Biosciences HiLoad 26/60 Superdex size exclusion column. The size exclusion fraction that exhibited the greatest amount of FAME activity was concentrated using an

Amicon Ultra centrifugal filter unit with a pore size of 10 kilodaltons. The concentrated supernatant was sequenced at the UCSD Biomolecular and Proteomics Mass Spectrometry Facility, and three candidate proteins were selected based on their known lipase properties and abundance in the supernatant fraction.

2.4. Cloning and Purification of Recombinant FAMEs

Standard PCR amplification, using the DNA polymerase Pfu (Thermo-Fisher), was employed to clone the genes for the FAME proteins. Cultures of *S. aureus* (Newman strain) cells were used as the source of template DNA. DNA primers, purchased from Integrated DNA Technologies, were designed to incorporate an Nco1 endonuclease cut site at the 5' end of the PCR product, and an Xho1 cut site at the 3' end. Additionally, a 6x His tag was added to the N-terminus of each construct. The PCR products were cut with Xho1 and Nco1 (Thermo-Fisher) for approximately two hours, purified using standard agarose gel electrophoresis, and the excised DNA was ligated into the pET22-b plasmid using T4 DNA ligase (Thermo-Fisher). Plasmid DNA was purified using Macherey-Nagel silica spin columns and transformed into BL21 *E. coli* for protein expression. Transformed BL21 cells were grown at 37º C to mid-logarithmic growth phase and induced with 1 mM IPTG. Protein expression was verified using standard SDS-PAGE. Wild-type FAME proteins were released from

bacterial cells via sonication, and the supernatant was subjected to chromatography using GE nickel affinity columns. This was followed by an additional purification step using sepharose ion exchange columns. The FAME-LUSH fusion was created by expressing the LUSH domain as a C-terminal fusion with the FAME protein designated 2603, which was originally isolated from the *S. aureus* USA300 strain. The linker between the 2603 FAME protein and the LUSH protein consisted of a short putative alpha helical linker [3]. The rationale for creating the fusion where the LUSH domain is positioned at the C-terminus of the 2603 FAME protein was to maintain the hexahistidine tag at the N-terminus of the FAME protein. Purification of the expressed proteins was accomplished using an FPLC system with an Amersham Biosciences HisTrap Nickel-affinity column, followed by a HiTrap Q HP anion exchange columns. The fusion protein was purified using the same method as for the wild-type FAME protein(s) except that strong denaturing (6 M guanidine HCl) conditions were employed during the nickel affinity step, and refolding was achieved via dialysis prior to ion exchange chromatography. SDS-PAGE showing 2603 FAME and the FAME-LUSH fusions is shown in supplementary Figure A-2.

2.5. Characterization of Lipase Activity

The following three recombinantly expressed *S. aureus* proteins from the USA300 strain were tested for lipase activity using nitrophenyl acetate:

SAUSA300_0320, SAUSA300_2518, and SAUSA300_2603. The nitrophenyl acetate assay was performed using 50 µg/mL nitrophenyl acetate and cell lysate in 50 mM bis-tris, pH 6.0, at 25º C. The evolution of p-nitrophenol was detected by measuring a change in the absorbance of the solution at 405 nm after 10 minutes. As a control, the rate of non-enyzmatic hydrolysis of the substrate was measured separately. Endogenous *E. coli* lipase activity was determined to be negligible at pH 6.0.

2.6. ANS Competitive Binding Assay

Purified wild-type FAME (SAUSA300_2603), FAME-LUSH fusion, and the FAME-LUSH-T57A mutant were each incubated at a concentration of 2 µM in 50 mM Bis-Tris (pH 6.0) with ethanol ranging between 0% and 15% v/v and up to 60 µM ANS. Fluorescence was measured with excitation at 360 nm and detection at 495 nm.

2.7. Determination of FAME Activity

The two isolated *S. aureus* lipases that met our criteria for being classified as FAME proteins (*i.e.,* 0320 and 2603) were assayed for FAME activity by incubating cell lysate (buffered with 50 mM bis-tris at pH 6.0 and normalized to the same cell concentration) with 250 µg/mL oleic acid and 5% butanol at 37º C. After 24 hours, the synthesized butyl oleate was extracted into hexane and

detected at m/z = 264 on a Saturn 3800 GC system with a Saturn 2000 mass spectrometer.

Comparison of FAME-positive recombinant wild-type (2603) and the FAME-LUSH fusion was achieved using a similar method as that described by Long et. al. [30] except that 50 mM bis-tris was used in place of sodium phosphate. A 3-mL volume containing buffer, 20 nM protein, 250 µg/mL of oleic acid, and between 1% and 40% ethanol was incubated at 37º C for 3 hours. Ethyl oleate was extracted into one volume of hexane and assayed quantitatively on a Hewlett-Packard GC-MS system at m/z = 264. The reaction rate was constant for 3 hours based on measurement of ethyl oleate levels after the first, second and third hours. In no case was a detectable amount of bis-tris alkyl ester produced.

A.3. Results and Discussion

3.1. Identification of *S. aureus* Fatty Acid Modifying Enzyme (FAME)

Previously, FAME activity has been observed in the supernatant of multiple *S. aureus* strain cultures [30]. FAME and lipase secretion is hypothesized to be an evolved strategy for proliferation in lipid-rich media, such as in human host lesions [30] and [32]. Consistent with this, FAME expression in laboratory media is also not constitutively uniform, and varies depending on the

particular growth media used to culture the bacteria. GC-MS was used to evaluate FAME activity (as described in Materials and Methods) for the following four *S. aureus* strains: USA300, Newman, ISP 479C, and SA113. In comparing FAME activity across these four strains (using two different growth media) it was observed that FAME activity depends not only on bacterial strain but is also impacted by the type of growth media used (Fig. A-1). This may be an important consideration in future identification of the FAME+ phenotype for other bacterial strains. In the case of the four strains tested, the culture supernatant of the USA300 strain exhibited the highest FAME activity. Interestingly, USA300 is one of the most virulent *S. aureus* strains [4], and thus this corroborates a demonstrable correlation between strain response to free fatty acids and strain virulence [24].

Size exclusion chromatography was used to fractionate proteins from the *S. aureus* USA300 culture supernatant and isolate the protein(s) exhibiting FAME activity (supplementary Fig. A-1). The proteins within the resulting fractions were subjected to LC(RP-C18)-MS amino acid sequence analysis which revealed the primary sequences for all fractionated proteins, and subsequent BLAST queries were used to determine their identities. The results demonstrated that of fifteen identified *S. aureus* secreted proteins twelve have putative functions not related to lipid synthesis. The three remaining proteins, designated as SAUSA300_2603, SAUSA300_0320, and SAUSA300_2518 [46],

hereafter abbreviated to 2603, 0320, and 2518 were shown to be lipases from the I.6 lipase/esterase family [48][49], a group of hydrolases found in *Staphylococcus* species (the prefix SAUSA300_ indicates that the enzymes originate from the USA300 strain of *S. aureus*). 2603 and 0320 were abundant in the most active fraction whereas only trace amounts of 2518 were detected. All three proteins express at similar levels in the pET22b recombinant periplasmic expression system, which was chosen because the periplasm of *E. coli* better emulates the extracellular environment in which the lipases fold *in vivo*. All three recombinant lipases exhibit lipase activity, as determined by the hydrolysis of p-nitrophenyl acetate (Fig. A-2) [12] and [22]. However, only the two of the three enzymes (*i.e.,* 2603 and 0320; also referred to as SAL1 and SAL2 by Cadieux et. al. [4]) naturally feature N-terminal signal sequences that direct the nascent polypeptides to *S. aureus* secretory pathway. *In vivo*, 2603 and 0320 are expressed as secreted pre-enzymes, with a catalytic domain rendered partially inactive by an N-terminal inhibitory domain [33], [39], [45], and [48]. Their activity is therefore modulated by the availability of secreted staphylococcal proteases, which cleave the inhibitory domain to yield a “mature” enzyme consisting solely of the lipase/FAME domain. In the context of the *E. coli* pET-22b recombinant expression system both proteins expressed and folded into an active conformation in the absence of the inhibitory domain. Sequence alignment reveals that these two lipases are much more similar to each other than to the

third lipase (*i.e.,* 2518). The 0320 protein, designated SAL2 by Cadieux et. al. [4], has 99% amino acid sequence identity with the staphylococcal lipase SAL3 [20] and [21]. Proteins 2603 and 0320 also have high sequence similarity to the structurally characterized *S. hyicus* phospholipase [19], [38], and [42]. 2518, the putative cytoplasmic lipase, has a significantly lower molecular weight (31 kD compared to 45 kD), and its sequence partially aligns with other staphylococcal members of the α/β hydrolase family [29] and [35] (supplementary Fig. A-3), but lacks the N-terminal signal sequence necessary for secreted proteins. The small amounts of 2518 found in the staphylococcal culture supernatant is therefore likely cytoplasmic lipase released from minor cell lysis. It was for these reasons that 2518 was not pursued as a FAME candidate protein. Sequence comparison of the detected proteins with other lipases in the USA300 genome shows some homology with several other staphylococcal lipases/esterases. 2603 and 0320 are distinct from the smaller, cytoplasmic lipases in possessing both a small (~40 amino acid) N-terminal secretion signal sequence and a larger N-terminal pre-protein sequence. One other protein, SAUSA300_0876, is a putative lipase which aligns with 2603 and 0320 over some portions of its sequence, but has no secretion signal sequence and has several predicted transmembrane helices according to the program PSORTb [50]. Recombinant expression of the two FAME candidate proteins (*i.e.,* 0320 and 2603) using standard *E. coli* expression results in enzyme products that recapitulate *in vitro* the catalytic activity observed

for the secreted FAME proteins isolated from staphylococcal growth media (Fig. A-3).

Previous work that demonstrated the presence of fatty-acid modification in staphylococcal lesions has left open the question of which specific enzyme or enzymes are responsible for this phenomenon *in vivo*. We have identified enzymes that catalyze fatty acid alkyl ester synthesis *in vitro* under aqueous conditions. Not surprisingly, they are highly similar (but not identical) to other esterase/lipase proteins in the staphylococcal lipase family, such as the aforementioned *S. epidermis* lipase, and one of the two (*i.e.,* 0320) is likely a homologue of the SAL3 lipase that has been shown to synthesize fatty acid alkyl esters in hexane by Horchani et. al. [21]. It is possible that FAMEs are derived from an ancestral protein that functioned as a lipase or phospholipase. Staphylococcal FAMEs certainly live up to the lipase designation, exhibiting lipase activity under laboratory conditions [4], [20]. It is not clear whether this versatility indicates a dual *in vivo* role for these enzymes or whether one of the functions is an evolutionary or experimental artifact; FAME activity is often studied in the context of non-aqueous environments that have little biological relevance. More recent investigation of the effect of staphylococcal lipases on pathogenicity suggests that their activity has farther-reaching consequences for bacterial populations. This includes not simply conferring resistance to

bactericidal fatty acids, but also playing a supporting role in the formation of biofilms [22].

3.2. Two Similar Enzymes in the I.6 Staphylococcal Lipase Family Exhibit FAME Activity

The fact that the enzymatic activities demonstrated for the 2603 and 0320 enzymes are highly similar is not surprising given their similar putative functions and amino acid sequences (*i.e.,* 57% primary sequence identity and 70% primary sequence similarity - supplementary Fig. A-3). Further work is required to elucidate the evolutionary cause of this apparent redundancy in the staphylococcal proteome. There may be some subtle yet crucial *in vivo* differences in activity or specificity between the two similar lipases. Another possible explanation for these observations is that the expression of the two FAME enzymes may be regulated differently. We have shown that FAME activity levels not only vary across strains, but also across different growth conditions. The Newman strain shows lower FAME activity in cultured supernatant when grown in LB instead of TSB, but the mature forms of the Newman FAMEs have the same primary amino acid sequences as their USA300 homologues. This indicates that the difference in FAME activity between the two strains is likely attributable to inter-strain differences in expression and regulation.

In addition to the strong similarities between 2603 and 0320 (as well as the 0320 homologue SAL3), these enzymes also have >50% sequence identity with lipase L62 from *Staphylococcus haemolyticus*. L62 has been used *in vitro* as a catalyst for fatty acid methyl ester synthesis [28] and [34]. In addition, the 2603 and 0320 enzymes are also >50% identical to the structurally characterized *S. hyicus* phospholipase [38]. The program Swissmodel was used to map the 2603 and 0320 sequences onto the *S. hyicus* crystal structure and revealed no significant deviations in the positions of the putative catalytic Asp-His-Ser catalytic triad with respect to the two hydrophobic binding cavities on the face of the enzyme(s). In the case of the *Staphylococcus hyicus* phospholipase, the two binding cavities coordinate acyl chains, which causes the substrate lipid's glycerol-acyl ester bond to come into close proximity to the catalytic serine positioned immediately between the two binding cavities. We propose that the alkyl ester synthesis observed for 2603 and 0320 proceeds in a similar manner, with one binding pocket coordinating the free fatty acid substrate and the other coordinating the alcohol substrate. This would explain the fact that *in vitro* FAME activity for 2603 and 0320 is notably higher when the supplied alcohol substrate is larger and more hydrophobic, such as butanol [32]. An alcohol that is more similar to a putative *in vivo* substrate moiety (such as cholesterol for example) likely better fits within the larger hydrophobic binding pocket. This preference for large alcohols may be a relic of the fact that the FAMEs, as I.6 lipase family

proteins, have binding sites adapted to bind fatty acyl chains. Whether the actual *in vivo* substrate is cholesterol for ester synthesis or triglycerides for lipid hydrolysis appears to be a matter of debate; both functions are observed *in vitro.* Resistance to triglycerides and resistance to free fatty acids seem to be required for staphylococcal survival under certain experimental conditions [4] and [6]. Though the initial screens we employed to test for FAME activity used butanol as the alcohol substrate, the large-alcohol bias of wild-type FAMEs presents a problem for potential applications in the field of biofuel production, as small alcohols (methanol and ethanol) are more common alcohol sources for biodiesel synthesis. The use of an aqueous reaction system in which substrate molecules are lower in concentration or less available makes substrate affinity a more significant factor in considering enzyme engineering strategies.

3.3. Engineering the SAUSA300_2603 FAME for use with Ethanol

Re-engineering the alcohol binding pockets of the FAME proteins (*i.e.,* 2603 or 0320) to better bind shorter chain alcohols such as methanol or ethanol is not a trivial endeavor, as amino acid substitutions in proximity to the substrate-binding pocket could potentially perturb the overall structure of the proteins. This is especially true if we assume that the 2603 and 0320 enzymes adopt a fold that is similar to that of the *S. hyicus* phospholipase, as the deeply recessed lipid/alcohol binding pockets place the relevant sidechains near the core of the

protein. Therefore we chose to undertake a more straightforward approach to improve the catalytic activity of the FAMEs with respect to small alcohol substrates.

Hydrophobic compounds, the typical substrates of lipases, spontaneously partition in aqueous systems and are thus not usually uniformly distributed throughout the solution. For many lipase/esterases, localization to substrate structures such as micelles or lipid droplets is necessary for catalysis as lipid substrates are scarce or absent in bulk solution. In other cases the actual conformations of some enzymes are altered by proximity to lipids or membranes [40], [44] and [47]. This effect, called interfacial activation, is partially due to the change in the dielectric constant of the solution in close proximity to micelles or lipid droplets. Under the *in vitro* assay conditions we employed, in which oleic acid and alcohol were the substrates for an esterification reaction, oleic acid partitions into droplets, resulting in catalysis occurring at the droplet surface where both substrates and enzyme interact. The 2603 and 0320 FAMEs are part of the staphylococcal lipase family, and therefore we hypothesized that these enzymes may depend in part on either substrate localization or interfacial activation. Following this line of reasoning, FAME activity could potentially be improved by enhancing localization of a smaller alcohol substrate to enzyme (and, indirectly, alcohol substrate to lipid substrate). We pursued this goal by appending an alcohol-binding protein to the C-terminus of the wild type 2603

FAME. This was accomplished by cloning and expression of the gene for an alcohol binding protein in frame with the gene for the 2603 enzyme. In principle, the presence of an alcohol-binding domain should increase the amount of alcohol rebinding by the protein. Increased rebinding in turn increases the local concentration of ethanol in proximity to the catalytic FAME protein, and therefore the frequency of ethanol-FAME binding events. There is evidence that the staphylococcal lipase SAL3 forms tetramers under physiological conditions. If the USA300 FAMEs also form tetramers then there may already be a weak rebinding effect taking place. However, the magnitude of such an effect is determined by the affinity of the binding sites for the substrate; FAME domains themselves have low affinity for small alcohols that thus the FAME domain is not appealing as a facilitator of rebinding. An alcohol binding domain with much higher affinity for ethanol can potentially create a more pronounced rebinding effect, at least partially overcoming the FAME's weak affinity for small alcohols.

Many characterized alcohol-binding proteins are transmembrane proteins [36], limiting their usefulness in recombinant expression systems such as *E. coli*. However, the *Drosophila melanogaster* alcohol receptor protein, known as LUSH, is a soluble rather than a membrane-associated protein and has been well studied [1] and [44]. LUSH is normally found in the chemoreceptor hairs that serve as the *Drosophila* olfactory system. It has been demonstrated by Kim et. al. that LUSH is required for the alcohol avoidance response in wild-type

Drosophila [25]. Later work established that LUSH itself is the alcohol-binding protein in these chemoreceptors and has a well-defined alcohol binding site [26] and [41].

We chose LUSH for the appended alcohol-binding domain, incorporating the primary sequence for LUSH C-terminally to the 2603 enzyme. Additionally, we engineered a LUSH-T57A mutant variant of the fusion protein (Fig. A-5) as threonine 57 provides an important contact in the LUSH ethanol binding site, and the alanine substitution functions to remove an important hydrogen bond interaction. This substitution has previously been shown by Thode. et. al. to be deficient in alcohol-binding function, due to loss of a crucial hydrogen bond between threonine and the hydroxyl group of ethanol, without leading to a loss of overall protein stability [41]. To examine the effect of this alteration on the interaction between the 2603-LUSH fusion and the alcohol substrate, we used ethanol to displace anilino-1-naphthalene-sulfonic acid (ANS) out of the alcohol-binding site(s) of the enzymes. As expected, a dose-dependent decrease in the fluorescence of ANS was observed at increasing ethanol concentrations (Fig. A-4). Treating ethanol as an inhibitor and using the Michaelis-Menten model to derive its k_i, similar values were observed for wild type 2603 and the 2603-LUSH T57A mutant, but a lower k_i for the 2603-LUSH wild-type fusion. Because k_i is effectively equivalent to the k_d of the inhibitor, it follows that the 2603-LUSH fusion has a lower effective k_d with respect to ethanol.

Expression of the staphylococcal 2603 enzyme as a fusion with the *Drosophila* LUSH domain results in a protein that catalyzes the formation of ethyl oleate at a greater rate than the wild-type enzyme (Fig. A-5). The increase in catalysis is most pronounced at low ethanol concentrations. At high ethanol concentrations the difference in reaction velocity between wild-type and fusion enzymes diminishes, as the availability of ethanol to the active site becomes a less significant constraint to the rate of reaction. Thus the wild type 2603 enzyme and the 2603-LUSH fusion show comparable V_{max}, but differing V_i at substrate levels below saturation. As a result, the effective K_M for the 2603-LUSH fusion is lowered. This data was analyzed using the program GraphPad Prism, which demonstrated that the K_M of the 2603-LUSH fusion is approximately threefold lower than that of the wild type (Table A-1). This suggests that the fusion protein gains its increased activity by virtue of increased substrate binding, as the kinetics of substrate-to-product conversion (k_{cat}) would not be changed. Since the structure of the 2603 binding site was not subjected to manipulation, the increased substrate binding can be attributed to increased localization of ethanol molecules to the 2603 FAME domain via the closely associated LUSH domain. Co-localization increases the effective substrate concentration in proximity to the enzyme active site.

An alternative explanation for the improved ability of the fusion protein to catalyze ethyl oleate formation is that the LUSH domain potentially stabilizes an

active form of the 2603 enzyme. It was therefore worth considering the possibility that improved catalytic activity was a consequence of domain-domain stabilization rather than improved substrate localization. We have shown that stabilization of the 2603 enzyme by the LUSH domain is not the cause of improved catalytic ability of the fusion protein. The T57A mutation in the LUSH domain of the 2603-LUSH fusion exhibits catalytic kinetics comparable to that of wild type 2603, including a comparable K_M. In the absence of alcohol-binding ability the presence of the mutated LUSH protein does not increase the catalytic activity of the 2603 enzyme. This demonstrates that the increased fame activity of the 2603-LUSH fusion is not the result of inadvertent stabilization of a more active form of the FAME domain by the LUSH domain.

A.4. Conclusion

Our data indicate that two fatty acid modifying enzymes, 2603 and 0320, are likely responsible for the observed *in vivo S. aureus* esterase activity. These two enzymes closely resemble at least one other staphylococcal lipase that exhibits FAME activity in hexane [21]. Previous research demonstrated that the FAME+ phenotype correlates to the virulence of staphylococcal strains [24]. As a result, these two enzymes could potentially serve as anti-MRSA drug targets in the future. We have experimentally demonstrated that appending a ligand (ethanol) binding domain to the 2603 enzyme greatly improves its catalytic

ability. It does so by increasing substrate localization to the catalytic domain, which increases the overall residence time of substrate in proximity to the enzyme active site. These results represent an important step towards the use of engineered enzymes that favorably contribute to the field of biofuel synthesis. Fatty acid modifying enzymes, engineered to be effective at lower ethanol (or methanol) concentrations, may be more compatible with other components of bioreactors (such as live algae) that are less tolerant of high alcohol concentrations.

A.5 References

[1] L. Ader, D.N.M. Jones, H. Lin, Alcohol binding to the odorant binding protein LUSH: Multiple factors affecting binding affinities, Biochemistry. 49 (2010) 6136–6142. doi:10.1021/bi100540k.

[2] E. Antonian, Recent advances in the purification, characterization and structure determination of lipases, Lipids. 23 (1988) 1101–1106. doi:10.1007/BF02535273.

[3] R. Arai, H. Ueda, a Kitayama, N. Kamiya, T. Nagamune, Design of the linkers which effectively separate domains of a bifunctional fusion protein., Protein Eng. 14 (2001) 529–532. doi:10.1093/protein/14.8.529.

[4] B. Cadieux, V. Vijayakumaran, M.A. Bernards, M.J. McGavin, D.E. Heinrichs, Role of Lipase from Community-Associated Methicillin-Resistant *Staphylococcus aureus* Strain USA300 in Hydrolyzing Triglycerides into Growth-Inhibitory Free Fatty Acids, J. Bacteriol. 196 (2014) 4044. http://dx.doi.org/10.1128/jb.02044-14.

[5] G. Carta, J.L. Gainer, a H. Benton, Enzymatic synthesis of esters using an immobilized lipase., Biotechnol. Bioeng. 37 (1991) 1004–1009. doi:10.1002/bit.260371104.

[6] M.L. Cartron, S.R. England, A.I. Chiriac, Bactericidal activity of the human skin fatty acid cis-6-hexadecanoic acid on *Staphylococcus aureus*, Antimicrob. Agents 58 (2014) 3599-3609.

[7] N.R. Chamberlain, S. a. Brueggemann, Characterisation and expression of fatty acid modifying enzyme produced by *Staphylococcus epidermidis*, J. Med. Microbiol. 46 (1997) 693–697. doi:10.1099/00222615-46-8-693.

[8] N.R. Chamberlain, B. Imanoel, Genetic regulation of fatty acid modifying enzyme from *Staphylococcus aureus*, J. Med. Microbiol. 44 (1996) 125–129. doi:10.1099/00222615-44-2-125.

[9] R.C. Chang, S.J. Chou, J.F. Shaw, Synthesis of fatty acid esters by recombinant *Staphylococcus epidermidis* lipases in aqueous environment, J. Agric. Food Chem. 49 (2001) 2619–2622. doi:10.1021/jf001337n.

[10] C.L. Chu, J.A. Buczek-Thomas, M. a Nugent, Heparan sulphate proteoglycans modulate fibroblast growth factor-2 binding through a lipid raft-mediated mechanism., Biochem. J. 379 (2004) 331–341. doi:10.1042/BJ20031082.

[11] S.J. Cordwell, M.R. Larsen, R.T. Cole, B.J. Walsh, Comparative proteomics of *Staphylococcus aureus* and the response of methicillin- resistant and methicillin-sensitive strains to Triton X-100, Microbiology. (2002) 2765–2781.

[12] C.M.A. dos Santos, J.-W.F.A. Simons, M.D. van Kampen, I. Ubarretxena-Belandia, R.C. Cox, M.R. Egmond, H.M. Verheij, Identification of a Calcium Binding Site in *Staphylococcus hyicus* Lipase: Generation of Calcium-Independent Variants, Biochemistry. 38 (1999) 2.

[13] E.S. Dye, F. a. Kapral, Partial characterization of a bactericidal system in staphylococcal abscesses, Infect. Immun. 30 (1980) 198–203.

[14] a M. Farrell, T.J. Foster, K.T. Holland, Molecular analysis and expression of the lipase of *Staphylococcus epidermidis*., J. Gen. Microbiol. 139 (1993) 267–277. doi:10.1099/00221287-139-2-267.

[15] A.D. Ferrão-Gonzales, I.C. Véras, F. a L. Silva, H.M. Alvarez, V.H. Moreau, Thermodynamic analysis of the kinetics reactions of the production of FAME and FAEE using Novozyme 435 as catalyst, Fuel Process. Technol. 92 (2011) 1007–1011. doi:10.1016/j.fuproc.2010.12.023.

[16] N.S. Gandhi, S.B. Sawant, J.B. Joshi, Specificity of a liapse in ester synthesis : Effect of Alcohol, Biotechnol. Prog. 11 (1995) 282–287. doi:10.1021/bp00033a007.

[17] H. Ghamgui, M. Karra-Chaâbouni, Y. Gargouri, 1-Butyl oleate synthesis by immobilized lipase from *Rhizopus oryzae*: A comparative study between n-hexane and solvent-free system, Enzyme Microb. Technol. 35 (2004) 355–363. doi:10.1016/j.enzmictec.2004.06.002.

[18] M. Gopalakrishnan, K. Forsten-Williams, M. a Nugent, U.C. Täuber, Effects of Receptor Clustering on Ligand Dissociation Kinetics: Theory and Simulations, Biophys. J. 89 (2005) 3686–3700. doi:10.1529/biophysj.105.065300.

[19] F. Götz, F. Popp, E. Kom, K.H. Schleifer, Complete nucleotide sequence of the lipase gene from *Staphylococcus hyicus* cloned in *Staphylococcus carnosus*, Nucleic Acids Res. 13 (1985) 5895–5906. doi:10.1093/nar/13.16.5895.

[20] H. Horchani, H. Mosbah, N. Ben Salem, Y. Gargouri, A. Sayari, Biochemical and molecular characterisation of a thermoactive, alkaline and detergent-stable lipase from a newly isolated *Staphylococcus aureus* strain, J. Mol. Catal. B Enzym. 56 (2009) 237–245. doi:10.1016/j.molcatb.2008.05.011.

[21] H. Horchani, S. Ouertani, Y. Gargouri, A. Sayari, The N-terminal His-tag and the recombination process affect the biochemical properties of *Staphylococcus aureus* lipase produced in *Escherichia coli*, J. Mol. Catal. B Enzym. 61 (2009) 194–201. doi:10.1016/j.molcatb.2009.07.002.

[22] C. Hu, N. Xiong, Y. Zhang, S. Rayner, S. Chen, Functional characterization of lipase in the pathogenesis of *Staphylococcus aureus*, Biochem. Biophys. Res. Commun. 419 (2012) 617–620. doi:10.1016/j.bbrc.2012.02.057.

[23] J. V Karabinos, H.J. Ferlin, Bactericidal activity of certain fatty acids, J. Am. Oil Chem. Soc. 31 (1954) 228.

[24] J.G. Kenny, D. Ward, E. Josefsson, I.M. Jonsson, J. Hinds, H.H. Rees, J. a. Lindsay, A. Tarkowski, M.J. Horsburgh, The *Staphylococcus aureus* response to unsaturated long chain free fatty acids: Survival mechanisms and virulence implications, PLoS One. 4 (2009) e4344. doi:10.1371/journal.pone.0004344.

[25] M.S. Kim, A. Repp, D.P. Smith, LUSH odorant-binding protein mediates chemosensory responses to alcohols in *Drosophila melanogaster*, Genetics. 150 (1998) 711–721.

[26] S.W. Kruse, R. Zhao, D.P. Smith, D.N.M. Jones, Structure of a specific alcohol-binding site defined by the odorant binding protein LUSH from *Drosophila melanogaster*., Nat. Struct. Biol. 10 (2003) 694–700. doi:10.1038/nsmb0104-102b.

[27] V. Kukreja, M.B. Bera, Lipase from *Pseudomonas aeruginosa* MTCC 2488: Partial purification, characterization and calcium dependent thermostability, Indian J. Biotechnol. 4 (2005) 222–226.

[28] K.P. Lee, H.K. Kim, Transesterification reaction using *Staphylococcus haemolyticus* L62 lipase crosslinked on magnetic microparticles, J. Mol. Catal. B Enzym. 115 (2015) 76. http://dx.doi.org/10.1016/j.molcatb.2015.02.002.

[29] N. Lenfant, T. Hotelier, Y. Bourne, P. Marchot, A. Chatonnet, Proteins with an alpha/beta hydrolase fold: Relationships between subfamilies in an ever-growing superfamily, Chem. Biol. Interact. 203 (2013) 266–268. doi:10.1016/j.cbi.2012.09.003.

[30] J.P. Long, J. Hart, W. Albers, F. a. Kapral, The production of fatty acid modifying enzyme (FAME) and lipase by various staphylococcal species, J. Med. Microbiol. 37 (1992) 232–234. doi:10.1099/00222615-37-4-232.

[31] T. Lu, J. Park, K. Parnell, L.K. Fox, M. a McGuire, Characterization of fatty acid modifying enzyme activity in staphylococcal mastitis isolates and other bacteria, BMC Res. Notes. 5 (2012) 323. doi:10.1186/1756-0500-5-323.

[32] J.E. Mortensen, T.R. Shryock, F. a. Kapral, Modification of bactericidal fatty acids by an enzyme of *Staphylococcus aureus*, J. Med. Microbiol. 36 (1992) 293–298. doi:10.1099/00222615-36-4-293.

[33] K. Nikoleit, R. Rosenstein, H.M. Verheij, Comparative biochemical and molecular analysis of the *Staphylococcus hyicus*, *Staphylococcus aureus* and a hybrid lipase, Eur. J. Biochem. 228(3) (1995) 732-738.

[34] B.-C. Oh, H.K. Kim, J.-K. Lee, S.-C. Kang, T.-K. Oh, *Staphylococcus haemolyticus* lipase: biochemical properties, substrate specificity and gene cloning , FEMS Microbiol. Lett. 179 (1999) 385.

[35] D.L. Ollis, E. Cheah, M. Cygler, B. Dijkstra, The α/β hydrolase fold, Protein Eng. 5(3) (1992) 197-211.

[36] S.M. Paul, Alcohol-sensitive GABA receptors and alcohol antagonists., Proc. Natl. Acad. Sci. U. S. A. 103 (2006) 8307–8308. doi:10.1073/pnas.0602862103.

[37] S. Ramamurthi, A.R. McCurdy, Lipase-Catalyzed Esterification of Oleic Acid and Methanol in Hexane - A Kinetic Study, Jaocs. 71 (1994) 927–930.

[38] S. Ransac, M. Blaauw, B.W. Dijkstra, a T. Slotboom, J.W. Boots, H.M. Verheij, Crystallization and preliminary X-ray analysis of a lipase from *Staphylococcus hyicus*., J. Struct. Biol. 114 (1995) 153–155. doi:10.1006/jsbi.1995.1014.

[39] J. Rollof, S. Normark, In vivo processing of *Staphylococcus aureus* lipase, J. Bacteriol. 174 (1992) 1844–1847.

[40] J. Skjold, Altering the activation mechanism in *Thermomyces lanuginosus* lipase, Biochemistry. 53(25) (2014) 4152-4160.

[41] A.B. Thode, S.W. Kruse, J.C. Nix, D.N.M. Jones, The role of multiple hydrogen bonding groups in specific alcohol binding sites in proteins: Insights from structural studies of LUSH, J Mol Biol. 376 (2008) 1360–1376. doi:10.1016/j.jmb.2007.12.063.

[42] J.J.W. Tiesinga, G. Van Pouderoyen, M. Nardini, S. Ransac, B.W. Dijkstra, Structural Basis of Phospholipase Activity of *Staphylococcus hyicus* lipase, J. Mol. Biol. 371 (2007) 447–456. doi:10.1016/j.jmb.2007.05.041.

[43] A.R.M. Yahya, W. a. Anderson, M. Moo-Young, Ester synthesis in lipase-catalyzed reactions, Enzyme Microb. Technol. 23 (1998) 438–450. doi:10.1016/S0141-0229(98)00065-9.

[44] J.J. Zhou, G.A. Zhang, W. Huang, M. a. Birkett, L.M. Field, J. a. Pickett, P. Pelosi, Revisiting the odorant-binding protein LUSH of *Drosophila melanogaster*: Evidence for odour recognition and discrimination, FEBS Lett. 558 (2004) 23–26. doi:10.1016/S0014-5793(03)01521-7.

[45] R. Rosenstein; F. Götz, Staphylococcal lipases: Biochemical and molecular characterization, Biochimie. 82 (2000) 1005–1014.

[46] H. Fukuda, A. Kondo, H. Noda, Biodiesel fuel production by transesterification of oils, J. Biosci. Bioeng. 92 (2001) 405–416. doi:10.1016/S1389-1723(01)80288-7.

[47] R. Verger, “Interfacial activation” of lipases: Facts and artifacts, Trends Biotechnol. 15 (1997) 32–38. doi:10.1016/S0167-7799(96)10064-0.

[48] B.A. Diep, S.R. Gill, R.F. Chang, T.H. Phan, J.H. Chen, M.G. Davidson, F. Lin, J. Lin, H.A. Carleton, E.F. Mongodin, G.F. Sensabaugh, F. Perdreau-Remington, Complete genome sequence of USA300, an epidemic clone of community-acquired meticillin-resistant *Staphylococcus aureus*, Lancet. 367 (2006) 731–739. doi:10.1016/S0140-6736(06)68231-7.

[49] A.B. Salleh, R.N.Z.R.A. Rahman, M. Basri, New Lipases and Proteases, Nova Science Publishers, New York, 2006.

[50] PSORTb v3.0: N.Y. Yu, J.R. Wagner, M.R. Laird, G. Melli, S. Rey, R. Lo, P. Dao, S.C. Sahinalp, M. Ester, L.J. Foster, F.S.L. Brinkman, PSORTb 3.0: Improved protein subcellular localization prediction with refined localization subcategories and predictive capabilities for all prokaryotes, Bioinformatics 26(13) (2010) 1608-1615.

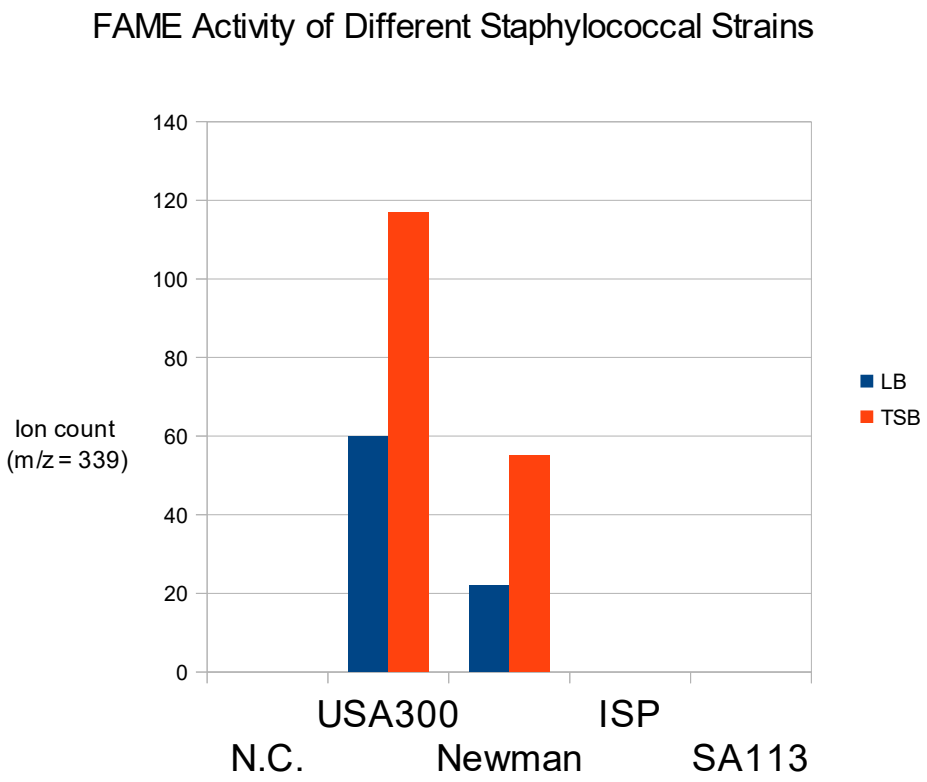

Figure A-1: GC-MS identification of FAME activity for staphylococcal culture supernatants, using LB and TSB media. Ion counts were measured at an m/z ratio of 339 amu, the mass of butyl oleate. In the case of sterile media filtrate in which no cells were cultured (N.C.), the ISP 479C staphylococcal strain, or the SA113 strain, no detectable amount of butyl oleate product was detected, whereas FAME activity was detected for the USA300 and Newman strains.

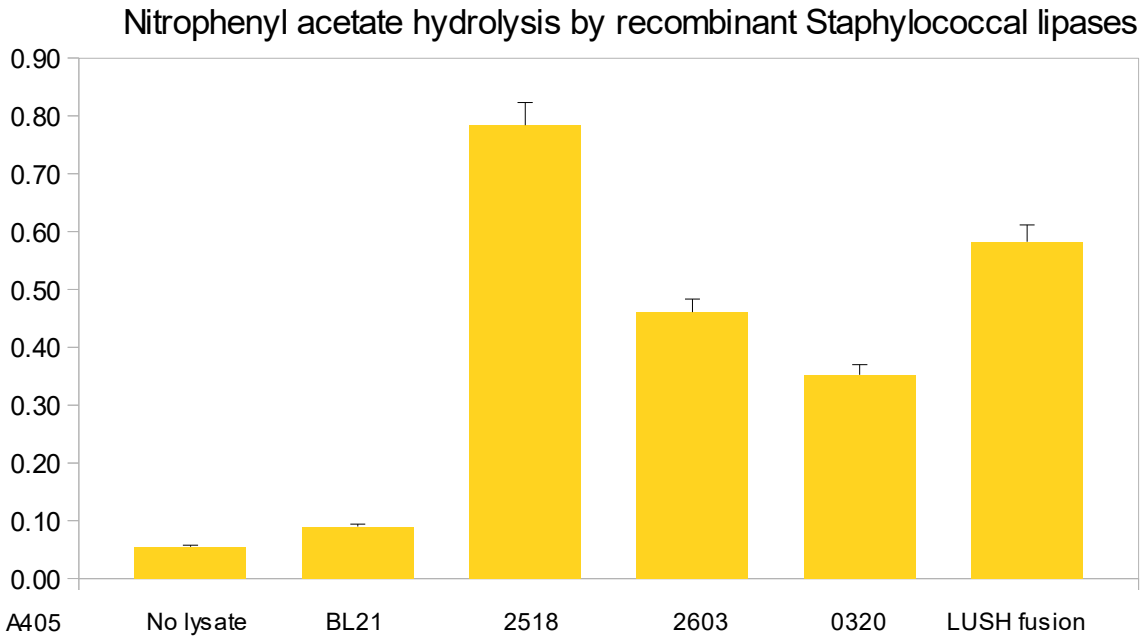

Figure A-2: Nitrophenyl acetate hydrolysis of *E. coli* expressed staphylococcal lipases. Absorbance measured at 450 nm indicates the evolution of p-nitrophenol, a lipolytic product. All three of the tested lipases, in addition to the 2603/LUSH fusion variant, catalyzed the formation of relatively similar amounts of p-nitrophenol. Lipases endogenous to the BL21 expression strain of *E. coli* are minimally active under these conditions (2nd bar).

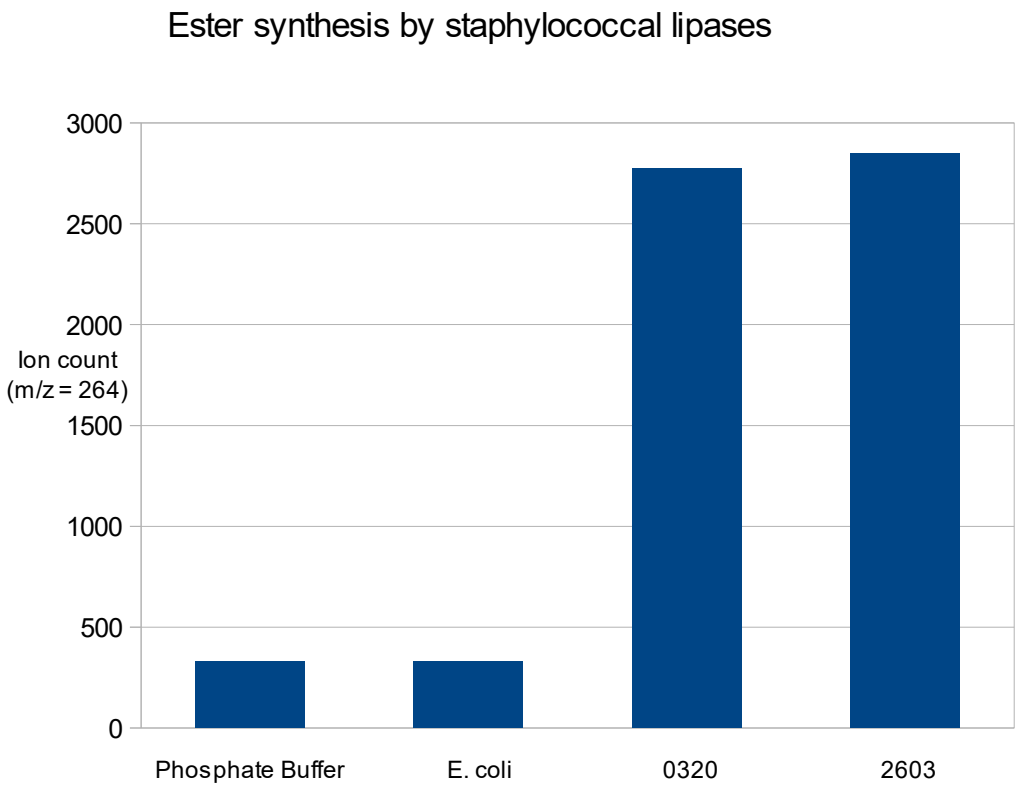

Figure A-3: GC-MS measurement of ester formation catalyzed by two recombinantly expressed staphylococcal esterases from *E. coli* cell lysate (enzymes 0320 and 2603). The fragmentation patterns of alkyl oleates have pronounced peaks at an m/z ratio of 264 amu. Fragmentation of alkyl oleates creates a distinctive peak at 264 amu corresponding to the fragment lacking the alkyl group. The increased counts at 264 amu for lysate of cells expressing the lipases 0320 and 2603 indicate successful catalysis of oleate ester formation.

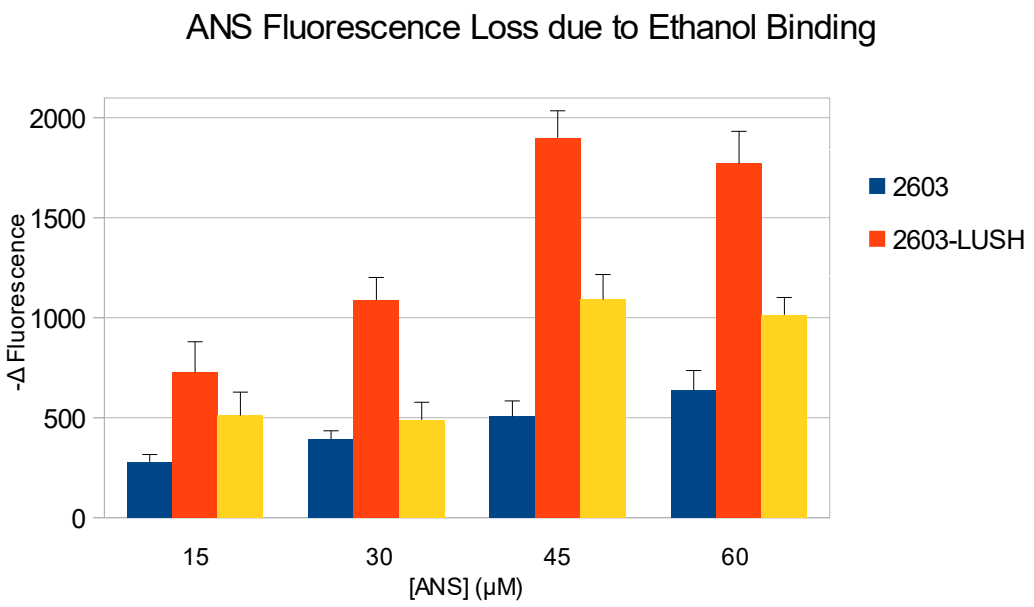

Figure A-4: Loss of ANS fluorescence due to ethanol binding. At 15, 30, 45, and 60 μM ANS, the difference in fluorescence between 0% ethanol and 15% ethanol (v/v) is indicated by the corresponding y-axis values. ANS fluoresces upon nonspecific interaction with a protein's exposed hydrophobic surfaces. Ethanol binding (both specific and nonspecific associations) excludes ANS from protein surfaces, resulting in a loss of fluorescence. A greater loss in fluorescence indicates more association between protein and ethanol.

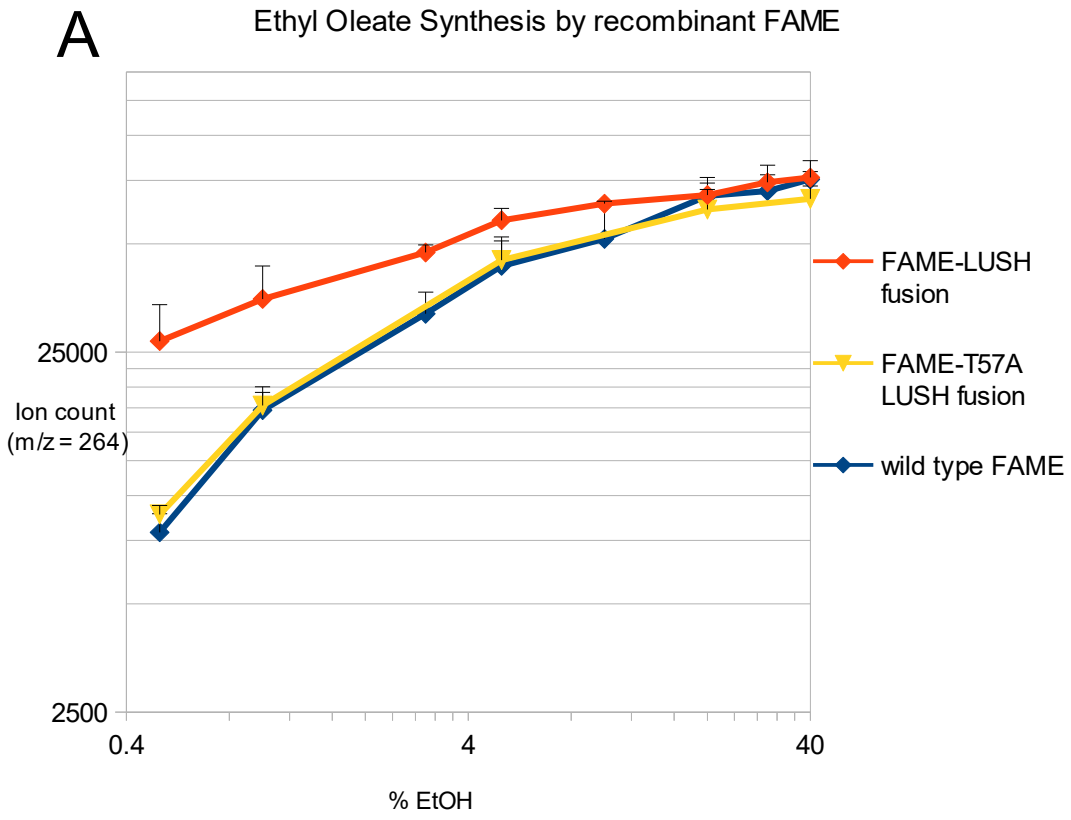

Figure A-5: (A) GC-MS assessment of ester synthesis as a function of ethanol concentration. Although the variants all have similar activities at higher ethanol levels, the 2603 FAME-LUSH fusion catalyzes esterification at a greater rate at low alcohol concentrations. The LUSH point mutant T57A, which has been demonstrated to not bind ethanol, mimics the wild-type FAME's catalytic ability.

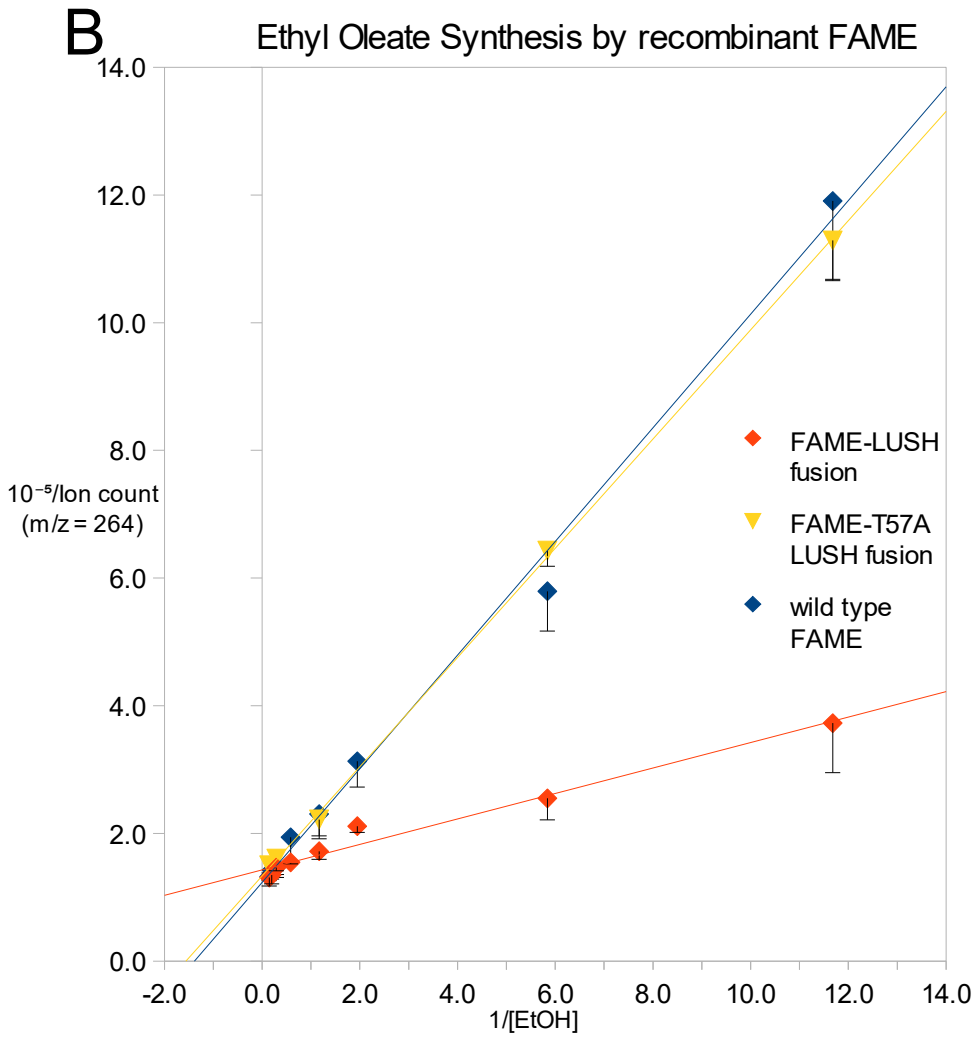

Figure A-5 (continued): (B) A Lineweaver-Burk double reciprocal plot shows similar $1/V_{max}$ for all three enzymes but greater $1/K_M$ (and therefore a lower K_M) for the 2603 FAME enzyme fused to the wild-type LUSH protein.

Table A-1: Analysis of the data using GraphPad Prism (C) indicates that the FAME-LUSH fusion has a >3-fold lower K_M with respect to ethanol.

Variant	K_M (mM)
Wild type FAME	622 ±59
FAME-LUSH fusion	180 ±21
FAME-LUSH T57A	616 ±75

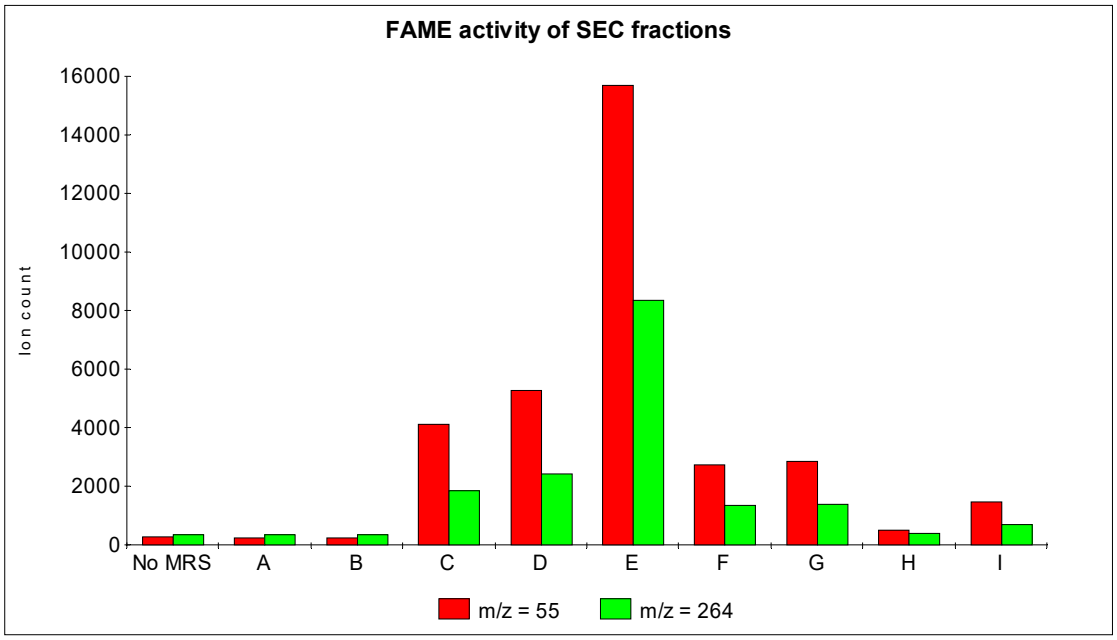

Supplementary figure A-1: Mass spectrometric determination of FAME activity in successive 15 mL size exclusion eluent fractions of staphylococcal culture supernatant. Ions were counted at two characteristic m/z values, 55 (a four-carbon fragment of the acyl chain) and 264 (the fragment lacking the alkyl group).

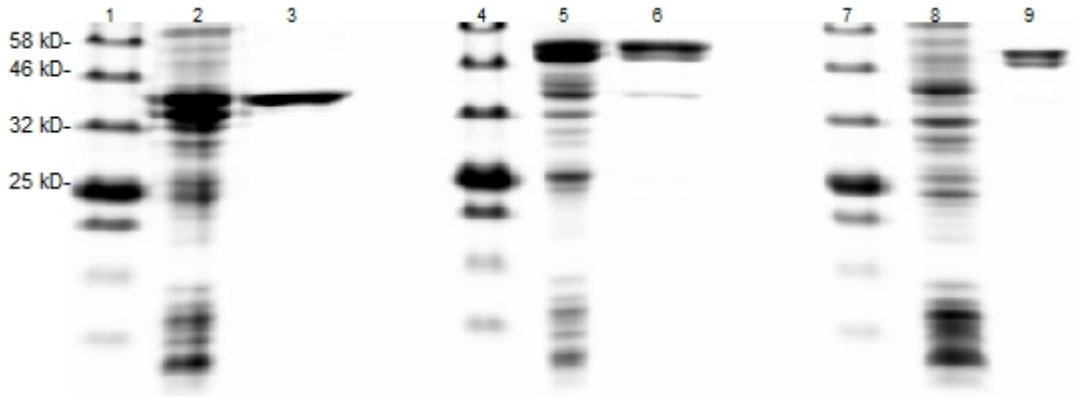

Supplementary figure A-2: SDS-PAGE showing 2603 FAME. Lanes 1, 4, 7: NEB molecular weight marker. Lane 2: total cell lysate of *E. coli* expressing 2603. Lane 3: purified 2603. Lane 5: lysate of *E. coli* expressing FAME-LUSH fusion. Lane 6: purified 2603-FAME. Lane 8: lysate of *E. coli* expressing FAME-LUSH-T57A. Lane 9: purified FAME-LUSH-T57A. Some visible scarring of the purified proteins is due to the incomplete removal of the N-terminal signal sequence.

```
2603        M---KSQNKYSIRKFSVGASSILIATLLFLSGGQAQAAEKQVNMGNSQEDTVTAQSIGDQ
0320        MLRGQEERKYSIRKYSIGVVSVLAATMFVVSSHEAQASEKTSTNAAAQKETLNQPG---E
0876        MNKTKGFTKYKKMRYIPGLDGLRAIAVL-----------GIIIYHLNKQWLTGGFLGVD
2473        ------------------------------------------------------------
RS13450     ------------------------------------------------------------
0641        ------------------------------------------------------------
2518        ------------------------------------------------------------
0430        ------------------------------------------------------------

2603        QTRENANYQRENG--VDEQQHTENLTKNLHNDK-TISEENHRKTDDLNKDQLKDDKKSSL
0320        QGNAITSHQMQSGKQLDDMHKENGKSGTVTEGKDTLQSSKHQSTQNSKTIRMQNDNQVKQ
0876        TFFVISGYLITSL-----LLKEYDDTGIIKLKSFWIRRLKRLLPAVIVLLMVVGTATLLL
2473        ------------------------------------------------------------
RS13450     ------------------------------------------------------------
0641        ------------------------------------------------------------
2518        ------------------------------------------------------------
0430        ------------------------------------------------------------

2603        NNKNIQRDTTKNNNANPSDVNQGLEQAINDGKQSKVASQQQSKEADNSQDSNANNNLPSQ
0320        DSERQGSKQSHQNNATNNTERQ------NDQVQNTHHAERNGSQSTTSQSNDVDKSQPSI
0876        KSDNIIRVK-------------------HDIIAAIFYVSNWWYIAKDVNYFEQFSFMPLK
2473        ------------------------------------------------------------
RS13450     ------------------------------------------------------------
0641        ------------------------------------------------------------
2518        ------------------------------------------------------------
0430        ------------------------------------------------------------

2603        SRIKEAPSLNKLDQTSQREIVNETEIEKVQPQQNNQANDKITNYN--------FNNEQEV
0320        PAQKVIPNHDKAAPTSTTPPSNDKTAPKSTKAQDATTDKHPNQQDTHQPAHQIIDAKQDD
0876        HLWSLAIEEQFYIFFPVILVTLLLTIKKRYKIGFIFWGVSIISLGLMMFIYS-INGDHSR
2473        ----MRKKWSTLAFGFLVAAYAHIRIKEKRSVKSYMLEQGIR-----------LSRAKRR
RS13450     ------------------MSQTEYQIKSGNIKGNSEETSTVSNIS-----YE-IENANNS
0641        ------------------------------------------------------MNKDNKW
2518        ------------------------------------------------------------
0430        ------------------------------------------------------------
```

Supplementary figure A-3: Kalign CLUSTAL protein sequence alignment of USA300 strain *Staphylococcus aureus* lipases, showing >50% sequence identity between 0320 and 2603. Highlighted are the characteristic “YSIRK” of staphylococcal secretion signal sequences and signal peptide cleavage sites for 0320 and 2603; the other lipases lack secretion signal sequences.

```
2603        KPQKDEKTLSVSDLKNNQKSPVEPTKDNDKKNGLNLLKSSAVATLPNKGTKELTAKAKDD
0320        TVRQSEQKPQVGDLSKHIDGQNSPEKPTDKNTDNKQLIKDALQAPKTRSTTNAAADAKKV
0876        VYFGTDTRLQTLLLGVILAFLWPPFKLKNDPPKVVKYVIDSIGSLSFIVLILLFFIINDE
2473        FMYKEEAMKALEKM--------APQTAGEYEGTNYQFKMPVKVDKHFGSTVYTVNDKQDK
RS13450     GLKQNKIDKQIKKLQEKNKFPKNLSYLKSYTDPKTGTTTSAFLNKDTGKVTLGMTGTNVH
0641        TMITALFITVISVLLAFHLKQHYDQITNENHANKDKINIKNKNVRIYQNLTYNRVFPNSK
2518        ----------------------------------------METLELQGAKLRYHQVGQG
0430        -------------------------------------------MRIKTPSPSYLKGTNG

2603        QTNKVAKQGQYKNQDPIVL-VHGFNGFTDDINPSVLAHYWGGNKMN--IRQDLEENGYKA
0320        RPLK-ANQVQPLNKYPVVF-VHGFLGLVGDNAPALYPNYWGGNKFK--VIEELRKQGYNV
0876        TNWI-YDGGFYLISILTLF-I---------IASVVHPSTWIAKIFSNPVLVFIGKRSYSL
2473        HQRV------------VLY-AHG--------------GAWFQDPLK--IHFEF-------
RS13450     KDAI-------------------------------------------LKQTFGVPSYQG
0641        LDIITPVDMSSNAKLPVIFWMHG-GGYIA-----------GDKQYKNPLLAKIAEQGYIV
2518        PVLI--------------F-IPGANG--------------TGDIFL-PLAEQL-KDHFTV
0430        HAIL--------------L-LHSFTG--------------TNRDVK-HLAAELNDQGFSC

2603        Y--EASISAFGSNY--DRAVELY-YYIKGGRVDYGAAHAAKYGHERYGKTYEGIYK-DWK
0320        H--QASVSAFGSNY--DRAVELY-YYIKGGRVDYGAAHAAKYGHERYGKTYKGIMP-NWE
0876        YLWHFAVISFVHSYYVDGQIPVYVYFIDISLTIIFAELSYRFIETPFRK--EGIKALNWR
2473        ------IDELAETL--NAKVIMP-VYPKIPHQDYQATYVL------FEKLYHDLLN-QVA
RS13450     Y---IDVSETLKDI--GADVNI-------------GLHSVTDKDPHYKNT-QDFIK-NIK
0641        V-----------NV----------NYALAPQYKYPTPLIQMNQATQFIK--ENKM--NLP
2518        V--AVDRRDYGES---ELTEPLP-DSASNPDSDYRVKRDAQDIAE---------LA-KSL
0430        Y---------APNY-PGHGLLLK-DFMTYNVDDWWEEVEKAYQF-------------LVN

2603        PGQKVHLV-GHSMGGQTIRQLEEL-----LRNGNREEIEYQKKHGGEI--SPLFKGN-HD
0320        PGKKVHLV-GHSMGGQTIRLMEEF-----LRNGNKEEIAYHKAHGGEI--SPLFTGG-HN
0876        PSYIPQFI-RMAI---VVTLLIPF-----MLILVGAFNKYGKDIIGEK--ANSFDTTIED
2473        DSKQIVVM-GDSAGGQIALSFAQL-----L----KEKHIVQPGHIVLI--SPVLDAT---
RS13450     KDYDIDIITGHSLGGRDAMILG-------MSNDIKHIVVYNP--------APL-------
0641        IDFNQVIIGGDSAGAQLASQFTAIQTNDRLREAMKFDQSFKPSQIK----GAILFGG---
2518        SDEPVYIL-GSSSGSIVAMHVLKD-----YPEVVKKIAFHEPPINTFLPDSTYWKDK-ND
0430        EGYESISATGVSLGGLMTLKLAQH—YP-LKRIAVMSAPKEKSDDGLI--EHLVYYS---
```

Supplementary figure A-3, continued.

```
2603        NMISSITTLGTPH-------NGTHASDLAGNEALV---RQIVFDIG----KMFGNK--NS
0320        NMVASITTLATPH-------NGSQAADKFGNTEAV---RKIMFALN----RFMGNK--YS
0876        NYLMRIAPIDNIHIDGLVSEKKKESSDVYNNIKPLLIGDSVMVDIG----ESFKSSVPKS
2473        ----------------M---QHPEIPDYLKKDPMVGV-DGSVFLAE----QWAGDT----
RS13450     --------------------AIKDVSGLYADQEEL---KKLIEKYDGHIVRFVSDE---D
0641        --FYNMQTVRETEFP-----RIQLFMKSYTGEEDW---EKSFKNIS----QMSTVK--QS
2518        DIVHQILTEGLEK-------GMKTFGETLNIAPID---AKMMSQPA----DTEEGR--IE
0430        QRMSNILNL-----------DQQASSAQLAAIDDY---EGEITKFQ----HFIDDI----

2603        R-------VDFGLAQWGLKQKP--NESYIDYVKRVKQSNLWKSKDNGFYDLTREGATDLN
0320        N-------IDLGLTQWGFKQLP--NESYIDYIKRVSKSKIWTSDDNAAYDLTLDGSAKLN
0876        R-------IDGKVGRQLYQTLPLVKANYSQYKK---------SSDQVVLELGTNGDFTVK
2473        P-------LD------NYKVSP--INGDLDGLGRITLTV---GTKEVLYPDALN-LSQLL
RS13450     E-------LDAGVRNHLYETAG--EKIVLKNGEGHAMSGILMSRTQAIILAELN---KVK
0641        T-------KNYPPTFLSVGDSDPFESQNIEFSKKLQELNV--PVDTLFYDGTHH------
2518        QYKRTMFWLEFEIRQYTHSNIT--LDDFTKYSDKITLLNG--TDSRGSFPQDVN--FYIN
0430        ------------MTNLNVIKMP--ANILFG------------GKDAPSYETSAH--FIYE

2603        RKTSLNPNIVYKTYTGEATHKALNSDRQKADLNMFFPFVITGNLIGKATEKEWRENDGLV
0320        NMTSMNPNITYTTYTGVSSHTG-PLGYENPDLGTFFLMATTSRIIGHDAREEWRKNDGVV
0876        QLDDL-----LNQFGKAKIYLV------NTRVPRIYE-ANVNRLLADAAKR--KSNVTLI
2473        SAKGIEHDF-IPGYYQFHIYPV----FPIPERRRFLY--QVKNIIN--------------
RS13450     GYQDENNKA-LKSVRKQTRHRL----HKVETLRANWI-QTTGGSLSSSQQQ----LLEAL
0641        ----------LHHQYQFHLNKP----ESIDNIKKVLL-FLSRNTSSSGIQT---EEKPQI
2518        KETGIP----IVDIPGGHLGYI----QKPEGFADVLL-----NMWG--------------
0430        HLGSVDKE--LNGLKDSHHLMT------HGEGRDILE-ENVIRFFNALT-----------

2603        SVISSQHPFNQAYTKATDK---IQKGIWQVTPTKHDWDHVDFVGQDSSDTVRTREELQDF
0320        PVISSLHPSNQPFVNVTNDEPATRRGIWQVKPIIQGWDHVDFIGVDFLDFKRKGAELANF
0876        DWYKRSQGHSEYF---------APDGV-----------HLEYKGV---------------
2473        ------------------------------------------------------------
RS13450     TALTIAEGLNQLVNEESQH---LKKCI-------TRW-HINLETTGKKR-----------
0641        ENPSNELPLNPLN-------------------------------------------------
2518        ------------------------------------------------------------
0430        ------------------------------------------------------------
```

Supplementary figure A-3, continued.

```
2603        WHHLADDLVKTE----KLTDTKQA
0320        YTGIINDLLRVEATESKGTQLKAS
0876        -LALKDEILKA---------LKKK
2473        ------------------------
RS13450     -KKLEMKLVKN-------------
0641        ------------------------
2518        ------------------------
0430        ------------------------
```

Supplementary figure A-3, continued.

Appendix I, in part is currently submitted for publication of the material. Saylor, Benjamin D.; Love, John J. The dissertation author was the primary investigator and author of this material.